ABSTRACT OF DISSERTATION

VERTICAL MOVEMENT OF ACTINIDE-CONTAMINATED SOIL PARTICLES

The vertical distribution of actinide-contaminated soil particles was investigated. Contaminated, but undisturbed soils were separated into their constituent mineral particles and the distribution of contaminants on each size fraction was examined for evidence of migration as a function of particle size and depth in soil. Physical mechanisms of movement were also examined in the laboratory for their potential to cause contaminant migration in soil systems. Mechanisms examined included water as a driving force, volume changes in soils resulting from freezing, and cracking as a result of drying.

Soil samples were collected from an undisturbed, actinide-contaminated, natural grassland site. The soils were size-fractionated and analyzed for $^{238, 239\text{-}240}$Pu and ^{241}Am alpha and gamma spectroscopy. The clay particle size fraction (0.45 - 2 μm) had the highest activity concentration for both elements. Approximately 50% of the total inventory resided in the coarse silt (10 - 53 μm) fraction. There was no evidence that contaminated soil particles of different sizes migrated at different rates into the soil. The mean value (7.6) of the $^{239\text{-}240}$Pu to ^{241}Am ratios were statistically indistinguishable with depth ($p=0.15$) but were statistically higher ($p = 0.001$) for the dissolved (< 0.45 μm) fraction. The mean value (75) of the $^{239\text{-}240}$Pu to ^{238}Pu ratios was not statistically different over all depths and particle sizes ($p = 0.5692$ and 0.9183).

Three mechanisms of physical transport: migration by water; frost heaving and thawing; and soil cracking, were evaluated for their potential to move soil particles through a homogenous soil medium. Five soil fractions: sand (50 - 250 μm), coarse silt (10 - 50 μm), fine silt (2 - 10 μm), clay (0.45 - 2 μm), and "dissolved" (< 0.45 μm) were labeled with ^{234}Th and applied to soil columns containing a sandy clay loam. Water equivalent to 130 year of rainfall was not a statistically significant factor ($p = 0.17$) in moving labeled particles into the columns. An experiment to assess the effects of freezing and cracking the soil resulted in significant migration ($p = 0.0001$) of ^{234}Th labeled clay particles. The migration was largely attributed to bypass flow through macropores (cracks) created during the shrinkage of the soil as it dried ($p = 0.0001$); less extensive but significant ($p = 0.0001$) migration was also attributed to volume changes caused by frost heaving and subsequent soil contraction upon thawing.

Kathryn A. Higley
Radiological Health
Sciences Department
Colorado State University
Fort Collins, CO 80523
Fall 1994

2

ACKNOWLEDGEMENTS

This research was partially supported by the Pacific Northwest Laboratory (PNL) through Associated Western Universities Inc., Northwest Division (AWU NW) under Grant DE-FG06-89ER-75522 with the U.S. Department of Energy and DOW Chemical Company under contract YCD000, and the Colorado Department of Health under contract ENV930778.

There are many individuals who deserve acknowledgement and thanks in the realization of this work. I would like to thank Andy Wallo, III, Gary Roles, John Tseng and Ray Pelletier from the Department of Energy for their continued support and encouragement. From Battelle, I would like to thank Jim Droppo, one of the finest gentlemen I have had the pleasure to work for, as well as Joe Soldat, Bruce Napier, Bill Kennedy, and Ernest Antonio. My trusty assistant Jeff Thompson (a.k.a "Bob") deserves special recognition for his skill in translating my back-of-the envelope-scratchings into functional designs and workable systems, as well as his willingness to tolerate my bossiness for the last 2 years. I would also like to thank Matt Gosch, the designer of the world's best soil-core extrusion tool. Lastly, I would like to thank the members of my graduate committee for their support, insight, and encouragement in seeing this work to completion.

This work is dedicated to the memory and spirit of Anna Jean Higley, the best role model a daughter could ever have asked to have.

3

TABLE OF CONTENTS

LIST OF TABLES

5

LIST OF FIGURES

Figure Page

THE DISTRIBUTION OF $^{238, 239-240}$PU AND ^{241}AM ON SOIL PARTICLES FROM THE ROCKY FLATS PLANT SITE

MOVEMENT OF ^{234}TH-LABELED SOIL PARTICLES THROUGH A HOMOGENOUS SOIL MEDIUM

7

INTRODUCTION

In 1989 the Radioecology Group at Colorado State University staff resampled an area they had surveyed for plutonium contamination in the early 1970s. The main purpose of the 1989 effort was to determine if any further migration of this radionuclide through the ecosystem had occurred since its initial contamination in the late 1960s. The data from the first visit were recorded and interpreted in the Ph.D. dissertation of Little (1976); the second in the M.S. thesis of Webb (1992).

Surprisingly, Webb observed no additional migration of plutonium into the soil in the 25 y since Little first conducted his research. In fact, Webb reported the same, statistically indistinguishable, gradient of plutonium concentration versus depth in soil as had Little. Webb's work, conducted using sampling methods identical to those employed by Little, raised the question: how had the plutonium moved rapidly to depth in the 1960s, yet remained apparently immobile in the intervening 25 y?

The research presented in this dissertation represents a first step in addressing the question of mechanics of plutonium migration into the soils of the U.S. Department of Energy's Rocky Flats Plant site (RFP). The work is presented in two parts. The first part examines the distribution of plutonium and americium on soil particles. Its purpose was to provide insight on possible mechanisms of movement into the soil that was contaminated at the RFP by asking whether contaminated soil particles of different sizes appeared to have different rates of penetration into soil. The second part of the research evaluates three physical mechanisms of movement and assesses their potential to cause migration of labeled soil particles of different sizes into uncontaminated soils.

The work is presented as a multipart dissertation: references are included at the end of each chapter, as are figures, tables, and endnotes. There are three appendices which contain information on analytical procedures, experimental apparatus, and the raw data used to generate figures and tables presented in the body of the work.

REFERENCES

Higley, K. A. Assessment of a model to describe the environmental transport and fate of ^{241}Am and $^{238,239}Pu$. M.S. Thesis. Fort Collins, CO: Colorado State University, 1992.

Little, C.A. Plutonium in a grasslands ecosystem. Ph.D. dissertation. Fort Collins, CO: Colorado State University, 1976.

Webb, S. B. A study of plutonium in soil and vegetation at the Rocky Flats Plant. M.S. Thesis. Fort Collins, CO: Colorado State University, 1992.

9

THE DISTRIBUTION OF $^{238, 239-240}$PU AND ^{241}AM ON SOIL PARTICLES FROM THE ROCKY FLATS PLANT SITE

BACKGROUND

The distribution of ^{241}Am, ^{238}Pu, and $^{239-240}$Pu on soil particles collected in 1993 from the RFP was examined. The RFP is located approximately 26 km northwest of Denver, Colorado and was established in 1950 as part of the U.S. Government's plan to expand and diversify the nation's nuclear weapons research, development and production complex (U.S. DOE, 1980, Vol.1). The Radioecology Group at Colorado State University (CSU), along with numerous other federal, state and private organizations, has been investigating the presence of these radiocontaminants since 1970 in the ecosystems surrounding the site. These studies have yielded a wealth of information on the distribution of these radionuclides. However, questions remained unanswered on how the contaminants moved rapidly into the soil soon after the principal contaminating event and then remained essentially immobile for the next 25 years. The objective of this study was to provide insight into potential mechanisms of plutonium and americium movement through the soils by evaluating the distribution of these radionuclides as a function of soil particle size.

A 50-ha hillside was inadvertently contaminated with plutonium and americium during remediation of an adjacent area (known as the 903 pad) in the late 1960s (Krey et al., 1976). The contamination originated from the outdoor storage of metal barrels containing waste cutting oil. The oil contained mostly submicron-sized particles of unrecoverable plutonium and its decay product, americium (U.S. DOE, 1980, Vol. 1). These radionuclides were initially present

10

as metallic filings maintained in a cutting oil - carbon tetrachloride suspension (Navratil and Baldwin, 1977). Their chemical speciation at the time of release has never been conclusively determined (Bondietti and Tamura, 1980). Other than being the subject of numerous sampling and field studies, and occasional weed control efforts, this hillside has been largely undisturbed since the original contaminating event[a]. As such, it presents an intact record of the contaminants in soil. Approximately 15 GBq of plutonium was estimated to remain in the area in 1980 (U.S.DOE, 1980, Vol. 2).

Previous studies defined the plutonium and americium inventory in soils, flora, and fauna of the hillside and adjacent areas (Krey et al., 1976; Little, 1976; EG&G, 1990; Webb, 1992; Schierman, 1994). Samples collected within 2 to 4 y of the original deposition revealed an exponentially decreasing concentration of plutonium with increasing depth in soil (Krey et al., 1976; Little, 1976). Approximately 50 % of the inventory was found in the top 3 cm of soil and greater than 90% in the top 12 cm. Plutonium was detected as deep as 20 cm in the soil profile (Little, 1976). Twenty-five years after the Krey et al. (1976) and Little (1976) studies, the same statistically indistinguishable, exponentially decreasing concentration-depth gradient was observed by Webb (1992). These results raise the question of how the plutonium and americium initially moved to depth within a few years and then apparently remain immobile through the intervening 20 y?

Comparisons have been made as to the mobility and bioavailability of plutonium at this site relative to plutonium-contaminated sites at other locations (Bondietti and Tamura, 1980). For example, the plutonium at RFP was found to be more insoluble than that from sites at the Oak Ridge Plant (ORP), located near Oak Ridge, Tennessee, or Mound Laboratories (ML), located near Miamisburg, Ohio, but similar to that from the Nevada Test Site (NTS) near Las Vegas, Nevada (Bondietti and Tamura, 1980). The solubility differences were attributed to the original source of material - metallic plutonium at the NTS and RFP sites versus a soluble form at the ORP and ML locations. Bondietti and Tamura (1980) highlighted the inherent problem of

trying to compare the environmental behavior of plutonium and americium across locations without knowing the chemical form of the source material.

Obvious differences in the behavior of americium and plutonium in soils at different locations can be attributed to four major factors: 1) chemical and physical form at the time of release; 2) soil type; 3) climate; and 4) biotic factors. For example, studies were conducted in Germany on an undisturbed slightly wet Alfisol classified soil to estimate the residence times of plutonium and americium (Bunzl et al., 1994). This soil is similar in many respects to the Aridisol classified soil of the 50-ha hillside site at the RFP. The German soils were undisturbed for approximately 30 y, slightly longer than those at RFP. Vertical depth distributions of these radionuclides were determined by collecting lifts in layers of 2 to 10 cm thick to a total depth of 40 cm. Both elements exhibited peak concentrations approximately 5-10 cm below the soil surface, indicating that either migration through the soil was occurring or new soil was being developed on the surface. In contrast, repeated investigations at the RFP show the peak activity concentration has remained in the 0-3 cm profile over the 20+ y since the release occurred (Webb, 1992).

The objective of this study was to provide insight into possible mechanisms of movement of the contaminants into the soil by examining their distribution in soils as a function of particle size and depth. Contaminated soils were tested to determine: 1) if there was preferential attachment to different sized soil particles; 2) if the decrease in radionuclide concentration with depth reported in other studies (Little, 1976; Webb, 1992) was constant over all particle sizes; 3) if there was a particle size and depth interaction, such as might result from one particle size migrating through the soil at a rate different than other particle sizes; 4) if the $^{239\text{-}240}Pu$ to ^{241}Am ratios were constant over all particle sizes and depths (suggesting similar mechanisms of movement through the soil); and, 5) if the $^{239\text{-}240}Pu$ to ^{238}Pu ratios were constant over all particle sizes and depths (i.e., to test the possible differences in mobility of these plutonium isotopes, as per the discussions in Kercher and Gallegos, 1993).

12

METHODS AND MATERIALS

Collection

The sampling site was chosen to coincide with an area previously investigated and identified as Macroplot 1 by Little (1976) and Webb (1992). Three locations, randomly selected within an 100-m^2 grid, were identified as CX15, CX16 and CX17. Four stacked lifts of soil, 20 cm wide by 12 cm long by 3 cm high were collected from each location at depths of 0-3, 3-6, 6-9, and 9-12 cm. The maximum sampling depth was chosen based on results of earlier studies which had shown that for this general location 90% of the plutonium and americium inventory resided in the top 12 cm (Webb, 1992; Schierman, 1994).

Collection methods were consistent with previously established soil sampling protocols (Little, 1976; Webb, 1992). Prior to collection, the area was cleared of vegetation using garden shears to cut plants level with the soil surface. Large plant debris (e.g., twigs) was removed by hand. Litter was sampled intact with the top 0-3 cm lift. Stones large enough to encompass more than one soil lift were discarded, all others were collected with the lift sample and returned to the laboratory for separation and analysis with the remainder of the soil.

Soil Fractionation

The size fractions used in this analysis were based on the textural classifications of the U.S. Department of Agriculture (Miller and Donahue, 1990). The size fractions included gravel (> 2 mm), sand (2 mm - 53 μm), coarse silt (53 - 10 μm), fine silt (10 - 2 μm), clay (2 - 0.45 μm), and a "dissolved" fraction (< 0.45 μm).

Bulk soil was dried at 105 °C for 24 h, weighed, and passed through a 2 mm sieve to separate the gravel fraction. The gravel was washed with deionized water to remove any remaining soil, redried, and weighed to obtain a total gravel mass per lift. The soil that was washed from the gravel was collected on a tared 0.45 μm membrane filter, dried and

recombined with the other soil for analysis. Typically, the mass of soil rinsed from the gravel was only a few percent of the total soil mass for the lift.

The soil was separated into smaller size fractions using a wet separation method specifically designed to minimize damage to the clay minerals (Gee and Bauder, 1986). The fractionation process consisted of a series of timed sedimentations with decantation and extraction to obtain an approximate particle size range. This was followed by filtration through a tared membrane filter of the desired minimum pore-size diameter. Repeated extractions were performed to provide at least 95% separation of particle sizes. The recovered soils were again dried at 105 °C for 24 h and weighed. The samples were homogenized using a mortar and pestle and split for americium and plutonium analyses. The dissolved fraction was recovered by evaporation and concentrated into tared 250 ml beakers.

An important assumption was made with regard to the fractionation process: namely, that the analytical method used to separate the soil particles did not substantially mobilize the radionuclides. The purpose of the soil separation procedure was to break up soil aggregates while leaving the radionuclides bonded to mineral particles. Studies have suggested the extractability of actinides from soils is strongly pH dependent, with the lowest extraction of americium and plutonium (0 - 2 %) occurring in the pH range of 3 - 6 (Tamura, 1977; Nishita et al, 1981; Nishita and Haug, 1981). The method used in this study required initial suspension of the soils in a dilute acetic acid (pH 5) solution to cause disaggregation.

The assumption that the disaggregation procedure did not appreciably extract americium or plutonium from the soil particles was experimentally tested. Six replicate samples of CX17 surface soil, each weighing 33 g, were each placed in 150 ml of acetic acid/sodium acetate solution. At intervals of 0, 4, 8, 20, 32 and 56 hours a sample was removed and filtered through a 0.45 micron filter (this particular time frame was chosen because it covered the duration of the initial separation step). The soil was dried for 24 h and counted for 1600 s. The filtered solution was recovered and also counted (300 to 86,400 s).

The americium concentration (Bq ml^{-1}) in the solution increased over the first 8 h and then remained constant at 0.01 ± 0.002 Bq ml^{-1} (n=4). The ^{241}Am activity concentrations (1.2 Bq g^{-1}) in the six soil fractions recovered and recounted after the experiment were within ± 1 standard deviation of the concentrations found in the soil prior to the experiment. The distribution coefficient calculated from the "equilibrium" concentration data was 120 ml g^{-1}, within the reported ranges for americium in soil-water systems (Jirka et al., 1983, Nishita et al, 1981).

The change of ^{241}Am concentration in the solution with time suggested buildup to and attainment of an equilibrium state between the aqueous and solid phases. If the experimental procedure resulted in the disaggregation of soil particles (a moderately paced process) one would expect to observe an increase in americium concentration in solution. The concentration in solution would eventually stabilize after all soil structure was lost and the < 0.45 μm particles dispersed into the solution. Conversely, if the procedure resulted in the leaching of americium from the soils, one would also expect to see an increase in solution concentration with time. However, an equilibrium concentration would not be expected because: 1) the solution concentration of americium is very dilute; 2) and solubility limits are not likely to have been reached; 3) the amount of americium in the solid phase is substantially greater than that in the aqueous one. Based on that rationale it was concluded that the soil separation procedure was not likely to have substantially remobilized americium (and by inference, plutonium), and the equilibrium concentration observed in solution was a consequence of disaggregation of soil structure.

In addition, earlier work on the particle size distribution of surface grab soil samples taken approximately 1 km from the original spill site were reviewed for the effect of various pretreatment methods on the distribution of plutonium among several particle sizes. A mild dispersive treatment (such as used in this study) resulted in 60% of the plutonium activity remaining on the silt soil fractions. Not until a more aggressive treatment was used, with

15

decomposition of the organic fraction, did the distribution of total activity shift to the clay fraction (Tamura, 1977).

Analysis

Gamma spectroscopy was used for ^{241}Am analysis. Aliquots of dried soil were placed in tared steel tins and counted on a shielded GeLi detector[c]. Soil standards, spiked with National Institute of Standards and Technology (NIST) traceable ^{241}Am solutions, were used to determine total sample activity. With two exceptions, all samples had measurable quantities of ^{241}Am. Sample masses ranged from 1 to 30 g, except for the gravel fractions which were counted in toto (masses ranged from 60 to 800 g). Count times varied between 1 and 12 h.

Plutonium analyses were conducted by a commercial firm[d] (detailed procedures are described in Appendix A). Briefly, soil samples were ground to a fine powder with ^{242}Pu tracers added to a 2 g aliquot. Dissolution of the soil was accomplished through the use of nitric, hydrochloric, and hydrofluoric acids. Amphoteric elements were removed from the sample by use of a hydroxide precipitation. Anion exchange was used to separate plutonium from other interfering radionuclides. The plutonium was microprecipitated on a 25 mm filter and subsequently counted on surface barrier detectors for ^{238}Pu and $^{239\text{-}240}$Pu. The < 0.45 μm fraction was submitted for analysis as a liquid (approximately 150 ml) concentrate.

The accuracy of the fractionation method was verified by use of a commercial service[e] to independently assess the percentage of sand, silt, and clays of a test soil. Blank and duplicate samples were run for every 20 th plutonium analysis; duplicates were consistently within the propagated uncertainty as reported by the commercial laboratory. Samples split between the commercial facility and inhouse laboratories at CSU were within the 95 % confidence intervals. The results of the americium gamma spectroscopy were compared with ongoing radiochemical analyses from the same location to verify the accuracy of the method (Schierman, 1994).

16

Statistical Analyses

The 3 microplots served as statistical replicates. Examination of the results indicated a significant difference in both radionuclide concentration and total inventory among the three microplots. Previous studies had shown an extremely strong correlation between distance from the 903 pad and microplot inventory (Little, 1976; Webb, 1992). Although inventory differences were found for the three sites, it was assumed that the same physical, biological and chemical processes would be acting on them. Data analyses were limited to simple linear regressions due to the small (n=3) number of replicates within each data set. The microplot data were analyzed both as raw inventory and as microplot-normalized inventory to control for the influence of inventory differences. They were also were evaluated as linear and natural log-transformed values of both inventory and activity concentration. Examination of residuals was used to select the best data transform.

Statistical analysis of the data were performed with the SAS® statistics software package using the general linear models procedure. Dependent variables examined included microplot, sample depth, particle size, and the depth by particle size interaction. Statistical significance was assessed at the 0.05 level.

RESULTS AND DISCUSSION

The activity concentrations and the inventory data were tested as linear and natural log-transformed values using the SAS® univariate procedure to test for normality. The results indicated that the data were most likely lognormally distributed. This observation was consistent with previous assessments of the radionuclide distribution in soils for this site. Consequently, statistical results reported here are for the natural log-transformed data. Results of the statistical analyses are listed in Table 1 and discussed in the following sections.

Mass Distribution

The relative distribution of masses recovered from the sampling plots is given in Fig. 1. The gravel content varied considerably among lifts, from as low as 6% of the lift mass at microplot CX16 at the 9-12 cm depth, to a maximum value of 48% for microplot CX15 in the 3-6 cm lift (Appendix C). The gravel content peaked in the 3-6 cm layer of soil in microplots CX15, CX16 and in the 6-10 cm layer for CX17. Conversely, the combined silt fraction, which totalled approximately 32% of all lift masses in the three microplots, was at a minimum in the 3-6 cm layer (26%) and maximum (41%) in the 9-12 cm layer.

Based on the total content of sand, silt and clay, this soil would be classified as a loam (Miller and Donahue, 1990). This finding is consistent with soil surveys of the area which classify it as a Denver/Kutch clay loam transitioning to Nederland cobbly gravely sandy loam (U.S. DOE, Vol. 2, 1980; USDA, ca. 1980).

Denver/Kutch soils are fine, montmorillonitic, mesic Torrertic Argiustolls, formed in calcareous, clayey material derived from mudstone and shale. The rock fragment content ranges from 0 to 15 %. Typically the surface layer is a grayish brown clay loam about 13 cm thick. Montmorillonite clays have cation exchange capacities that range from 800 to 1200 mmol $(+)^{9}$ kg^{-1} and have a strong affinity for actinides and lanthanides (Bohn et al., 1985). The typical profile of the Nederland cobbly gravelly sandy loam is a grayish brown, cobbly sandy loam surface layer about 10 cm thick. The upper part of the subsoil is brown cobbly sandy loam approximately 15 cm thick.

Activity Concentrations of ^{241}Am

The average activity concentration of ^{241}Am in the three microplots, expressed as a function of depth and particle size, is shown in Fig. 2. This graph illustrates the general distribution in ^{241}Am concentration versus depth and particle size which was observed across all microplots.

The ^{241}Am activity concentrations were log transformed and then statistically tested to determine if there were significant differences in concentration as a function of microplot, particle size, sampling depth, and if there was a particle size by depth interaction. Considerable variation in ^{241}Am activity concentrations existed between microplots, as can be seen from the F^h (9.2) and p values (0.0005) for the variable "microplot" (Table 1). Statistically significant differences in concentrations were observed among the five particle sizes ($p=0.0001$). Similar to results reported elsewhere in the literature, the dissolved (or colloidal) particle size fraction (< 0.45 μm) had the highest activity concentration. There was also a significant decrease in concentration with depth ($p=0.0001$).

Statistical tests on ^{241}Am activity concentrations indicated that differences existed as a function of depth. There also were significant differences among at least one of the particle sizes. Tukey's Studentized Range test was used to determine which particle size was statistically different from the others (Table 2).

Activity concentrations were significantly different across several, but not all particle sizes. For example, the activity concentration of sand was significantly different from all other particle sizes. A similar test on depth showed that with the exception of the 9 - 12 cm lift, adjacent layers were not *statistically* different from each other (i.e., the 0 - 3 cm layer was not statistically different from the 3-6 cm layer; however it was different from the 6 - 9 and the 9 - 12 cm layers). This is not a surprising result, as the sampling intervals are part of a dependent continuum, where the concentration in one layer is expected to be related to that in adjoining layers, as opposed to being independent, discrete entities.

Those data sets that were found to be statistically indistinguishable (e.g., ^{241}Am concentrations in coarse and fine silt) were combined and evaluated again. No significant change was observed in any of the descriptive statistics.

There was an absence of a statistically significant depth by particle size interaction ($p = 0.9642$, Table 1). Its absence indicates that the slopes of the lines describing particle size-specific activity concentrations as a function of depth are statistically indistinguishable across all

particle sizes, even though visual inspection of Fig. 2 might suggest otherwise (i.e., removing the 9-12 cm layer and rerunning the statistical analysis did not change the result). One possible explanation for this common slope is that the separation technique mobilized and redistributed the radionuclides among the sand, silt, and clay fractions of each lift during the soil size separation process. However, if redistribution of ^{241}Am did occur, it should, theoretically, follow the relative affinity (e.g., distribution coefficients or cation exchange capacities) for each particle size. The activity concentration would be based on the mass of each fraction present in a particular lift. One could predict the relative distribution of ^{241}Am for any soil layer based on knowledge of its distribution in any other layer. To test this assumption, the distribution of ^{241}Am in the top soil layer of each microplot was used to predict the distribution in the remaining layers. There was no significant correlation between the predicted and observed distributions. Therefore, remobilization of contaminants during the soil separation process was considered unlikely to have occurred.

Another interpretation of the lack of a particle size by depth interaction is that all particle sizes were moving through the soil at the same rate. This could have occurred in two ways: 1) physical mixing of the soil layers in a manner that did not discriminate based on gross particle size; or, 2) a one-time distribution to depth of contaminants initially distributed to the surface soil, such as might occur by migration along a macropore or soil crack (Shipitalo et al., 1990). Further work will need to be undertaken to assess the potential importance of this phenomenon.

Activity Concentrations of ^{238}Pu $^{239-240}$Pu

Five soil size fractions were analyzed for ^{238}Pu $^{239-240}$Pu content at four depths and at each of the three microplots (Figs. 3 and 4). The gravel fraction was not analyzed for plutonium content, as gamma spectroscopy had yielded very low and extremely variable concentrations of ^{241}Am. The concentrations of the plutonium isotopes differed in magnitude from that of ^{241}Am, but their profiles in soil generally mimicked the americium data. The results

20

of statistical tests on ^{238}Pu and $^{239\text{-}240}Pu$ ln-transformed values, given in Table 1, show the same microplot effect (p=0.0001), depth effect (p = 0.0001), size effect (p = 0.0001), and absence of the depth by size interaction (p = 0.7068, and 0.5798, respectively). As with ^{241}Am, the R^2 values were relatively strong (i.e., larger), indicating a reasonable fit of the data to a simple linear model.

Inventory Distribution

The ^{241}Am, $^{239\text{-}240}Pu$, and ^{238}Pu inventories for each location, sample depth and size fraction were calculated for each size fraction as the product of the recovered soil mass and the activity concentration (Appendix C). No inventory estimate was made for plutonium isotopes in gravel. However, by analogy to the ^{241}Am inventory in gravel, less than 1% of the total plutonium inventory was likely to have been overlooked by the omission of this component.

Distinct inventory differences were observed among the five particle sizes. As discussed in the previous section, the dissolved particle size fraction (< 0.45 μm) had the highest activity concentration for both americium and the plutonium isotopes. However, because of its larger mass, the greatest proportion of the total inventory (approximately 50 %) resided in the coarse silt (10 - 53 μm) fraction. The microplot-averaged contribution to inventory, by particle size and depth, for ^{241}Am, $^{239\text{-}240}Pu$, and ^{238}Pu, are shown, respectively, in Figs. 5 - 7.

The ^{241}Am inventory and the $^{239\text{-}240}Pu$ and ^{238}Pu inventories were normalized on a microplot basis and then ln-transformed. Using the SAS® general linear model (a regression) procedure, the data were found to decrease in inventory with depth (p=0.0001 in all cases); the inventories varied among particle sizes (p=0.0001 in all cases); but the slope of the line that describes the decrease in inventory with depth did not vary significantly for different particle sizes (p = 0.43, 0.99 and 0. 65, respectively). A Tukey's Studentized Range test with a significance level of 0.05 was used to determine which particle sizes were significantly different from each other. These results are shown in Table 3 for americium and indicate that the

21

inventory distributions are significantly different across most particle sizes. This test indicates a greater number of differences between particle sizes than did the test on americium concentrations. Similar results were found for the plutonium isotopes.

Those data sets that were found to be statistically indistinguishable (e.g., ^{241}Am inventories in coarse and fine silt) were combined and rerun. No significant improvement was observed in any of the descriptive statistics. As with the concentration data, there was no statistically significant depth and particle size interactions.

$^{239\text{-}240}Pu$ to ^{241}Am Ratios

The mean value of 7.6 was calculated as the ratio of activity for each radionuclide and size fraction. A comparison of the $^{239\text{-}240}Pu$ to ^{241}Am inventory data[1] is shown in Fig. 8. Statistical analysis of the $^{239\text{-}240}Pu$ to ^{241}Am ratio over all particle sizes indicated a significant particle-size effect ($p = 0.001$); depth and the depth by size interaction were not statistically significant ($p = 0.15$ and 0.17). Application of the Tukey's Studentized Range test indicated that only the dissolved fraction was significantly different from all other particle sizes, with this fraction having a higher $^{239\text{-}240}Pu$ to ^{241}Am ratio. Selection of a less stringent ($p = 0.1$) value did not substantially alter the results, although the coarse silt and sand fractions become marginally significantly different at the $p = 0.1$ significance level.

Inspection of Fig. 8 indicates that americium values are low relative to plutonium in the dissolved fraction. The basis for this difference is uncertain; it may be an artifact of the low number of dissolved sample sets ($n = 12$). Other possible reasons for this difference are: 1) different sources of contaminants (i.e., the americium and plutonium did not originate from the same source); or 2) differences in sorption-desorption kinetics for these elements. Surveys conducted at the RFP (EG&G Energy Measurements, 1990), discount the possibility of a separate source of americium. Quantitative differences in sorption kinetics is more likely: the literature suggests that for certain soil conditions, the distribution coefficients (K_d's) are higher for americium than plutonium (Essington et al., 1981; Nishita et al., 1981; Sheppard, 1985). The

22

difference in distribution may be explained if the americium, being preferentially sorbed to clays, is depleted in the dissolved fraction. An alternative explanation is a relatively higher K_d value for plutonium on the dissolved fraction (Sheppard et al., 1979; Garten, et al., 1987). Further experiments would need to be conducted to determine if the americium was moving independently of the plutonium and whether their K_d values were different for the clay and dissolved fractions.

$^{239-240}Pu$ to ^{238}Pu Ratios

Recent studies have alluded to possible differences in mobility of $^{239-240}Pu$ and ^{238}Pu isotopes (Kercher et al., 1993). However, the $^{239-240}Pu$ to ^{238} Pu activity ratios determined in this study were constant over all depths, particle sizes, and concentrations. These results were consistent with the work of Webb (1992) who noted that for soils with relatively high concentrations of ^{238}Pu and $^{239-240}Pu$ (such as these), the isotopic ratios were relatively constant.

SUMMARY AND CONCLUSIONS

Three replicate sets of soil samples were collected from the Rocky Flats Plant site in an area of known plutonium and americium contamination. Samples were taken to a depth of 12 cm in 3 cm increments and then fractionated into particle size ranges using a wet separation/sedimentation method. Inventory and activity concentrations of both elements decreased exponentially with depth, with the smallest particle size (< 0.45 μm) having the highest concentration. The radionuclide inventory was primarily contained in the silt fraction (10 - 53 μm) which is a reflection of the abundance of this size fraction in a loam soil. Statistical analysis of the plutonium to americium ratios indicated that the dissolved fraction (< 0.45 μm) ratios were significantly higher than the other size fractions. One possible explanation for this difference in sorption-desorption kinetics for these contaminants.

REFERENCES

Bondietti, E. A.; Tamura, T. Physicochemical associations of plutonium and other actinides in soils. In: Transuranic elements in the environment. U. S. Department of Energy, National Technical Information Service; DOE/TIC-22800; 1980:145-164.

Bohn, H. L.; McNeal, B. L.; O'Connor, G.A. Soil chemistry. Second Edition. John Wiley & Sons, Inc. New York. 1985.

Bunzl, K.; Förster, H., Kracke, W.; Schimmack, W. Residence times of fallout $^{239+240}Pu$, ^{238}Pu, ^{241}Am and ^{137}Cs in the upper horizons on an undisturbed grassland soil. J. Environ. Radioactivity 22 (1994) 11-27.

EG & G Energy Measurements. An aerial radiological survey of the United States Department of Energy's Rocky Flats Plant, Golden CO. EGG-10617-1044. May 1990.

Essington, E. H.; Fowler, E. B.; Polzer, W. L. The interactions of low-level, liquid radioactive wastes with soils: 2. Differences in radionuclide distribution among four surface soils. Soil Sci. 132:13-18; 1981.

Garten, C. T., Jr; Bondietti, E. A.; Trabalka, J. R.; Walker, R. L.; Scot, T. G. Field studies on the terrestrial behavior of actinide elements in East Tennessee. In: Environmental research on actinide elements, in proceedings of a symposium held at Hilton Head, South Carolina, November 7-11, 1983. U.S. Department of Energy: CONF-841142; 1987:109-119.

Gee, G. W.; Bauder, J. W. Particle size analysis. In: Methods of soil analysis, Part 1 - Physical and Mineralogical Methods. 2nd Edition. American Society of Agronomy. Number 9 (part 1) in

124

the series Agronomy. American Society of Agronomy, Soil Science Society of America, Inc Pubs. 1986.

Kercher, J. R.; Gallegos, G. M. Possible differences in biological availability of isotopes of plutonium: report of a workshop. UCRL-ID-110051. Lawrence Livermore National Laboratories, 1993.

Krey, P.; Hardy, E. Plutonium in soil around the Rocky Flats. USAEC Report, Health and Safety Laboratory. HASL-235. 1971.

Krey, P.; Hardy, E.; Volchok, H., et al. Plutonium and americium contamination in Rocky Flats Soil - 1973. US ERDA - Health and Safety Laboratory. HASL-304. March 1976.

Little, C.A. Plutonium in a grasslands ecosystem. Ph.D. dissertation. Fort Collins, CO: Colorado State University, 1976.

Miller, R. W.; Donahue, R. L. Soils, and introduction to soils and plant growth. Prentice Hall, Englewood Cliffs, NJ, 1990.

Navratil, J. D.; Baldwin, C. E. Recovery studies for plutonium machining oil coolant, ERDA report RFP-2579, University of Utah. NTIS. 1977.

Nishita, H.; Wallace, A.; Romney, E. M.; Schultz, R. K. Effect of soil type on the extractability of ^{237}Np, ^{239}Pu, ^{241}Am, and ^{244}Cm as a function of pH. Soil Sci. 132:25-34; 1981.

Nishita, H.; Haug, R. M. Some factors that influence the extractability of Pu (IV) from several clay minerals. Soil Sci. 132:35-39; 1981.

125

Puls, R. A.; Powell, R. M.; Clark, D. A.; Paul, C. J. Facilitated transport of Inorganic contaminants in ground water: part II. Colloidal transport. United Stated Environmental Protection Agency. EPA/00/M-91/040, 1991.

Schierman, M. J. Characterization of americium and plutonium concentrations in soil profiles at the Rocky Flats Plant. Master's Thesis. Fort Collins, CO; Colorado State University, 1994.

Sheppard, J. C.; Campbell, M. J.; Kittrick, J. A.; Hardt, T. L. Retention of neptunium, americium, and curium by diffusible soil particles. Environ. Sci. Technol. 13:680-684.

Sheppard, M. I. Radionuclide partitioning coefficients in soils and plants and their correlation. Health Phys. 49:106-111; 1985.

Shipitalo, M. J.; Edwards, W. M.; Dick, W. A.; Owens, L. B. Initial storm effects on macropore transport of surface-applied chemicals in no-till soil. Soil Sci. Soc. Am. J. 54:1530-1536; 1990.

Tamura, T. Effect of pretreatment on the size distribution of plutonium in surface soil from Rocky Flats, pp 173- 186, In: Transuranics in Desert Ecosystems, Nevada Applied Ecology Group, November 1977. NVO-1871 UC-11.

U.S. Department of Agriculture, Soil Conservation Service. Soil survey of Golden area, Colorado, parts of Denver, Douglas, Jefferson, and Park counties. Undated, ca 1980.

U.S. Department of Energy. Final environmental impact statement (final statement to ERDA 1545-D): Rocky Flats Plant Site; Golden, Jefferson County, colorado. Washington, D.C.: National Technical Information Service; DOE/EIS-0064 (3 vol); 1980.

Table 2. Results of Tukey's Studentized Range test for minimum significant difference ($p=0.05$) between mean ln-activity concentrations of ^{241}Am. The table represents a pairwise comparison to determine the significant differences between particle sizes. Those comparisons which were significant at $p=0.05$ are underlined.

Sand (S)	S-S				
Coarse Silt (CS)	S-CS	CS-CS			
Fine Silt (FS)	S-FS	CS-FS	FS-FS		
Clay (CL)	S-CL	CS-CL	FS-CL	CL-CL	
Dissolved (D)	S-D	CS-D	FS-D	CL-D	D-D
	Sand (S)	Coarse Silt (CS)	Fine Silt (FS)	Clay (CL)	Dissolved (D)

Table 3. Results of Tukey's Studentized Range test for minimum significant difference ($p=0.05$) between the ln-transformed, normalized ^{241}Am inventory. The table represents a pair wise comparison to determine the significant differences between particle sizes. Those comparisons which were significant at $p=0.05$ are underlined.

Sand (S)	S-S				
Coarse Silt (CS)	S-CS	CS-CS			
Fine Silt (FS)	S-FS	CS-FS	FS-FS		
Clay (CL)	S-CL	CS-CL	FS-CL	CL-CL	
Dissolved (D)	S-D	CS-D	FS-D	CL-D	D-D
	Sand (S)	Coarse Silt (CS)	Fine Silt (FS)	Clay (CL)	Dissolved (D)

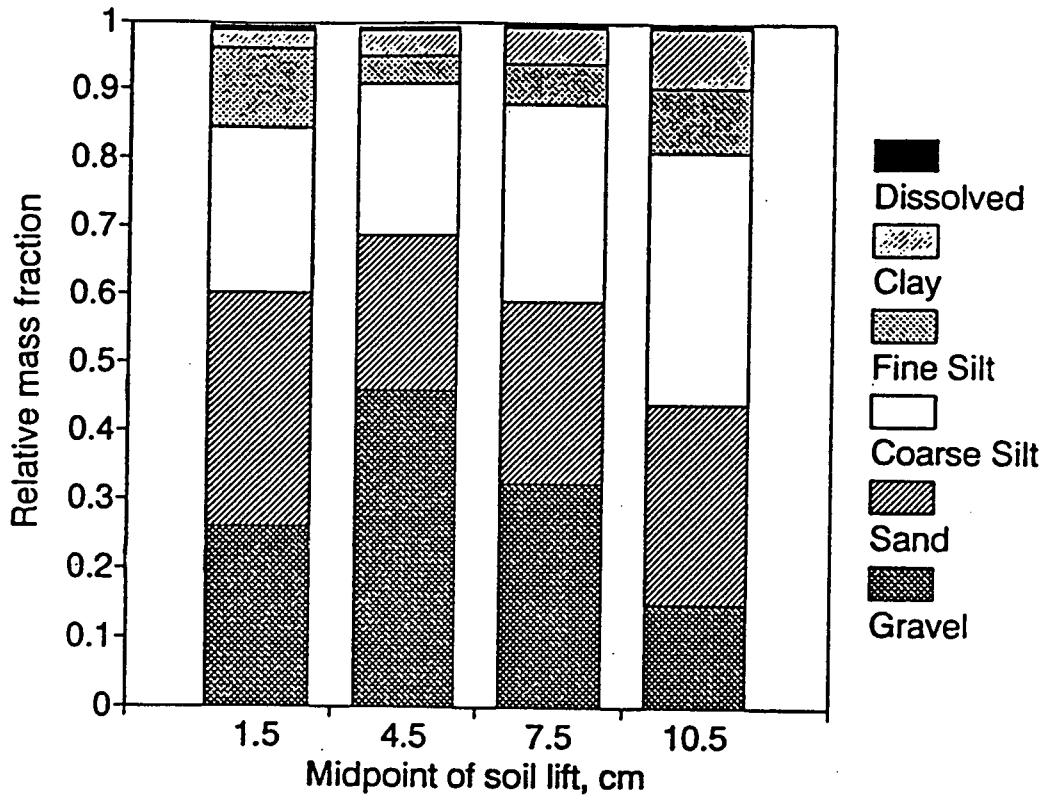

Fig. 1. The contribution to lift mass by particle size and depth, from the mean of three microplots sampled at the RFP site. The mass of each lift is approximately 1100 g.

28

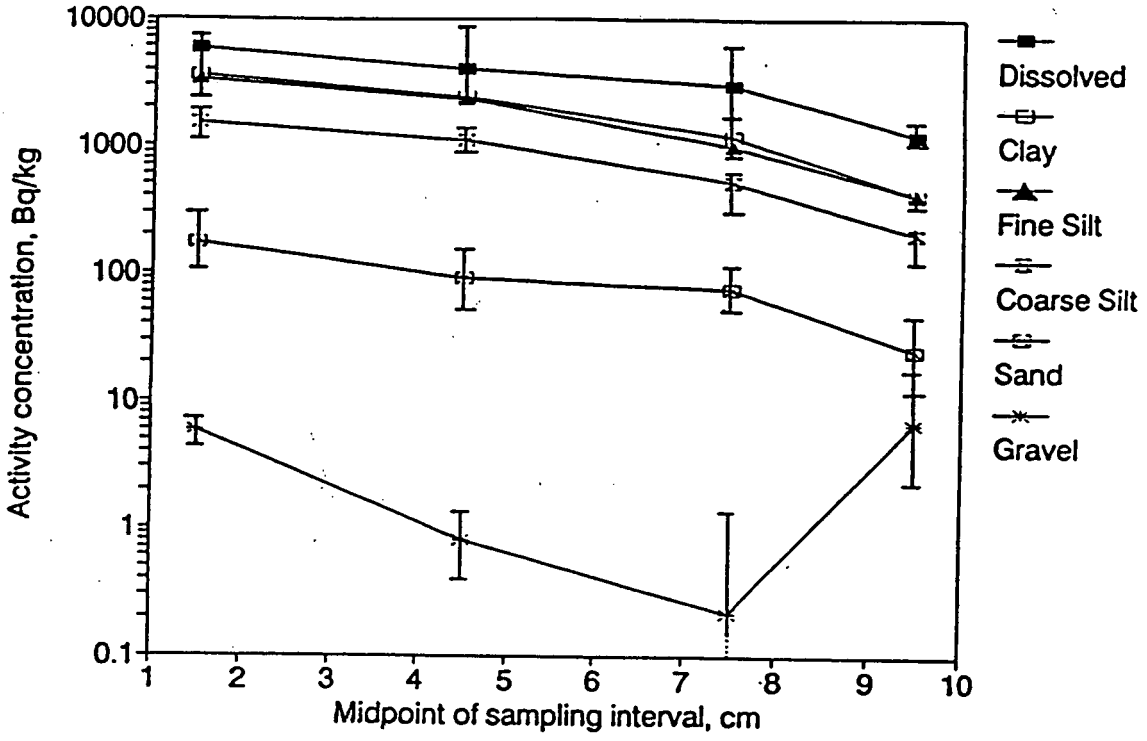

Fig. 2. Distribution of ^{241}Am activity concentrations as a function of particle size and depth, from the means of three microplots sampled at the RFP site. Error bars represent ± 1 standard error of the geometric mean (n = 3 per data point).

29

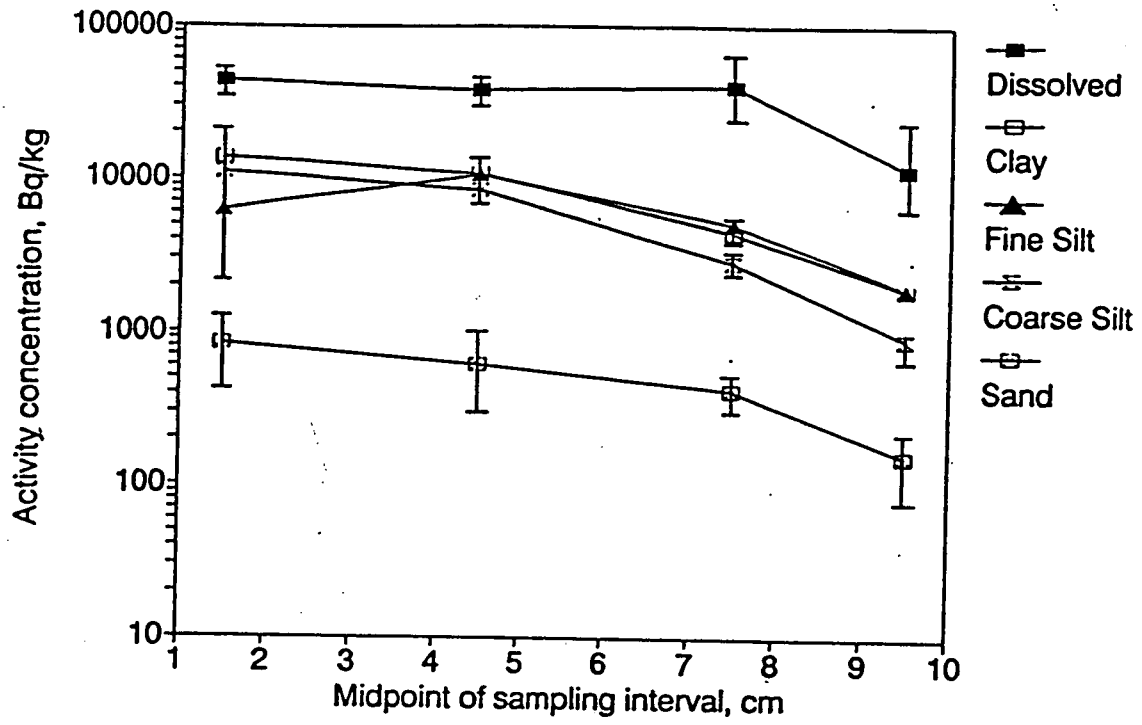

Fig. 3. Distribution of $^{239-240}Pu$ activity concentrations as a function of particle size and depth from the means of three microplots sampled at the RFP site. Error bars represent ± 1 standard error of the geometric mean (n = 3 per data point).

130

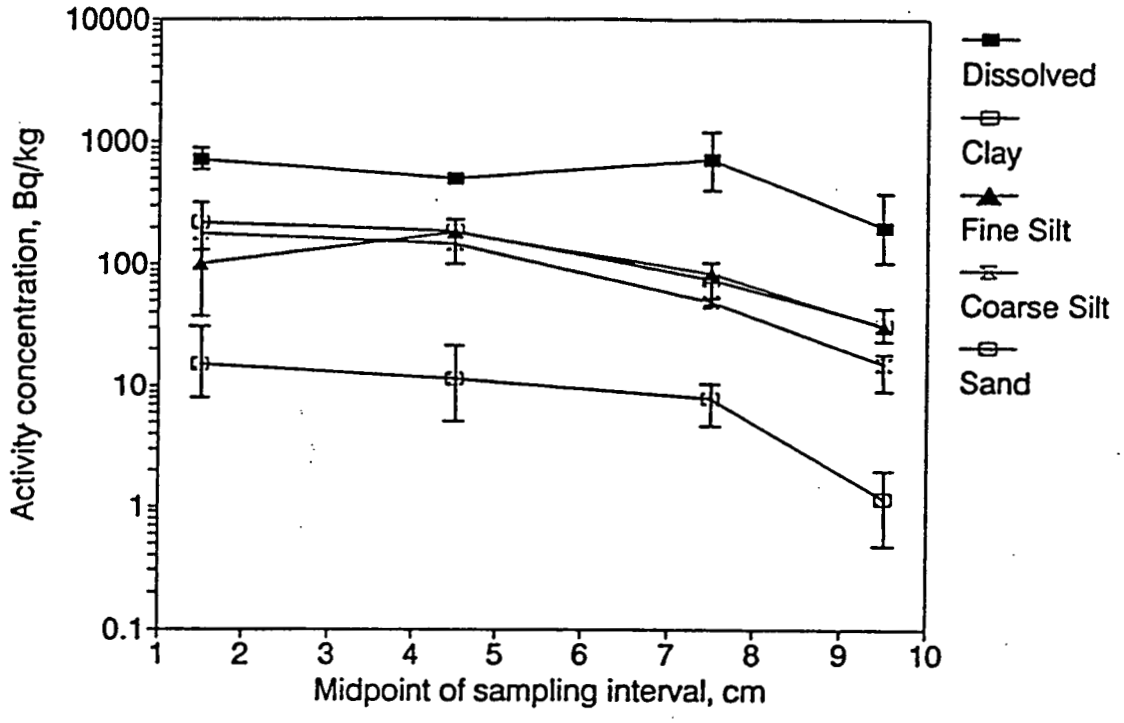

Fig. 4. Distribution of ^{238}Pu activity concentrations as a function of particle size and depth from the means of three microplots sampled at the RFP site. Error bars represent ± 1 standard error of the geometric mean (n = 3 per data point).

31

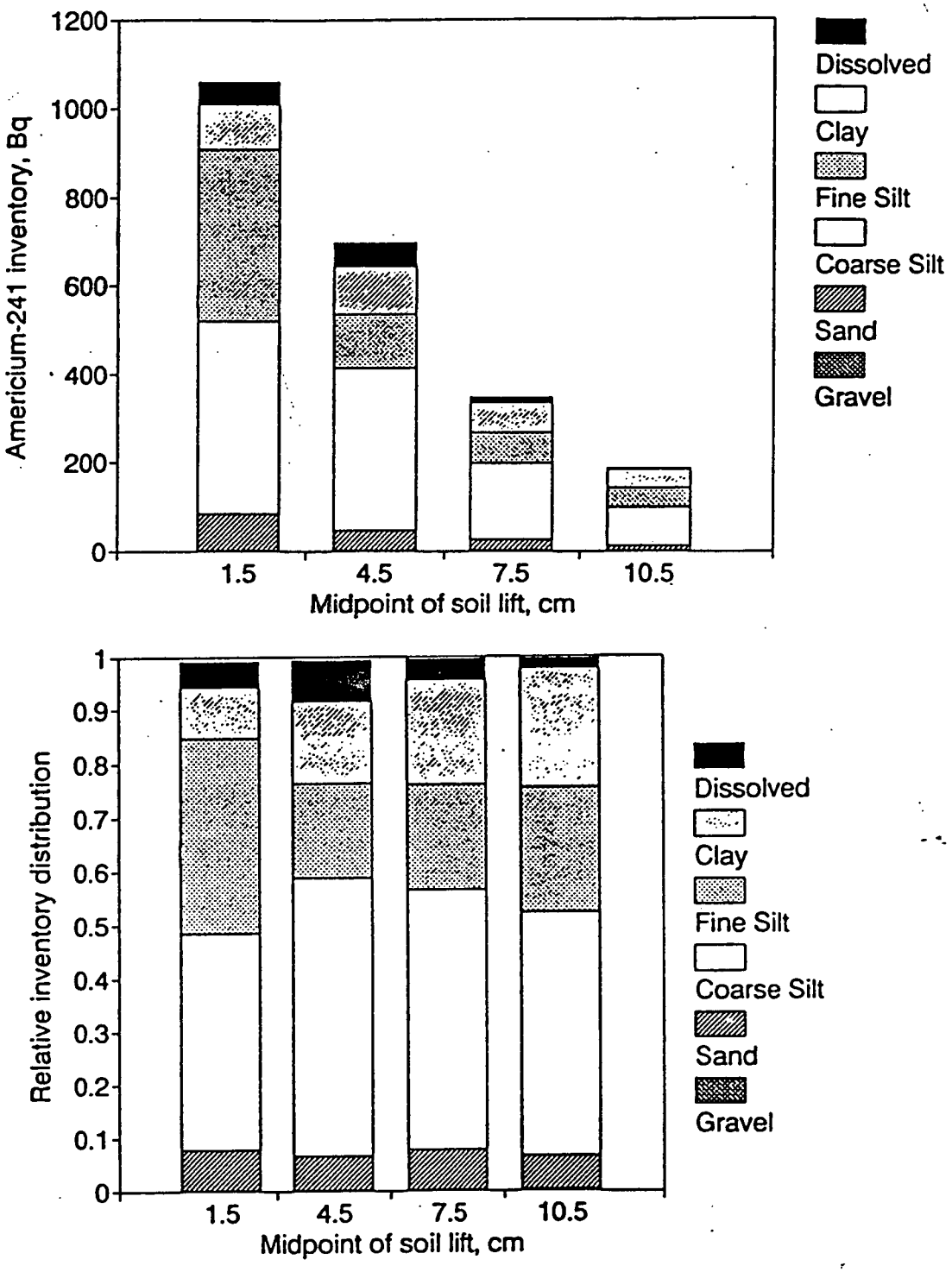

Fig.5. Top: ^{241}Am inventory by particle size and depth, from the means of three microplots sampled at the RFP site. Bottom: the relative inventory distribution by lift and particle size.

32

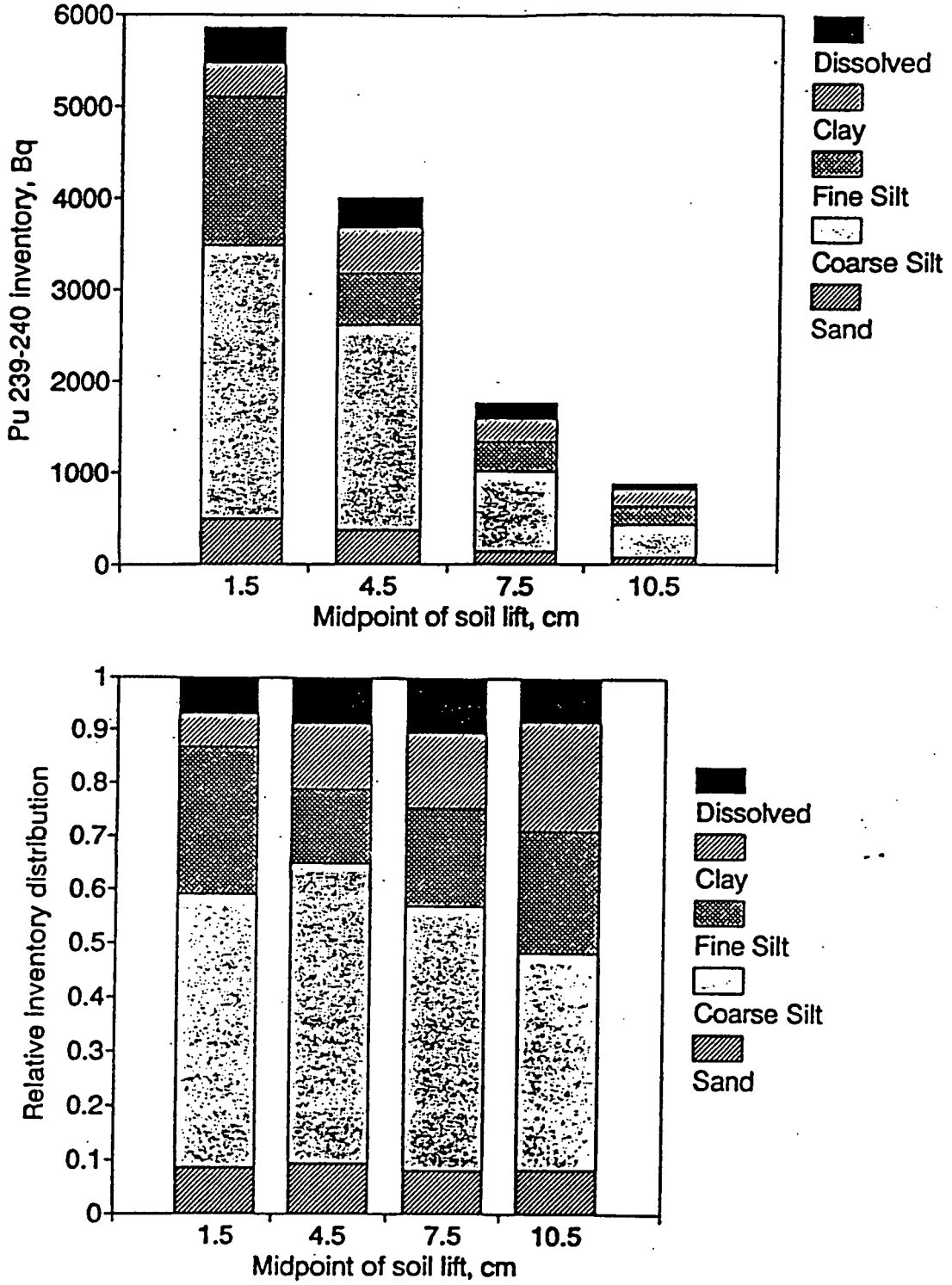

Fig.6. Top: $^{239-240}Pu$ inventory by particle size and depth, from the mean of three microplots sampled at the RFP site. Bottom: the relative distribution of inventory by lift and particle size.

33

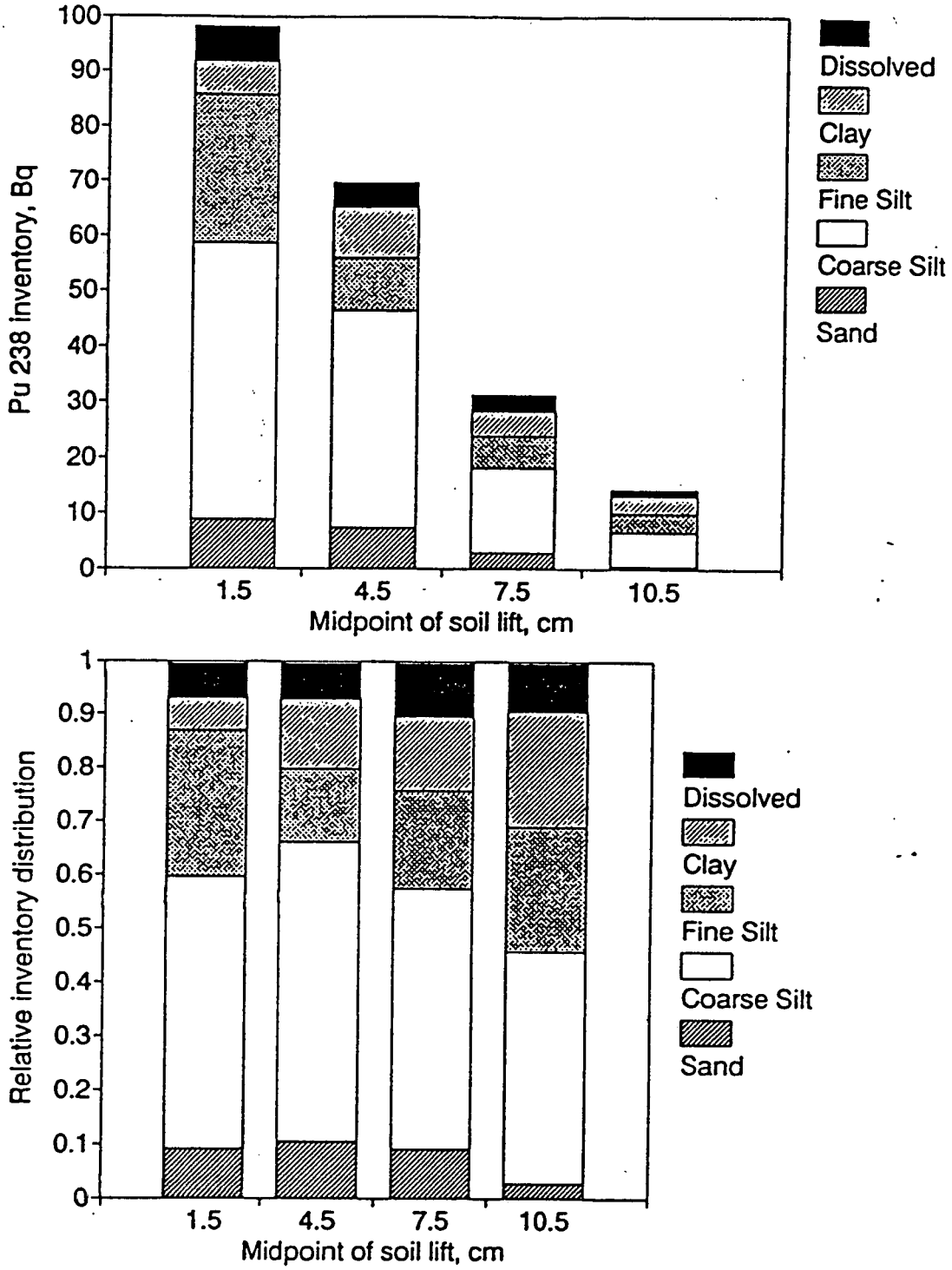

Fig.7. Top: ^{238}Pu inventory by particle size and depth, from the mean of three microplots sampled at the RFP site. Bottom: the relative distribution of inventory by lift and particle size.

34

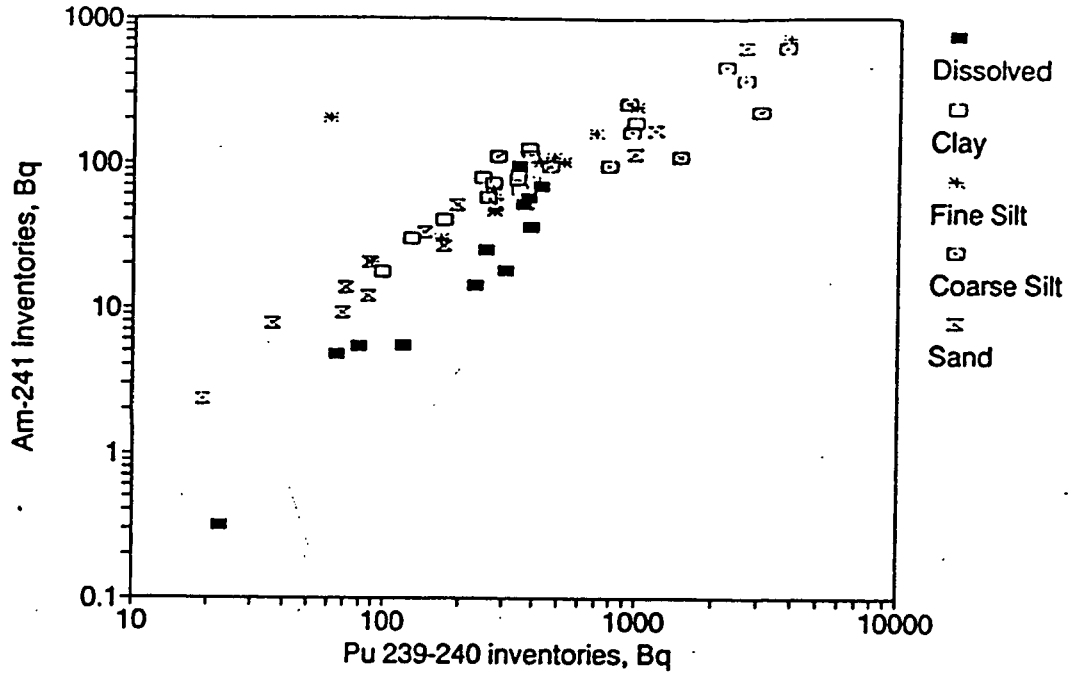

Fig. 8. A comparison of $^{239-240}Pu$ to ^{241}Am inventory values over all microplots and particle sizes.

35

ENDNOTES

a. Personal communication, L. Fraley, Department of Radiological Health Sciences, Colorado State University, Fort Collins, CO.

b. The term "dissolved" has historically been used to differentiate between that fraction of a sample that can pass through a 0.45 μm filter and larger, particulate phases in water samples (Puls et al., 1991).

c. ORTEC coaxial GeLi, 56.14 mm diameter x 66.8 mm length with a drift depth of 23 mm and 30.25 % measured efficiency relative to a 3 x 3 NaI at 1.333 MeV. ORTEC Incorporated, Midland Road, Oak Ridge, TN.

d. Analytical Technologies, Inc. Fort Collins, CO.

e. Soils Testing Laboratory, Colorado State University, Fort Collins, CO.

f. SAS is a registered trademark of SAS Institute, Inc., Cary, NC.

g. Cation exchange capacities are expressed in terms amount of positive charge, written as "mmol (+)" or "$mmol_c$" per kg of soil, clay, or organic colloid.

h. The F test is a test of the null hypothesis. Large values of F provide evidence for not accepting the null hypothesis.

i. The same comparison could be made between concentration data, as the plutonium and americium inventories were the result of multiplication of the same mass values with the plutonium and americium concentrations.

MOVEMENT OF ^{234}TH-LABELED SOIL PARTICLES THROUGH A HOMOGENOUS SOIL MEDIUM

BACKGROUND

Reinvestigation of the spatial distribution of plutonium in soils at the U.S. Department of Energy's Rocky Flats Plant (RFP) was recently conducted by the Radioecology Group at Colorado State University (Webb, 1992; Schierman, 1994). That effort raised the question as to how plutonium contamination, deposited on an undisturbed grassland, could move to depth within a few years and then remain apparently immobile for the next twenty (Higley, 1993). In an initial attempt to determine what factors might account for this phenomenon, three mechanisms of physical transport of particles in soil were investigated. Included in this chapter are a description and qualitative assessment of the significance of contaminant transport into soils by water migration, frost heaving, and soil cracking.

Soil Structure

Soil consists of a combination of physical particles (sands, silts, clays, etc.) cemented together by inorganic and organic constituents such as carbonates, oxides, and humic materials (Miller and Donahue, 1990; Jury et al., 1991). The result of irregular cementation (and other, biotic, factors) is many air-filled passages of varying diameters and lengths that serve to decrease the average density of soil from its mineral density of 2.65 g cm^{-3} to a typical bulk density of 1.2 g cm^{-3} (Miller and Donahue, 1990; Mermut, 1992; Horn et al., 1994). Because of particle rearrangement during wetting and drying cycles, bulk density is not static. It can

change in soils with time: initially increasing in new soils as aggregation occurs, and later decreasing as voids are developed in the soil (Horn, 1994).

Soils that contain more than 15 % clay (particle size < 2 μm) tend to form structured units known as aggregates or "peds" (Horn et al., 1994). Structure is created in unconsolidated soils during shrinking and swelling (when the soil is dried and wetted) and biological processes, such as earthworm activity and root penetration (Lee, 1985). The aggregates can vary greatly in size and shape, from a few mm to 100 mm or more for prisms and columnar structures (Horn et al., 1994).

The intra pedal area consists of unconsolidated particles and voids (pores). There are three distinct pore groups in undisturbed soils: 1) small circular voids (the most frequent); 2) irregular pores (called vughs) and cylindrical channels which are formed by root activity; and, 3) cracks (planar voids between peds with widths > 2 mm) formed by swell-shrink processes of the soil (Mermut, 1992). The size and distribution of these pore spaces are consequences of the soil type, i.e., sandy soils have large and continuous pores, whereas clay soils have more total pore space, but have smaller pore diameters (Miller and Donahue, 1990) within aggregates. Clay soils may contain planar voids, which although relatively few in number, often contribute substantially to total porosity (Mermut, 1992).

Water Migration

Soil pore spaces provide conduits for water, gas, and dissolved mineral transport (Jury, 1991). It has been observed that particles with diameters greater than 1 μm can move faster than the average ground-water flow velocity in porous media. This is attributed to effects such as size exclusion from smaller pore spaces (Horton, 1988; Puls et al., 1992).

Pore spaces can also be a route for the rapid migration of contaminants into soil (Bouma and Dekker, 1978; Bouma and Wösten, 1979; Shipitalo et al.; 1990; Booltink and Bouma, 1991; Horn et al., 1994). Soils with pronounced structure and large continuous macropores are subject to a phenomenon known as "bypass" flow (Booltink and Bouma, 1991).

38

Bypass flow results in rapid vertical movement of water along the macropores in unsaturated clays, with only limited movement of water into the soil adjacent to the pore (Booltink and Bouma, 1991).

Shrink Swell Processes

Soils can swell when wet and shrink when dried; the higher the clay content the greater the potential for heaving, cracking, subsidence, and void formation (Mermut, 1992; Tariq and Durford, 1993). Soils with certain types of expanding clay minerals, such as the montmorillonite found in some soils surrounding the RFP, have a particularly high shrink-swell potential (Miller and Donahue, 1980; U.S.DOE, 1980; USDA, ca 1980; Bohn, 1985).

Crack and void formation is not a completely random process that occurs during drying; the aggregated soil mass between cracks tends to remain cohesive, bound by inorganic and organic agents. In some instances the aggregates are coated with a cemented clay layer while the larger particles are contained on the inside (Horn et al.; 1994). Soils tend to crack repeatedly along the same weak planes, rehealing themselves following wetting, only to recrack again along the same lines (Bouma and Dekker, 1978; Miller and Donahue, 1990; Horn et al., 1994). Cracks may penetrate 0.5 m or more into soil (Bouma and Dekker, 1978; Bouma and Wösten, 1979; van Lanen et al., 1992; Wopereis et al., 1994).

In many soils the major functional macropores are cracks and planes between peds (Logsdon et al 1992). Because of the potential for rapid movement of rainwater into such voids, cracking is considered a potential mechanism for rapidly moving contaminants from the surface deeper into the soil (Bouma and Dekker, 1978; Booltink and Bouma, 1991; Shipitalo, 1990).

Frost Heaving

Soils that are frozen undergo expansion due to the presence of water in the pores (Pietrzyk, 1982; Blanchard et al., 1985). The extent of expansion is a function of both the water

content and soil type (Baker, 1975; Pietrzyk, 1982; Blanchard, 1985). Clay-type soils are considered some of the most expansive; the rapid freezing of clay soils that are near field capacity can result in expansion by 10% or more (Pietrzyk, 1982; Saetersdal, 1992) with crystallization of water in the soil causing "frost heaving" or upheaval of the surface particles. During freezing an ice lens forms behind the freezing front and forces migration of mineral particles out of the zone (Loch, 1982). The specific mechanisms of frost heaving and ice lens formation are beyond the scope of this paper (see Anderson and Williams, 1985, for a number of articles on this subject). However, because of the volumetric change inherent during freezing it may provide a mechanism for moving surface contaminants into soils.

Research Objectives

Contaminants deposited on surface soils can attach to soil particles, be chelated by organic and inorganic ligands in soils, or remain unattached and move with, or even faster than, water in soil (Horton, 1988; Puls 1991). Migration of monomeric, soluble contaminants through soil pores in saturated and unsaturated systems has been the subject of much study (Boast, 1973; Kurtz, 1973; Horton, 1988; Puls, 1991; Ela, 1992; Mermut 1992) and is not investigated here. In this study the potential for migration of contaminants that are strongly attached to soil particles was examined.

Previous work on the distribution of plutonium in the ecosystems of the RFP indicated > 99 % of the contaminants were attached to soil particles (Little, 1973; Tamura, 1977; Langer, 1986). This behavior is consistent with general knowledge of both plutonium and americium in environmental systems (Bondietti, 1980; Watters et al., 1980) and the soil type of the RFP which is classified as a Denver Kutch clay loam with montmorillonitic clay. As a first step in elucidating transport processes for these contaminants, physical mechanisms of movement were investigated. Limiting the number of experimental variables dictated the order of experimentation to assessing: 1) the potential for particle movement through a constant density, homogeneous, structureless soil system; 2) movement via crack formation in the same system;

and, 3) movement due to frost heaving and thawing. This was accomplished by investigating the movement of ^{234}Th-labeled soil particles of specific size ranges into soil columns.

METHODS AND MATERIALS

This work consisted of four phases: 1) collection, characterization, and preparation of soil for use in columns; 2) particle size separation and radiotracer labeling; 3) conduct of the water migration experiment; and 4) conduct of the freezing and cracking experiment.

Soil Sampling

Approximately 100 kg of a clay loam/sandy clay loam soil was collected from private property adjacent to the western perimeter of the RFP site. To facilitate flow in the column experiments a clay loam/sandy clay loam, instead of a clay soil was used. The collected soil was passed through a 2 mm sieve to remove rocks and vegetation fragments and dried for 24 h at 105 °C. Chemical and physical characteristics were established through independent laboratory analysis[a,b] (Table 1).

Preparation of Carrier-Free ^{234}Th and Soil Labeling

Soil in graded particle size ranges was labeled with ^{234}Th. Radiotracers are useful because they potentially allow easy detection of the extent of migration of soil particles. Key concerns in the choice of the radiotracer are that: 1) it binds strongly and does not desorb appreciably; and 2) it is easily detectable with minimal sample preparation. Thorium-234 was chosen as the tracer. It is a gamma emitter with a physical half-life of 24.10 d and emits a 63.3 keV photon (ICRP, 1983). The ^{234}Th was obtained from a natural uranium "cow". Approximately 500 g uranyl nitrate was loaded onto a DOWEX® 1x4 200 mesh chloride form anion exchange resin using the method of Sill and Willis (1964) and Berman et al. (1960).

M1

Thorium was eluted from the column as $ThCl_4$, and then neutralized by evaporation and redilution.

Five particle sizes were labeled with thorium. Particle size separation was achieved through a wet sieving/sedimentation/filtration method (Gee and Bauder, 1986). The particle size ranges used in the experiment were: 1) sand (50 - 250 μm); 2) coarse silt (10 - 50 μm); 3) fine silt (2 - 10 μm); 4) clay (0.45 - 2 μm); and, 5) "dissolved"[ed] (< 0.45 μm).

The ^{234}Th tracer was applied as a slightly acidic (pH 5.5) solution to the soil fractions and muffled (with the exception of the clay and dissolved fraction) for 24 h at 500 °C to convert the thorium to an oxide and provide a permanent bond to the soil. The clay and dissolved fractions were not muffled because of concerns for destroying the clay lattice at the elevated temperatures required for formation of the oxide. Instead, the clay and dissolved fractions were equilibrated with the thorium solution for 24 h. The clay was filtered onto a 0.45 μm membrane filter and sequentially rinsed with deionized water. The rinse water was counted for residual activity; rinsing was complete when no detectable activity could be found in a 20 ml sample in a 30-minute count. Because of thorium's position in the lyotropic series[e], it was assumed that it would largely remain bonded to this montmorillonitic clay fraction. Flow through leaching tests performed on the clay fraction supported this assumption.

Column Packing

Columns were constructed from polyvinyl chloride (schedule 40 PVC) pipe. The columns were 30 cm long by 5 cm i.d. The bottoms of the columns contained a mesh nylon screen which was covered with a PVC end cap that contained a tygon tubing drain. Soils were dried for 24 h at 105 °C, weighed, rewetted to 8% moisture content, and then packed into the PVC columns using the method described by Klute (1986) to achieve a constant density of 1.1 g cm^{-3}.

42

Water Migration

A 4-L water reservoir, constructed of PVC pipe (50 cm long by 10 cm in diameter), was attached to the top of each soil column. The soil columns were saturated and conditioned to a constant flow rate by the addition of water with 0.01 M $CaCl_2$ which was used to prevent loss of ions and resultant swelling and clogging of the pores[f]. A constant head system was designed to keep the water reservoirs full and provide continuous feed to the columns. Small variations in flow rates through the columns were regulated with screw clamps placed on the tygon drain lines.

Immediately prior to application of the ^{234}Th-labeled particles, the columns were drained to field capacity. The radiotracer-labeled particles were applied to the soil column surface either as a dry powder or suspension. Five g of clean sand was placed on top of the labelled material, a 10 μm filter placed over the clean sand, and 5 g of additional clean sand placed on top of the filter. Water was then carefully reapplied to the system. Each column received one specific particle-size fraction.

Three volumes of water, equivalent to 0[g], 3 and 130 y of precipitation at 38 cm y^{-1}[h], were passed continuously through the saturated soil columns. Four columns (replicates) of each particle size and water volume were analyzed at a time. The soil column was dismantled and the soil extruded and sectioned into 7 mm layers. Each layer was placed in a tared 20 ml glass vial; dried for 24 h at 105 °C, weighed, and gamma counted using a sodium iodide detector[i] with an integral multichannel analyzer; the approximate band of 50 -70 keV was used for peak analysis. Vials containing unspiked soils were used to determine the sample background count rates. Soil samples were counted 600 to 1800 s each.

The activity concentration in each core was normalized to itself to eliminate the effect of variations in the initial spike activity and to compensate for radioactive decay between sampling intervals. Statistical analysis was performed using the SAS[@][j] software and significance was assessed at the $p = 0.05$ level. Data were evaluated with the general linear model procedure using untransformed and ln-transformed values. Examination of residuals from the linear model

was used to select the ln-transformed data in each case for reporting the results of the statistical test.

Frost Heaving and Soil Cracking

The purpose of this experiment was to determine if freezing and thawing of soil was a possible mechanism for movement of contaminants through soil. It was coupled with a drying and cracking study, and designed such that the cracking component might be separated from the frost-heaving component during data analysis.

Twenty soil columns were packed and placed, 10 each, into two soil-filled insulated plastic tubs. At the center of each tub was an instrumented soil column with thermocouple wires placed every 5 cm along its length. The thermocouple wires were connected to a data logger that recorded soil temperature readings every 15 minutes. The purpose of the data logger was to monitor the extent and duration of the migration of the freezing front through the soil. Results for the first 3 thermocouples located at depths of 0, 5, and 10 cm are illustrated in Fig. 1 for one freeze thaw cycle (which lasted about 7 days). Typically the freezing front penetrated through the first 5 cm. Frost heaving and shrinkage during drying of soils was measured prior to application of the thorium spike. Initial soil heaving produced up to a 5 % increase in soil height relative to soils at field capacity; drying resulted in a 3 % decrease in height (Appendix C). Overall compaction of the soil was observed during the experiment; this was attributed to an aggregation forming process occurring in the homogenized soil cores (Horn et al., 1994).

Each soil column was brought to field capacity and spiked with 1 ml of a ^{234}Th-labeled clay suspension. The soils were taken through a series of freeze/thaw/heat/crack/rewet cycles using a combination of liquid nitrogen; heat lamps; and a misting hose; typically each complete cycle lasted one week. Four columns were removed at intervals of 0, 1, 4, 5, and 6 freeze thaw cycles, extruded and sectioned into 5 mm slices. The center of each slice was separated

from of the outer segment and both counted to determine the extent of migration of the ^{234}Th tracer.

RESULTS AND DISCUSSION

The normalized inventory data were tested as natural logarithm (ln) transformed and untransformed values. Examination of the residuals for increasing variance, cyclical behavior, and non-random distribution indicated that the data were most likely ln normally distributed. Statistical results, listed in Tables 2 and 3, are reported for ln-transformed data.

Water Migration

The column-normalized data were tested against labeled particle size, depth, and water volume to determine if there was a difference in migration of size fractions into the column as function of water volume. Water volume was not a statistically significant factor ($p = 0.17$) but depth ($p = 0.0001$) and soil particle size ($p = 0.0001$) were (Table 2). Differences between particle sizes were assessed using Tukey's Studentized Range test (Table 4). Only the fine silt fraction (2 - 10 μm) was significantly different from the other labeled soil particle fractions. It penetrated slightly further into the soil at each of the three water volumes relative to the other size fractions. At the time of initial application, the fine silt fraction migrated further into the soil. Its position relative to the other size fractions remained unchanged through the remainder of the experiment. The reason for this difference is unclear, as all soils were treated in the same manner. Results of the experiment that simulated 130 y of precipitation (Fig. 2), are typical of the other treatments. Based on these results, it was concluded that water migration through a saturated, homogenous, constant density soil medium is not likely to be a significant mechanism in the movement of soil particles to depth.

Frost Heaving and Soil Cracking

As much as a 5 % percent increase in volume was observed in the cores during freezing and a 3 % decrease during the drying portion of cycle. Repeated cycling of the initially homogeneous material resulted in an overall decline in volume. This is consistent with the observations of Horton (1988) who reported that unconsolidated soils may increase in bulk density after repeated shrink-swell events.

Columns were observed during each cycle. Cracking was observed in some instances over the entire core surface, but the cracks did not appear to penetrate the center of the core surface. It was more of a "flaking" type phenomenon, with individual flakes less than 1 - 2 mm thick, but covering 25 mm^2 area or more. However, as the soil dried it pulled away from the sides of the PVC, forming a large void, or artificial macropore, on the order of a few mm wide. After rewetting the soil to field capacity with a misting hose, these voids would disappear and the soil would once again be bonded to the side of the PVC.

Following a drying event, the soils were wetted to field capacity, extruded, sectioned into 5 mm thick slices, and the center segment (38 mm diameter) removed from the 9 mm outer ring. This particular approach was taken because the results of the water migration experiment determined that water movement alone was not sufficient to cause significant migration of particles. It was assumed that the outer sides of the core sections might be affected by the movement of labeled soil particles down along the voids at the sides of the PVC containers due to shrinkage of the soils. Conversely, the center segment was assumed to reveal information on the extent of movement that occurred primarily due to shrink/swell processes since deep cracks were not observed in the centers of the core sections.

The ln-transformed column-normalized inventory data were tested against the number of freeze/thaw/drying/wetting cycles (i.e., 0 to 6 cycles), segment depth, and cycle by depth to determine if there was a difference in the extent of soil particle migration into the column as a function of the number of cycles. The data were evaluated as inner, outer and combined core

segments (i.e., the summation of the inventory distributed in the inner and outer core segments equaled that in the combined core).

Statistical analyses of the ^{234}Th inventory present in the soil cores showed significant differences ($p = 0.0001$) between cycles, irrespective of how the core segments were partitioned or grouped (Table 3). Visual inspection of the combined core data (Fig. 3) indicated downward migration was occurring as the number of cycles increased. A similar result was observed for the separate inner and outer segments (Fig. 4), although the difference between the 0 and 6 cycle data was much more pronounced for the outer than the inner segments. Differences between cycles were assessed using Tukey's Studentized Range test; results for the outer core segments are shown in Table 5. Similar results were obtained for the inner and combined core data.

A significant difference in the ln transformed inventory versus depth was observed for all core segments ($p = 0.0001$), irrespective of cycle number, which was expected. The statistical significance of the cycle by depth interactions for the outer, inner and combined core segments were $p = 0.0001$, 0.02 and 0.0001, respectively. These results indicate that the slopes of the lines describing activity concentration as a function of depth and cycle are different. If mixing or migration had occurred in these cores, it was expected that concentration gradients would change over time. For example, a simple one dimensional diffusion equation of the form (Kocher, 1991):

$$C = \frac{1}{\sqrt{\pi D t}} e^{\frac{-z^2}{4Dt}}$$

describes concentration in one direction as a function of time (where C is concentration; D is the diffusion coefficient; z is depth; and t is time). Application of this equation to a variety of times results in the generation of a series of curves whose concentration gradients are not identical to those in Fig. 3 and 4, but exhibit qualitatively similar behavior (Fig. 5). The cores exhibit a steep decline in concentration with depth for no freeze thaw cycles, with a gradual

leveling off (approaching zero slope) as the number of cycles increase. The data indicate the inventory is being distributed to depth, that vertical mixing is occurring in the cores. Inspection of the combined segment data indicate an increase in activity in the 5 - 10, 10 - 15, and 15 - 20 mm depths as a function of number of cycles (Fig. 6). This suggests that migration from the surface into the core is occurring.

The combined core data were also evaluated using the minimum curvature (Briggs, 1974) contour plotting package in Surfer® to create contour plots for 0 and 6 cycles (Fig. 7). These contours were created using the normalized core values, expressed as percentages of column inventory. The 0 cycle data indicate the depth to which the spike initially penetrated at the time of application. The contours for this cycle were closely spaced, indicating the bulk of inventory was on the core surface, near its midpoint. After six cycles, the contours were more widely spaced, indicating the inventory had moved deeper into the core.

The contours in Fig. 7 suggest that some migration along the sides of the columns may also have occurred (note the shape and position of the 1 and 6 % contours). This is also supported by the results presented in Fig. 4. The inner core segments exhibit a sharp inventory decrease at the surface layer, but show only a modest change in deeper layers. Conversely, the outer core segments exhibit a modest change in inventory at the surface layer, but exhibit a dramatic change in distribution deeper in the column. This suggests a significant portion of the inventory in the outer segment has migrated down the container sides, whereas limited migration (due to shrink swell processes) has occurred in the inner core segments.

CONCLUSIONS

The movement of water was not a significant mechanism in the movement of insoluble ^{234}Th-labeled soil particles through a homogenous, saturated soil system. Volume changes of soil resulting from frost heaving and drying may provide a mechanism for limited mixing of contaminants into soil. Repeated experiments will need to be conducted to better assess the

long term impact of extended expansion and contraction cycles in contaminant transport. The cracking of soils during drying appears to provide a more effective route for migration of contaminants through bypass flow in soil. Statistically significant migration of contaminants was observed after only 6 cycles. As a consequence of this work, bypass flow should be further investigated as one possible mechanism responsible for the rapid migration of plutonium and americium to depth in the soils of the RFP.

REFERENCES

Anderson D. M. and Williams, P. J., ed. Freezing and thawing of soil-water systems. Technical Council on Cold Regions Monograph. American Society of Civil Engineers, ISBN 0-87262-506-0 1985.

Baker, T. H. W. Transportation, preparation, and storage of frozen soil samples for laboratory testing. In: Soil specimen preparation for laboratory testing. A symposium presented at the Seventy-eighth annual meeting of the american society for testing and materials. Montreal, Canada, 22-27 June 1975.

Berman, S.S.; McKinley, L.; Bednas M. E. The separation of carrier-free ^{234}Thorium (UX_1) from uranium by anion-exchange. Talanta 4:153-157; 1960.

Boast, C. W. Modeling the movement of chemicals in soils by water. Soil Sci. 115:224-230; 1973.

Blanchard, D.; Dupas, A.; Fremond, M.; Levy, M. Soil freezing and thawing. Modeling and application. In: Freezing and thawing of soil-water systems. Technical Council on Cold Regions Monograph. American Society of Civil Engineers, ISBN 0-87262-506-0 1985:10-17.

Bohn, H. L; McNeal, B. L; O'Connor, G. A. Soil chemistry. Second Edition. John Wiley & Sons, Inc. New York. 1985.

Bondietti, E. A.; Tamura, T. Physicochemical associations of plutonium and other actinides in soils. In: Transuranic elements in the environment. U. S. Department of Energy, National Technical Information Service; DOE/TIC-22800; 145-164:1980.

Booltink, H. W. G.; Bouma, J. Physical and morphological characterization of bypass flow in a well-structured clay soil. Soil Sci. Soc. Am. J. 55:1249-1254; 1991.

Bouma, J.; Dekker, L. W. A case study on infiltration into dry clay soil. I. Morphological characteristics. Geoderma 20:27-40; 1978.

Bouma, J.; Wösten J. H. M. Flow patterns during extended saturated flow in two, undisturbed swelling clay soils with different macrostructures. Soil Sci. Soc. Am. J. 43:16-22; 1979.

Briggs, I. C. Machine contouring using minimum curvature. Geophysics. 39:39-47;1974.

Ela, S. D.; Gupta, S. C.; Rawls, W. J. Macropore and surface seal interactions affecting water infiltration into soil. Soil Sci. Soc. Am. J. 56:714-721; 1992.

Gee, G. W.; Bauder, J. W. Particle size analysis. In: Methods of soil analysis, Part 1 - Physical and Mineralogical Methods. 2nd Edition. American Society of Agronomy. Number 9 (part 1) in the series Agronomy. 1986. American Society of Agronomy, Soil Science Society of America, Inc Pubs.; 1986:383-412.

50

Higley, K. A. How good is good enough: when do you go with what you've got? In: Proceedings of the twenty-sixth midyear topical meeting of the Health Physics Society Jan 24-28, 1993. Couer d'Alene, ID. Research Enterprises, Richland WA. 1993:267-280.

Horn, R.; Taubner, H.; Wuttke, M.; Baumgartl, T. Soil physical properties related to soil structure. Soil and Tillage Res. 30:187-216; 1994.

Horton, R.; Thompson, M. L.; McBride, J. F. Determination of effective porosity of soil materials. U.S. Environmental Protection Agency Project Summary. EPA/600/S2-88/045; 1988.

International Commission on Radiological Protection. Radionuclide transformations . Oxford: Pergamon Press: ICRP Publication 38, Volumes 11-13; ICRP 1095; 1983.

Jury, W. A.; Gardner, W. R.; Gardner, W. H. Soil physics. 5th edition. New York, N.Y.: John Wiley and Sons; 1991.

Klute, A. ed. Methods of soil analysis, Part 1 - Physical and Mineralogical Methods. 2nd Edition. American Society of Agronomy. Number 9 (part 1) in the series Agronomy. Madison, WI: American Society of Agronomy, Soil Science Society of America, Inc Pubs. 1986:649-650.

Kocher, D. C. A validation test of a model for long-term retention of ^{131}I in surface soils. Health Phys. 60:523-531; 1991.

Kurtz, L. T. and Melsted, S. W.; Movement of chemicals in soils by water. Soil Sci. 115:231-239; 1973.

51

Langer, G. Dust transport - wind blown and mechanical resuspension, July 1983 to December 1984. Rockwell International; RFP-3914; 1986.

Lee, K. E. Earthworms, their ecology and relationships with soils and land use. New York: Academic Press; 1985.

Little, C. A. Plutonium in a grasslands ecosystem. Ph.D. dissertation. Fort Collins, CO: Colorado State University, 1976.

Loch, J. P. G. State of the art report - frost heaving actions in soils. In: Developments in geotechnical engineering vol. 28: ground freezing, 1980. Selected papers of the Second International Symposium on Ground Freezing; held in Trondheim, June 24 ; 226, 1980. Elsevier Scientific Publishing Company, Amsterdam, 1982:213-224.

Logsdon,S. D.; McCoy, E. L.; Allmaras, R. R.; Linden, D. R. Macropore characterization by indirect methods; Soil Sci. 155:316-324; 1993.

Mermut, A. R.; Grevers, M. C. J.; de Jong, E. Evaluation of pores under different management systems by image analysis of clay soils in Saskatchewan, Canada; Geoderma 53:357-372; 1992.

Miller, R. W.; Donahue, R. L. Soils, and introduction to soils and plant growth. Englewood Cliffs, NJ, Prentice Hall, 1990.

Pietrzyk, K. An attempt at a new formulation of the criteria of frost heave. In: Developments in geotechnical engineering vol. 28: ground freezing, 1980. Selected papers of the Second

International Symposium on Ground Freezing; held in Trondheim, June 24 ; 226, 1980. Elsevier Scientific Publishing Company, Amsterdam, 1982:281-290.

Puls, R. W.; Powell, R. M.; Clark D. A.; Paul, C. J. Facilitated transport of inorganic contaminants in ground water: part II. colloidal transport. U.S. Environmental Protection Agency, Environmental Research Brief, EPA/600/M-91/040 1991.

Saetersdal, R.; Heaving conditions by freezing of soils. In: Developments in geotechnical engineering vol. 28: ground freezing, 1980. Selected papers of the Second International Symposium on Ground Freezing; held in Trondheim, June 24 ; 226, 1980. Elsevier Scientific Publishing Company, Amsterdam, 1982:291-306.

Schierman, M. J. Characterization of americium and plutonium concentrations in soil profiles at the Rocky Flats Plant. M.S. Thesis. Fort Collins, CO; Colorado State University, 1994.

Shipitalo, M. J.; Edwards, W. M.; Dick, W. A.; Owens, L. B. Initial storm effects on macropore transport of surface-applied chemicals in no-till soil. Soil Sci. Soc. Am. J. 54:1530-1536; 1990.

Sill, C. W.; Willis, C. P. Barium sulfate precipitation of submicrogram quantities of, and application to fluorometric determination of thorium in mineralogical and biological samples A. Chem 36:622-625; 1964.

Tamura, T. Effect of pretreatment on the size distribution of plutonium in surface soil from Rocky Flats, In: Transuranics in Desert Ecosystems, Nevada Applied Ecology Group. NVO-1871 UC-11; 173- 186; 1977.

53

Tariq, A.; Durnford, D. S. Soil volumetric shrinkage measurements: a simple method. Soil Sci. 155:325 - 330; 1993.

U.S. Department of Agriculture, Soil Conservation Service. Soil survey of Golden area, Colorado, parts of Denver, Douglas, Jefferson, and Park counties. undated, ca 1980.

U.S. Department of Energy. Final environmental impact statement (final statement to ERDA 1545-D): Rocky Flats Plant Site; Golden, Jefferson County, colorado. Washington, D.C.: National Technical Information Service; DOE/EIS-0064 (3 vol); 1980.

van Lanen, H. A. J.; Reinds, G. J.; Boersma, O. H.; Bouma, J. Impact of soil management systems on soil structure and physical properties in a clay loam soil, and the simulated effects on water deficits, soil aeration and workability. Soil Tillage Res. 23:203-220; 1992.

Watters, R. L.; Edgington, D. N.; Hakonson, T. E.; Hanson, W. C.; Smith, M. H.; Whicker, F. W.; Wildung, R. E. Synthesis of the research literature. In: Transuranic elements in the environment. U. S. Department of Energy, National Technical Information Service; DOE/TIC-22800; 1980:1-44.

Webb, S. B. A study of plutonium in soil and vegetation at the Rocky Flats Plant. M.S. Thesis. Fort Collins, CO: Colorado State University, 1992.

Wopereis, M. C. S.; Bouma, J.; Kropff, M. J.; Sanidad, W. Reducing bypass flow through a dry, cracked and previously puddled rice soil. Soil Tillage Res. 29:1-11; 1994.

Table 1. Characteristics of Rocky Flats soils; a comparison of data obtained by C. Little (1976) for MP1, 0-10 cm and from private property on the west side of the RFP.

Characteristic	C.Little MP1, 0-10 cm data	C.Little MP1, 10-20 cm data	Private Property 0 - 100 cm data
pH	7.7	8.0	7.4
conductivity, mmhos cm^{-1}	0.7	0.8	1.4
Ca^{++}, meq l^{-1}	7.0	5.5	7
Mg^{++}, meq l^{-1}	0.5	2.9	3.5
Na^{+}, meq l^{-1}	0.7	0.7	3.1
SO_4^{+}, meq l^{-1}	2.5	2.5	7.3
Cl^{-}, meq l^{-1}	0.6	0.8	4.4
CO_3^{-}, meq l^{-1}	0	0	0.2
HCO_3^{-}, meq l^{-1}	4.1	4.2	2.0
CEC, meq $100g^{-1}$	25.0	25.8	14.5
Total N, %	0.17	0.12	0.056
NO_3-N, ppm	45	99	5.54
NO_2-N, ppm	<1	<1	1.14
NH_4-N, ppm	9	7	9.34
Organic Matter, %	2.6	3.5	1.4
$NaHCO_3$ extractable P, mg kg^{-1}	20	9	4.0
1N NH_4OAc extractable K, mg kg^{-1}	418	413	152.3
2 Hour DTPA extractable Zn, mg kg^{-1}	1.9	6.6	0.61
2 Hour DTPA extractable Fe, mg kg^{-1}	16.1	17.4	13.6
2 Hour DTPA extractable Cu, mg kg^{-1}	2.4	23.6	1.7
2 Hour DTPA extractable Mn, mg kg^{-1}	15.2	15.2	11.6
% Sand	40	39	68
% Silt	24	21	12.0
% Clay	36	40	20
Texture	clay loam	clay loam clay	Sandy Clay Loam / Sandy Loam
Bulk Density, g cm^{-3}			1.4
% Saturation			40.2

55

Table 2. Evaluation of water volume, depth, particle size and depth by size as independent predictors of the migration of specific particle sizes into saturated soil columns.

	F Value (and probability, p, of attaining a more extreme statistic)				
Dependent Variable	Water Volume	Depth	Particle Size	Depth by Size	R^2
Ln(Inventory)	1.8 (0.17)	170 (0.0001)	14 (0.0001)	2.5 (0.0001)	0.82

Table 3. Evaluation of freeze thaw cycles, soil depth, and cycle by depth as independent predictors of the migration of clay-sized particles into soil columns.

	F Value (and probability, p of attaining a more extreme statistic)			
Dependent Variable	Freeze Cycle	Depth	Cycle by Depth	R^2
Outer core (ln (inventory))	5.13 (0.0001)	50 (0.0001)	5 (0.0001)	0.73
Inner core (ln(inventory))	6 (0.0001)	92 (0.0001)	1.6 (0.02)	0.78
Combined core (ln(inventory))	15 (0.0001)	8.3 (0.0001)	2.8 (0.0001)	0.51

56

Table 4. Results of Tukey's Studentized Range test on the water migration experiment. The table represents a pairwise comparison to determine the significant differences between particle sizes. Those comparisons that are significant at p=0.05 are underlined.

Sand (S)	S - S				
Coarse Silt (CS)	S - CS	CS - CS			
Fine Silt (FS)	S - FS	FS - CS	FS - FS		
Clay (C)	S - C	CS - C	FS - C	C - C	
Dissolved (D)	S - D	CS - CS	FS - D	C - D	D - D
	Sand (S)	Coarse Silt (CS)	Fine Silt (FS)	Clay (C)	Dissolved (D)

Table 5. Results of Tukey's Studentized Range test on the freeze/thaw experiment. The table represents a pairwise comparison of outer core segments to determine the significant differences between freeze thaw cycles. Those comparisons that are significant at p=0.05 are underlined.

Freeze thaw cycle					
0	0 - 0				
1	0 - 1	1 - 1			
4	0 - 4	1 - 4	4 - 4		
5	0 - 5	1 - 5	4 - 5	5 - 5	
6	0 - 6	1 - 6	4 - 6	5 - 6	6 - 6
	0	1	4	5	6

Freeze thaw cycle

57

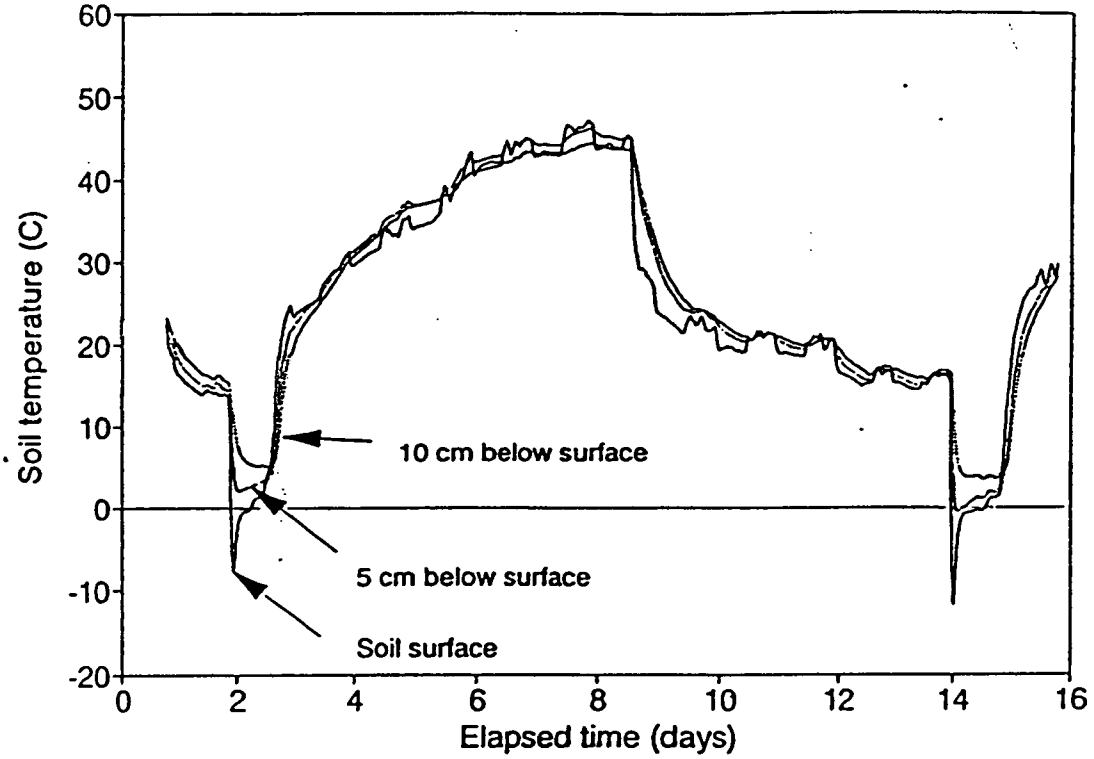

Fig. 1. Soil temperature profile for 0 - 10 cm and one freeze thaw cycle.

58

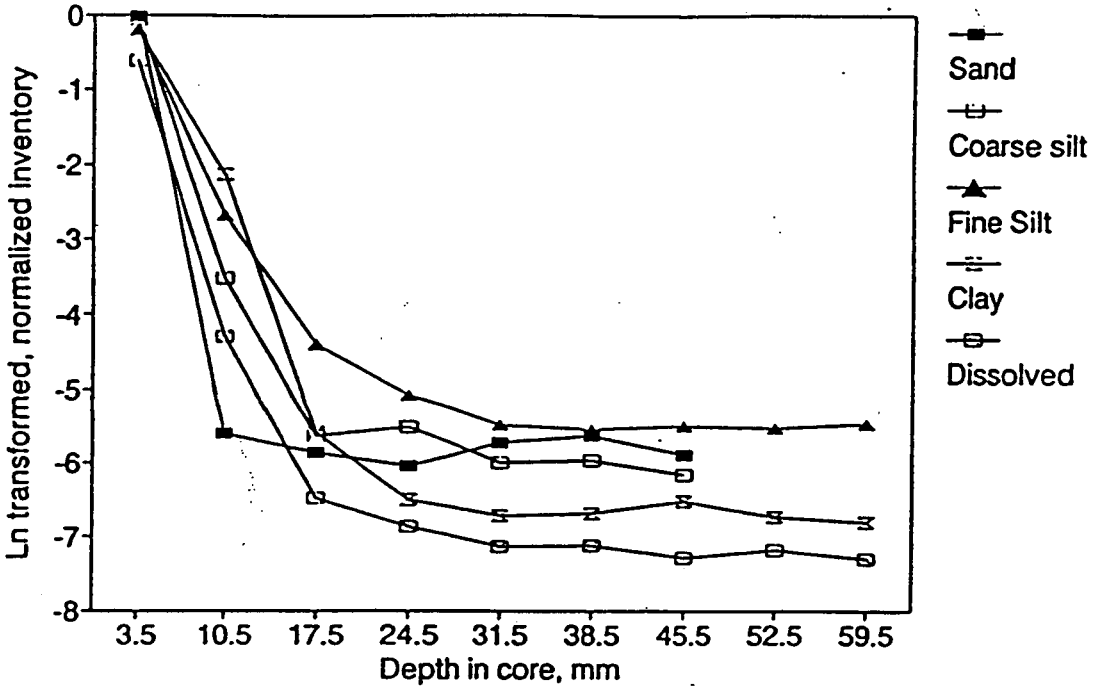

Fig. 2. Comparison of inventory distribution as a function of particle size and depth for the 130 y equivalent precipitation experiment

59

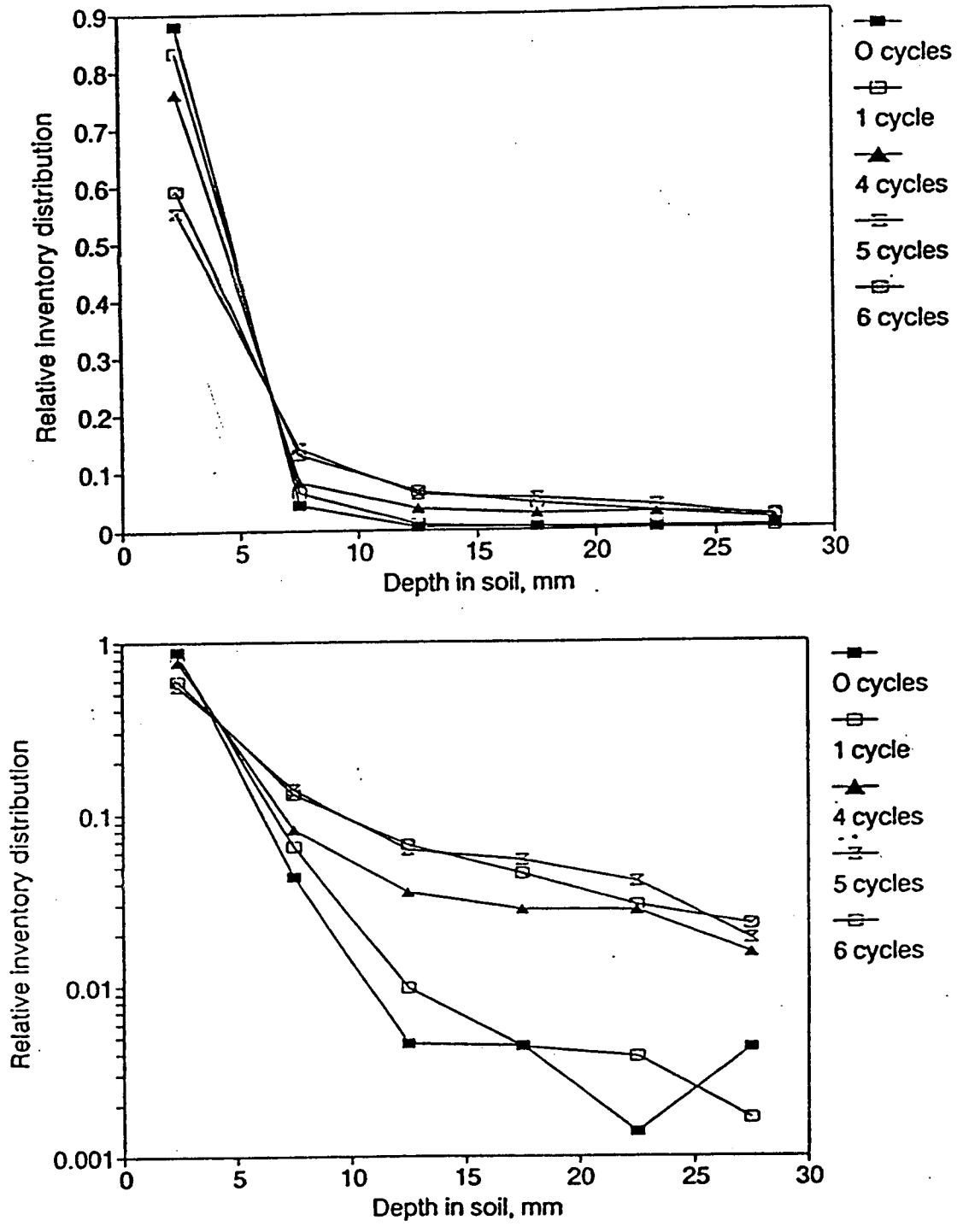

Fig. 3. Relative distribution of ^{234}Th inventory in combined soil cores as a function of depth and cycles; the inventory of each cycle sums to unity. Both linear and log scales are shown to better illustrate the results.

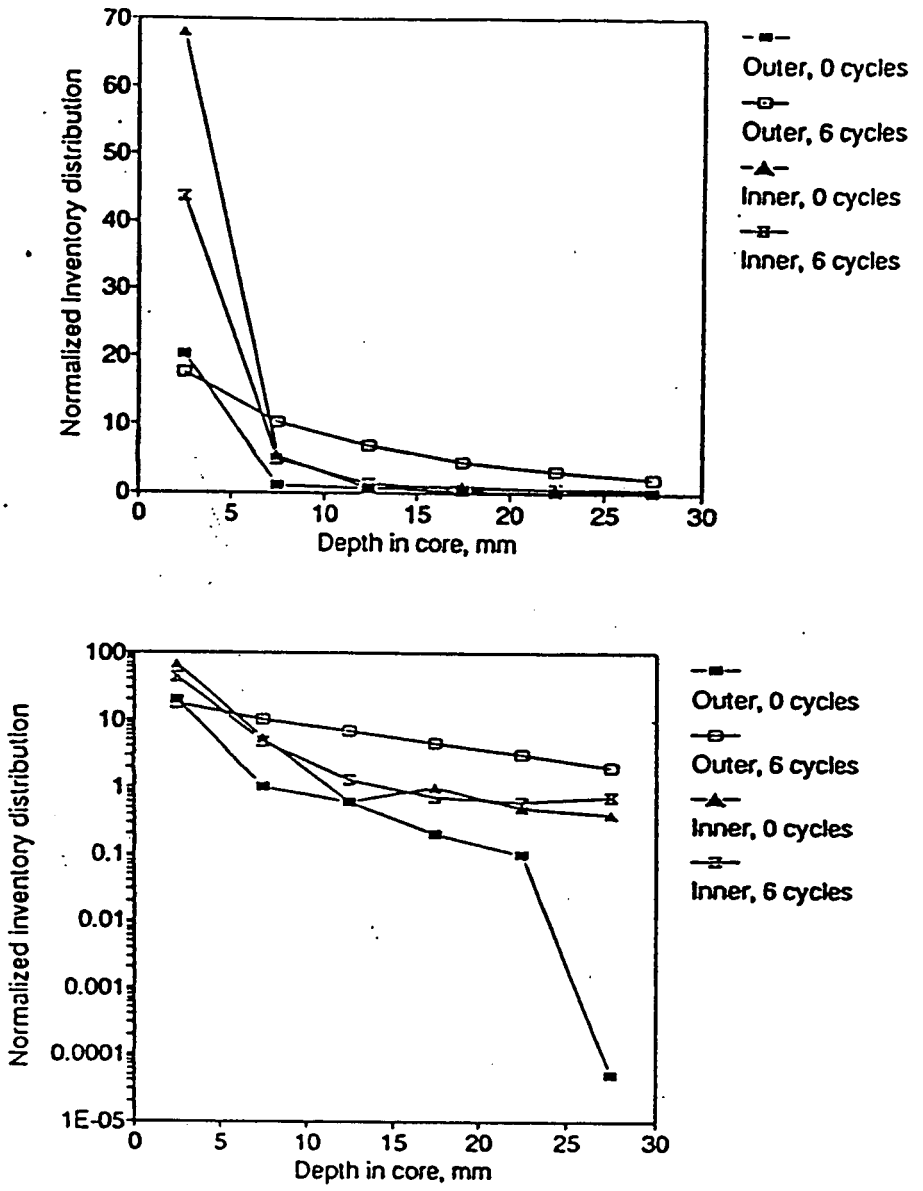

Fig. 4. Inventory distribution on inner and outer core segments as a function of soil depth and cycles. Both linear and log scales are shown to better illustrate the results.

61

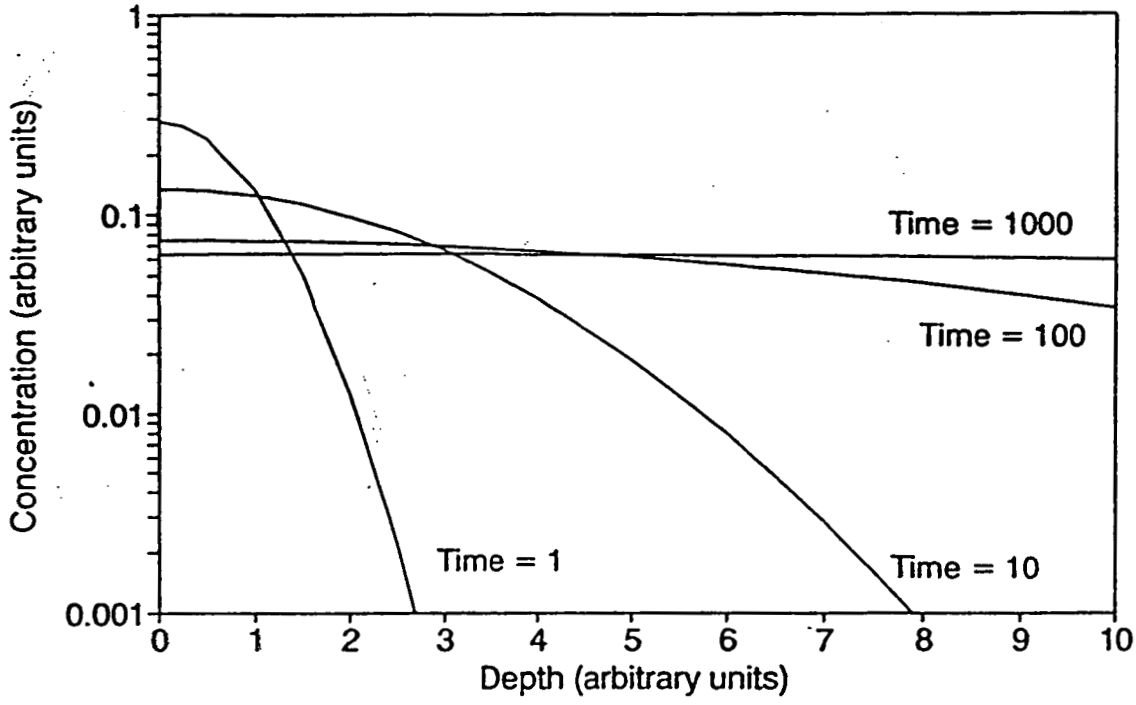

Fig. 5. Concentration versus depth curves for diffusion driven movement. This curves illustrates how contaminants migrate into soil over time.

62

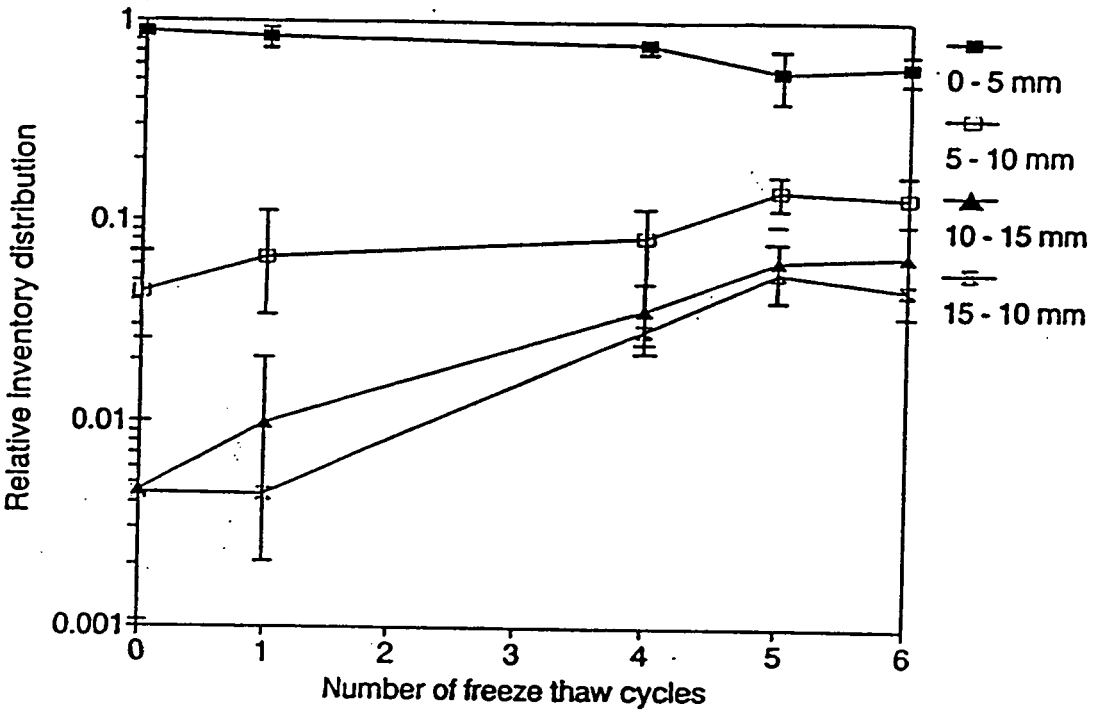

Fig. 6. Relative distribution of ^{234}Th in the combined soil core segments for the top four soil core layers as a function of depth and cycles; the inventory in each cycle sums to unity. Error bars represent ± 1 standard error of the geometric mean.

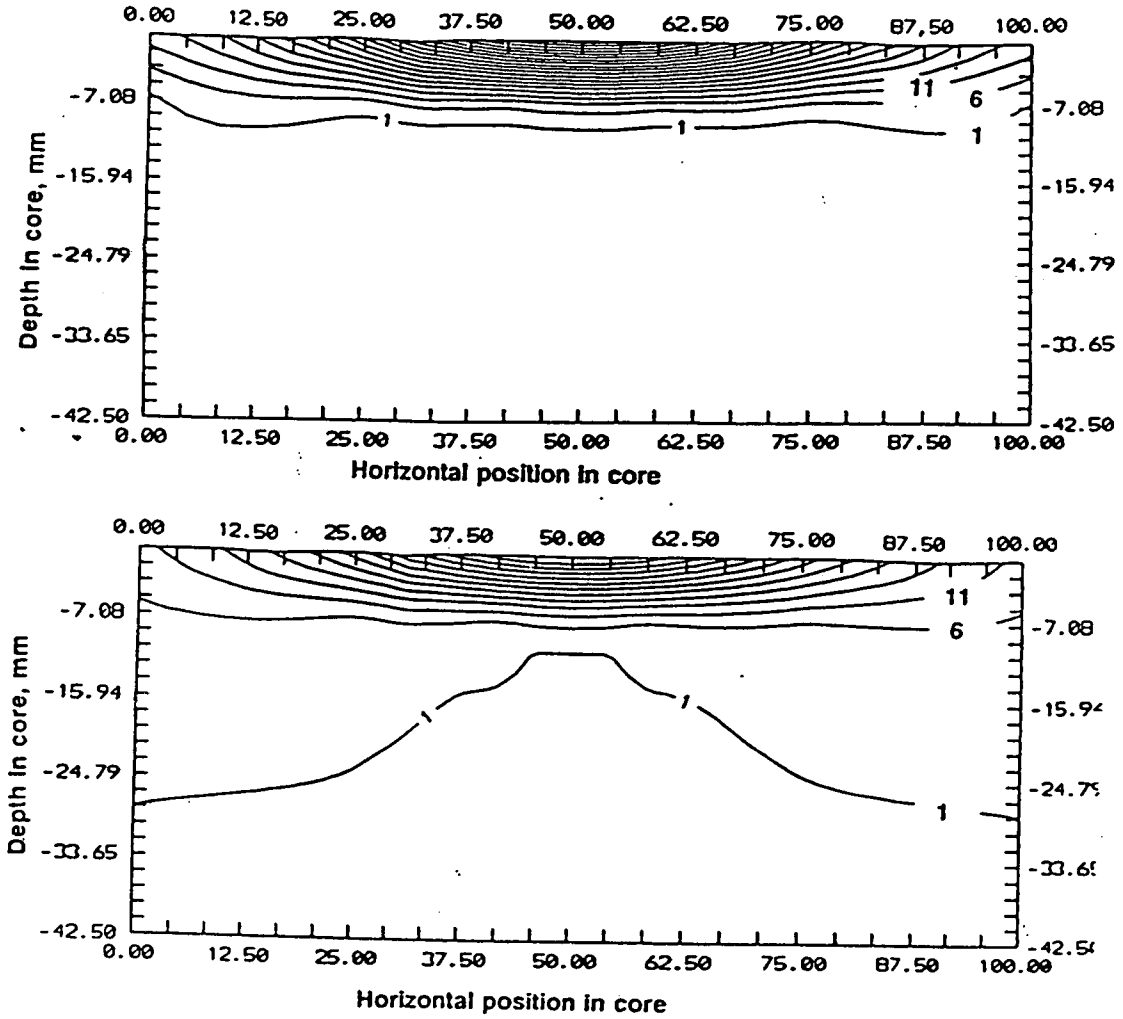

Fig. 7. Inventory contour plots indicating the percent of total inventory in the soil column. Inventory contour plot for a) zero cycles and b) after six cycles.

ENDNOTES

a. Soils Testing Laboratory, Colorado State University, Fort Collins, CO.

b. Plutonium analysis was performed in the laboratories of S. Ibrahim and F. Whicker in the Department of Radiological Health Sciences, Colorado State University, Fort Collins, CO.

c. Dowex is a registered trademark of DOW Chemical Co. This resin was distributed by Sigma Chemical CO, P.O. Box 14508, St. Louis, MO.

d. The term "dissolved" has historically been used to differentiate between that fraction of a sample that can pass through a 0.45 μm filter and the larger, particulate phases in water (Puls et al, 1991).

e. The lyotropic series is an indication of the relative replaceability of an ion from specific colloids. For example, in order of decreasing ease of removal: $Li^{+} > Ca^{2+} >> Th^{4+}$ (Bohn, 1985).

f. Personal communication, May 1993, K. Barbarick, Department of Agronomy, Colorado State University, Fort Collins, CO.

g. The "zero" precipitation columns were pulled and analyzed shortly after the radiotracer was applied to the saturated soils. The purpose was to determine the extent of migration of constituents due to wicking and physical pressure of the clean sand applied to the surface.

h. This particular rainfall rate was chosen to correspond with that observed in the vicinity of the RFP site (U.S.DOE, 1980).

i. A 3 in thallium activated sodium iodide crystal of through hole design. The Autogamma 5000 series, manufactured by Packard Instrument Company, One State Street, Meriden, CT 06450.

j. SAS is a registered trademark of SAS Institute, Inc., Cary, North Carolina.

k. Golden Software, Inc., P.O. Box 281, Golden, CO.

SUMMARY, CONCLUSIONS, AND RECOMMENDATIONS

Over the last 25 y, the Radioecology Group at Colorado State University has repeatedly sampled and analyzed soils, flora, and fauna at the RFP for the presence of plutonium and americium. The objective has been to document their concentrations and inventories and to ultimately determine their potential impact on human health and the quality of the environment. Mathematical models have been employed to project the cycling of the radionuclides through the food chain pathway and estimate the dose to individuals residing in the vicinity of the site.

Although short term projections of impact can be generated based on current concentrations, longer term projections require understanding of the dynamics of movement of these contaminants in soil, which is the primary reservoir and source of ^{238}Pu, $^{239\text{-}240}Pu$ and ^{241}Am. The research presented in this dissertation arose from the desire to understand how plutonium and americium could have migrated as far as 20 cm into the soil in a relatively-short time frame. The results of this work, will, ultimately be employed in the models used to estimate the long-term impacts of americium and plutonium in the environment around the RFP.

SUMMARY

Samples were taken from an undisturbed grassland soil that had been contaminated with plutonium and americium nearly 25 y earlier. The soils were separated into constituent mineral particle sizes and examined for the presence of these radionuclides. Statistical tests were used to evaluate the relationships between radionuclide inventory (or concentration), particle size, and depth in soil, with the intention of gaining insight into contaminant migration mechanisms. The fundamental question was: is there evidence that contaminated soil particles of different sizes migrate at different rates into the soil?

Physical mechanisms for moving soil particles into soil columns were also investigated. Water percolation, soil freezing, and soil cracking were each evaluated for their potential to move soil particles into constant density, homogenous, soil columns. The vertical migration of ^{234}Th-labeled soil particles into saturated soil columns as a function of water volume, labeled particle size, and depth were statistically tested to determine if preferential rates of particle migration existed. Vertical movement of thorium-labeled clay particles into soil columns as a function of: 1) freeze thaw cycle was tested to determine if soil volume changes could result in particle migration; and 2) extreme drying to show whether cracking could cause downward movement.

CONCLUSIONS

Soils collected from the plutonium and americium contaminated grassland site at RFP exhibited a preferential attachment of plutonium and americium to the smaller particle size fractions. The clay size fraction (0.45 - 2 μm) had the highest activity concentration for both actinides, but because of the preponderance of silt-sized particles in this soil, approximately 50% of the total inventory resided in the coarse silt (10 - 53 μm) fraction. The relative order of activity concentration was inversely related to particle size: the smaller particle size fraction had the highest activity concentration and the largest size fraction (gravel) had the lowest.

There was no evidence of a particle-size depth interaction. If the actinides were permanently attached to a specific size fraction, one might expect to have seen differences in the particle-size specific concentration gradients with depth into soil. However, radionuclide inventories and concentrations decreased exponentially into soil with no significant difference in slope among the particle size fractions. All particles sizes were found to have measurable concentrations of contaminants at all sampled depths. There was no evidence that one size fraction was migrating differently through the soil than another. This suggests, but does not prove, that colloid migration is not a dominant transport mechanism.

67

The mean value of the $^{239\text{-}240}Pu$ to ^{241}Am ratios (over all particles sizes and depths) was 7.6, but the dissolved fraction was statistically significantly higher ($p = 0.001$) than all other particle sizes, i.e. more plutonium than americium was present in the dissolved fraction. While the difference is likely due to varying chemical affinities of the two actinides, the specific reason for the occurrence is unknown at this time.

There was no evidence that ^{238}Pu was distributed differently than $^{239,240}Pu$ over all particle sizes and depths ($p=0.5692$ and 0.9183), consistent with previously reported results.

Three mechanisms of physical transport: migration by water; frost heaving and thawing; and soil cracking, were evaluated for their potential to move ^{234}Th-labeled soil particles through a homogenous soil medium. Five soil fractions: sand (50 - 250 μm), coarse silt (10 - 50 μm), fine silt (2 - 10 μm), clay (0.45 - 2 μm), and "dissolved" (< 0.45 μm) were radiotracer-labeled and applied to soil columns containing a sandy clay loam. Water volumes equivalent to between 0 and 130 y were applied to the columns. Water was not a statistically significant factor ($p = 0.17$) in moving labeled particles into the columns.

A second experiment was conducted using only clay-sized particles labeled with ^{234}Th. Freezing and cracking (through heating and drying) the soil resulted in significant migration ($p = 0.0001$) of labeled clay particles into the columns. The migration was largely attributed to bypass flow through macropores (cracks) created during the shrinkage of the soil as it dried ($p = 0.0001$); less extensive but significant ($p = 0.0001$) migration was also attributed to volume changes caused by frost heaving and subsequent soil contraction upon thawing.

RECOMMENDATIONS

The material discussed in this dissertation represents five years of research on plutonium and americium in the soils of the U.S. Department of Energy's Rocky Flats Plant site. This work has raised a number of questions regarding these contaminants. First and foremost is the analytical technique used to separate the soil particles for analysis. Although this is a

standard method which has been utilized by others, there is the potential for a certain amount of remobilization of the constituents which may mask our understanding of transport mechanics in the soil system. Further research clarifying the solubility of plutonium and americium in these soils is warranted.

It is common practice to employ various factors, such as distribution coefficients, to predict contaminant movement through soils. As part of the analysis of the redistribution issue described above, attempts were made to relate the distribution of contaminants across all depths as a function of particle size and mass of that size fraction. The rational was that if redistribution had occurred, it would follow along the lines of particle size affinity (i.e. distribution coefficients) and it would be possible to predict the inventory distribution as a function of particle size and mass of that fraction. The results were not successful, and the absence of such a relationship suggests that the system is not in equilibrium. Consequently, the use of equilibrium type calculations (such as distribution coefficients) to predict the partitioning of contaminants should be avoided.

Additional soil sampling techniques should be investigated to provide finer structure for assessing contaminant migration into the soil. These and previous sampling efforts collected 3 cm lifts which may have masked movement from the soil surface into the near surface layers.

Quantification of macropore structure at the RFP site would provide a better indication of likelihood of this route of transport. Techniques for macropore characterization have proliferated substantially in the last few years, and a number of options are now available, including the use of quick setting emulsions, soil thin sections, and computer imaging and pattern recognition techniques.

APPENDIX A

ANALYTICAL PROCEDURES

10

A. 1. PLUTONIUM RADIOCHEMISTRY

Analysis of Plutonium was conducted by Analytical Technologies, Inc., Fort Collins, CO. The following is a general description of the radioanalytical procedures employed by ATI in their analysis of plutonium in RFP soil samples (identified as ATI SOP 71OFCO, 11/3/93, new, rev 0).

SPECIAL NOTE:

This procedure details the steps for preparation of soil samples for quantitative measurement of isotopic plutonium. Although copied largely verbatim, a complete description of required apparatus, reagents, and procedures can be found by consulting ATI radiochemical procedure ATI SOP 71OFCO, 11/3/93, new, rev 0.

OVERALL PROCESS:

Soil samples are dried and ground to a homogenous fine powder. Tracers are added to a 2 g aliquot of the sample. Total dissolution of the soil is accomplished with nitric, hydrochloric, and hydrofluoric acids. Hydroxide precipitation is then done to remove many of the amphoteric elements from the dissolved sampled. The separation and purification of plutonium from extraneous materials and other actinides is accomplished by anion exchange.

Oxidizing-complexing acids with hydrofluoric acid are used to effect solubilization of the soil by breakdown of intractable materials, including refractory oxides, and removal of siliceous compounds.

As any soil prepared by is dried prior to sieving and grinding, the result of this analysis is automatically obtained on a dry weight basis.

REAGENTS

1) High purity Pu-242 standardized solution, approximately 20 dpm/ml activity

2) Nitric acid, 16 N (conc), 8 N.

3) 12 N HNO_3: cautiously add 750 ml conc. HNO_3 to 250 ml of distilled water.

4) 8 N HNO_3 cautiously add 500 ml conc. HNO_3 to 400 ml DI water and dilute to one liter.

5) Hydrofluoric acid, HF, 29 N (conc)), 3N

6) 3 N HF: dilute 104 ml concentrated HF to 1 L with DI water. Use plastic graduated cylinder and storage bottle.

7) Hydrochloric acid, HCL 12 N (conc), 9 N, 6 N, 1 N, 0.5 N, 0.1 N

9 N HCl: add 750 mil conc HCL to 250 ml DI water. Mix and allow to cool. 6 N HCL: add 500 ml concentrated HCL to 500 ml DI water

1 N HCL: add 83 ml conc HCL to 500 ml of DI water and dilute to 1 L

0.5 N HCL add 42 ml concentrated HCL to 500 ml di water and dilute to 1 L

8) 0.1 N HCL: add 8 ml concentrated HCL to 500 ml DI water and dilute to 1 L

9) Boric acid (H_3BO_3) reagent grade.

10) Sodium Bisulfite ($NAHSO_3$) reagent grade.

11) Sodium hydroxide, 50 percent (NaOH). Add 500 g reagent grade NaOH pellets to 500 ml of DI water. Stir until all materials are dissolved. Cool. dilute to 1 L final volume with DI water.

12) Nitric acid, 8 N, saturated with H_3BO_3 add 25 g of boric acid (H_3BO_3) to IL of 8 N HNO_3 and heat with stirring until all of the crystals are dissolved. Cool solution and store.

13) Ammonium hydroxide (NH_4OH) conc, 15 M, reagent grade.

14) AGIX8 bio rad (100-200 mesh) anion exchange resin.

15) Ammonium iodide (NH_4I)

16) 9 N HCL

17) Di-n-butyl N, N-diethylcarbamoyl phosphate (DDCP)

18) Toluene, reagent grade.

19) AG50WX4 bio rad cation exchange resin (100-200 mesh)

20) Ammonium thiocyanate (NH_4SCN) 1 N. Weigh out 7.6 g of NH_4SCN and dissolve in 100 ml of DI water. Prepare fresh for each use.

172

21) Lanthanum carrier, 0.1 mg La^{3+} ml^{-1}: dissolve 0.0779 g of high purity $La(NO_3)_3 \cdot 6H_2O$ in 250 ml of 1 N HCl.

22) Hydrogen peroxide, H_2O_2, 50 % reagent grade. Store in refrigerator.

SAMPLE PREPARATION

1) Weigh 1-2 gm aliquot to the nearest .01 g of the final sieved and ground sample into a labeled Vycor evaporating dish.

2) Add calibrated volume of tracer solutions to each sample, blank and blank spike.

3) Add appropriate calibrated spike solutions to the blank spikes. Dry samples in drying oven about 30 min to 1 h. Consult the spike/tracer data sheet (FM 721) for information on spike standard identification and volumes.

4) Place the Vycor dish in a muffle furnace and heat at 600 C for 1 hour.

SAMPLE DISSOLUTION:

1) Remove dish from muffle furnace and cool. Break up any lumps in ignited soil with plastic stir rod.

2) Transfer sample to a teflon beaker using concentrated nitric acid (HNO_3).

3) Add 40-50 ml to conc HNO_3 and 25 ml of concentrated hydrofluoric acid (HF) to the sample.

4) Heat the sample on a hot plate with frequent stirring for 1 hour using a plastic stir rod. Cover with a teflon watch glass. Do not allow the sample to go to dryness. If about to dry, add a small amount of conc. HNO_3.

5) Remove the teflon beaker from the hot plate and allow to cool.

6) Add 15-20 ml of conc. HF to the sample, and add concentrated HNO_3 as necessary to have a total volume of 60--70 ml.

7) Heat on a hot plate for 45 minutes, covered with teflon watch glass. Do not allow to go dry. If about to go dry, add additional concentrated HNO_3.

8) Add 10 ml of concentrated HNO_3 to the sample and heat the sample for 30 minutes uncovered with occasional stirring.

9) Repeat the step above with a second 120 ml amount of conc. HNO_3, with occasional stirring.

10) Continue heating sample until evaporates to approximately 10-15 ml volume.

11) Transfer the sample to a 250 ml Pyrex beaker using a plastic stir rod and a minimum amount of HNO_3 (conc) from a wash bottle.

12) Carefully add 30 ml of HCL (concentrated) and stir. Allow sample to set for a minimum of 20 minutes before heating at a low temperature for 45 minutes with occasional stirring (the sample can spatter easily while heating, adjust the heat accordingly).

13) Add about 5 g powdered H_3BO_3 and digest for an additional 15 minutes. Stir frequently.

14) Add 200 mg of sodium bisulfite ($NaHSO_3$) and digest on a hot plate.

15) Continue heating and evaporate to dryness.

16) Add 50 ml of 0.1 N HCL and digest sample on a hot plate to dissolve salts. Cool.

17) Using a wash bottle of 0.1 N HCL transfer the total sample into a 250 ml centrifuge tube.

18) Centrifuge sample 30 minutes at approximately 2500 rpm. Very carefully decant into 250 m l beaker. Avoid transferring insoluble material.

19) Break up insoluble residue in tube with 2 N HCL (approximately 10 ml) from a wash bottle and repeat centrifuge step. Add wash solution to beaker. Discard any residue.

20) Add a magnetic stir bar to sample solution and add 50 percent NaOH and stir to a pH of nine (check pH with pH paper). Add 5 to 10 ml excess of NaOH and continue stirring for five minutes.

21) Remove stir bar and transfer the mixture back to a 250 ml centrifuge tube. rinse beakers with a minimum amount of DI water from a wash bottle and add to centrifuge bottle.

174

22) Centrifuge sample for 30 minutes at approximately 2500 rpm. Discard the supernate. Avoid losing any precipitate.

23) Dissolve the precipitate with 25 ml of 8 N HNO_3- saturated H_3BO_3. Digest in a hot water bath to aid solubilization. Add 50 ml of DI water with agitation.

24) Add ammonium hydroxide (NH_4OH) dropwise, using a vortex mixer, to a pH 9 (a brown iron hydroxide precipitate will form)

25) Centrifuge the sample for 30 minutes at approximately 2500 rpm. Discard the supernate. Avoid losing any precipitate.

26) Dissolve the precipitate in 1-2 ml of con. HNO_3. Bring to 50 ml volume with 8 N HNO_3.

PLUTONIUM ION EXCHANGE:

1) Prepare an anion exchange column (AG1X8, 100 to 200 mesh) about 5.7 cm in length.

2) Add glass microbeads to a depth of 0.5 cm. Condition the column with 50 ml of 8 N HNO_3.

3) Filter the sample solution into the column through Whatman 41 filter paper.

4) Pass the sample through the column, collect the effluent in a 250 ml beaker if americium,curium analysis is needed. Rinse the sample beaker with 30 ml of 8 N HNO_3 and pass through the column, combining the rinse with the effluent in the same 250 ml beaker and save for americium analysis.

5) Rinse the column with an additional 20 ml of 8 N HNO_3 and discard the rinse.

6) Continue washing with 40 ml of 9 N HCL to remove thorium Repeat with an additional 20 ml of 9 N HCL. Discard effluent.

7) Elute the plutonium with 20 ml of 9 N HCl /NH_4I solution. Add 5 ml of concentrated HNO_3 to collected effluent.

8) Evaporate the solution to dryness. If yellow color does not disappear before going to dryness, add 5-10 ml conc. HNO_3 and evaporate to dryness.

9) Add 10 ml concentrated. HCL and evaporate to dryness.

175

MICROPRECIPITATION OF PLUTONIUM.

1) Dissolve sample in 15 ml of 1 N HCL. Heat gently on hotplate to complete dissolution. Cool sample, add 0.5 ml H_2O_2 and swirl gently

2) Add 1ml of lanthanum carrier and swirl gently.

3) Add 6-8 ml of 3 N HF and mix well.

4) Allow samples to set for 2 hour to complete microprecipitation.

5) Mount 25 mm filter in filter funnel and rinse with 5-10 ml of alcohol, then 5-10 ml of DI water, allowing each rinse to completely pass through the filter before adding next solution.

6) Using suction, filter co-precipitation sample through filter membrane.

7) Rinse sample beaker twice with 5 ml water and add to filter funnel.

8) When filtering is complete, remove membrane and dry for a few minutes in Pyrex beaker in drying oven.

9) Mount membrane on 1/1/4 " stainless steel cupped disc with double-sided tape.

10) Discard all liquid in suction flask into appropriate waste carboy.

Quality control

1) One reagent blank is run per batch of 20 samples or at a five percent frequency.

2) One sample duplicate is run per batch of 10 samples or at a 10 % frequency.

3) One lab control sample (spiked blank) is run for each batch of 20 samples (fiver percent frequency) with a range of 5 to 15 pCi of ^{239}Pu or ^{238}Pu.

76

A. 2. PREPARATION OF CARRIER-FREE THORIUM-234 TRACER

REFERENCE: This procedure has been adapted from that described by Sill (1964) and Berman (1964).

EXPERIMENTAL APPARATUS: 1000 ml buret with support stand; glass wool; glass stir rod of sufficient length to reach 1.5 times the length of the buret; hot plate; 1 L pyrex beaker; 0.75 kg Dowex 1x4-200 (chloride form) anion exchange resin; 500 g uranyl nitrate ($UNO_3 \circ 6\ H_20$); 8 L concentrated nitric acid; 1 L concentrated HCL.

CAUTIONARY NOTE: Preparation and packing of this column results in the evolution of HCL and HNO_3 gases. This work should be performed in a hood.

PROCEDURE: Place plug of glass wool above the stopcock in the 1000 ml buret using a glass rod; sufficient material should be used to cover hole but not restrict flow.

Suspend the resin as a slurry in 8 N HNO_3 and pour slowly into the column; gently tapping the column sides to facilitate packing and settling. Add the resin in small increments, allowing it sufficient time to settle. After the column has been packed, continue to pass 8 N HNO_3 (approximately 4 L) through until no evidence of HCL evolution is present. The column is now ready for addition of uranyl nitrate in equilibrium with progeny.

While heating, dissolve the $UNO_3 \circ 6\ H_20$ in sufficient 9.5 M HNO_3 to create a solution. Add solution slowly to the top of the column, collecting nitric acid from column base. **CAUTION:** significant bubbling and offgassing will be evident due to the evolution of chlorine gases and nitric fumes. This work must be done in a hood.

Extract the thorium by adding 9 M HCl to the column; elute by passing approximately 1 column volume of HCL (approximately 500 ml) through the resin and collecting the thorium as a chloride solution.

RECOMMENDATIONS: Because of the large volume of acid being used in the preparation of this resin column, secondary containment sufficient to catch and hold the volume of the column is recommended. Standard laboratory safety apparel is also suggested.

78

APPENDIX B

EXPERIMENTAL APPARATUS

79

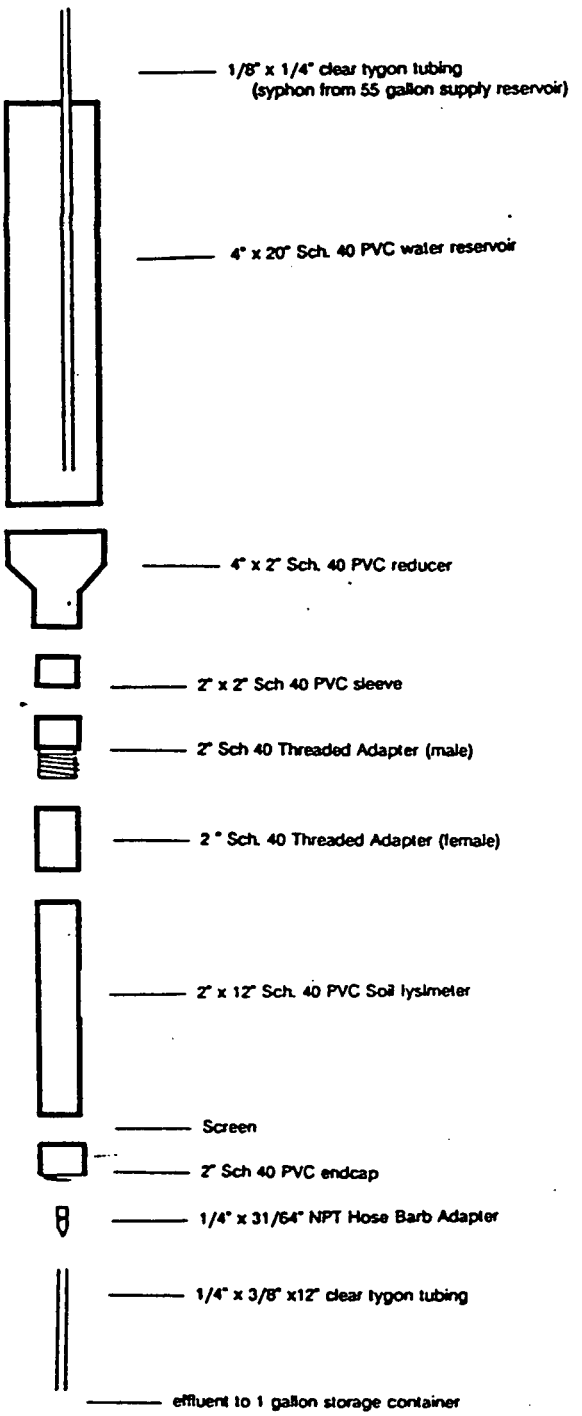

Figure B.1 Schematic of column used in water migration experiment.

80

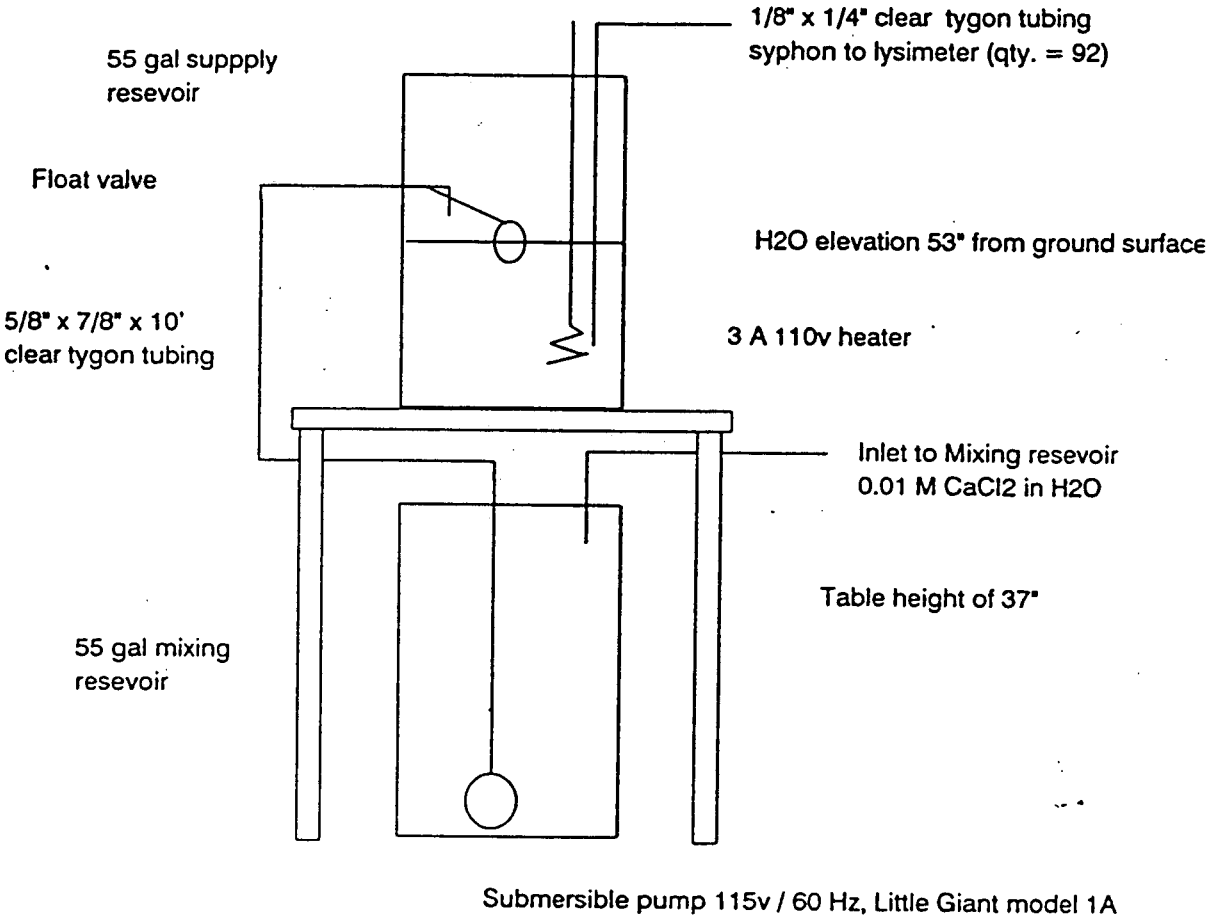

Figure B.2 Schematic of constant head system used in water migration experiment.

81

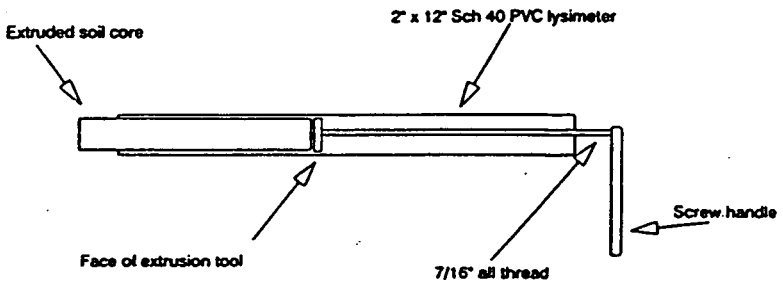

Figure B.3 Schematic of soil extrusion tool.

82

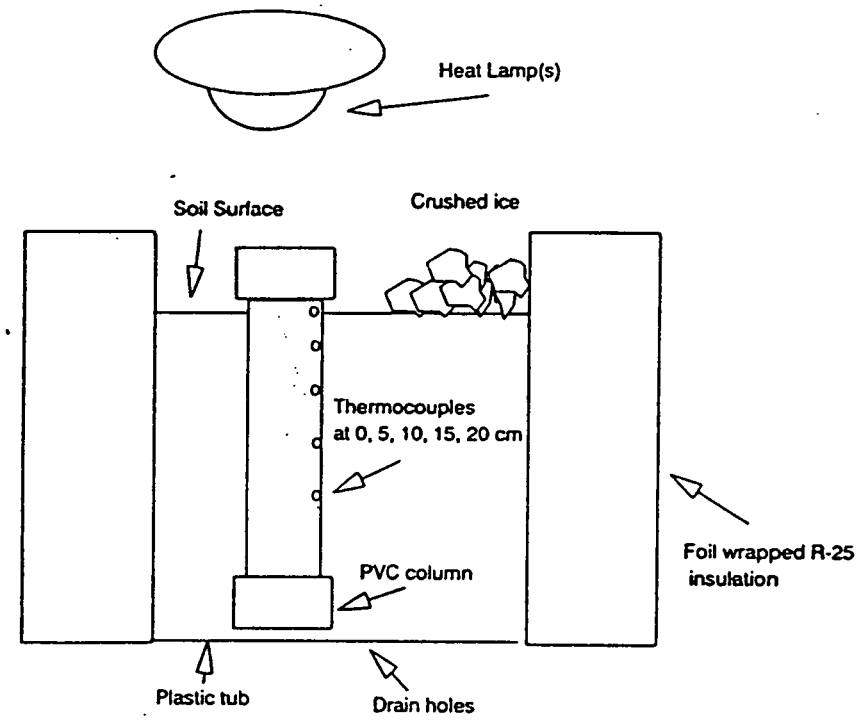

Figure B.4 Schematic of soil freezing and thawing system.

83

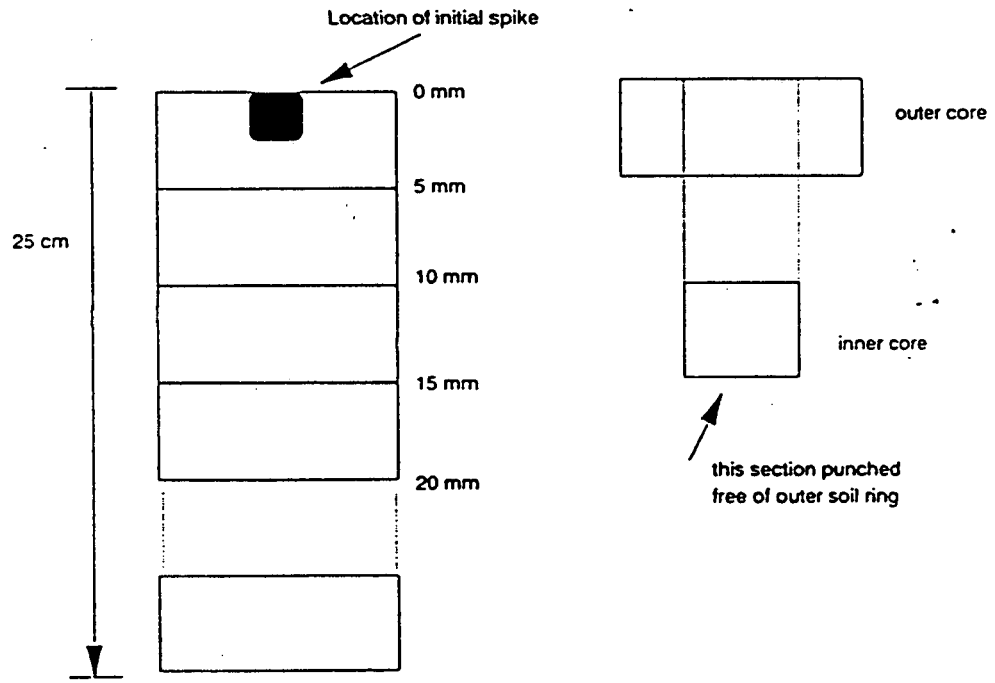

Figure B.5 Schematic of soil core as extruded and collected for freeze-thaw experiment.

84

Table C.1 Mass distribution per microplot, g (dry) (and percentage of total microplot mass contained in each size fraction).

Sampling depth	Size Fraction	Microplot designation		
		CX15	CX16	CX17
0-3 cm	Gravel	440 (8.4%)	220 (5.7%)	210 (4.4%)
	Sand	380 (7.1%)	410 (11%)	370 (7.7%)
	Coarse Silt	300 (5.7%)	190 (5.0%)	330 (6.9%)
	Fine Silt	79 (1.5%)	280 (7.1%)	44 (0.9%)
	Clay	47 (0.9%)	27 (0.7%)	16 (0.3%)
	Dissolved	8.2 (0.2%)	6.7 (0.2%)	14 (0.3%)
3-6 cm	Gravel	780 (15%)	480 (12%)	530 (11%)
	Sand	270 (5.2%)	250 (6.3%)	380 (8.0%)
	Coarse Silt	460 (8.7%)	150 (3.9%)	260 (5.4%)
	Fine Silt	63 (1.2%)	61 (1.6%)	37 (0.8%)
	Clay	32 (0.6%)	96 (2.5%)	19 (0.4%)
	Dissolved	11 (0.2%)	11 (0.3%)	6.2 (0.1%)
6-9 cm	Gravel	320 (6.1%)	63 (1.6%)	670 (14%)
	Sand	290 (5.6%)	230 (5.8%)	360 (7.6%)
	Coarse Silt	360 (6.8%)	340 (8.7%)	260 (5.4%)
	Fine Silt	89 (1.7%)	45 (1.2%)	61 (1.3%)
	Clay	84 (1.6%)	48 (1.2%)	42 (0.9%)
	Dissolved	5.9 (0.1%)	4.9 (0.1%)	2.2 (0.0%)
9-12 cm	Gravel	260 (4.9%)	58 (1.5%)	190 (3.9%)
	Sand	280 (5.4%)	250 (6.5%)	450 (9.5%)
	Coarse Silt	360 (6.8%)	540 (14%)	350 (7.4%)
	Fine Silt	160 (3.1%)	64 (1.6%)	97 (2.0%)
	Clay	170 (3.2%)	66 (1.7%)	59 (1.2%)
	Dissolved	4.7 (0.1%)	6.8 (0.2%)	4.4 (0.1%)

85

Table C.2. ^{241}Am inventory distribution microplot, Bq (and percent of total microplot inventory contained in each size fraction)

Sampling depth	Size Fraction	Microplot designation		
		CX15	CX16	CX17
0-3 cm	Gravel	4 (0.2%)	0.79 (0.04%)	1.3 (0.1%)
	Sand	34 (1.4%)	51 (2.6%)	170 (6.6%)
	Coarse Silt	460 (19%)	220 (11%)	620 (25%)
	Fine Silt	200 (8.4%)	720 (36%)	250 (9.8%)
	Clay	120 (5.1%)	67 (3.4%)	110 (4.4%)
	Dissolved	36 (1.5%)	58 (2.9%)	70 (2.8%)
3-6 cm	Gravel	2.0 (0.1%)	0.28 (0.01%)	0.19 (0.01%)
	Sand	12 (0.5%)	14 (0.7%)	120 (4.6%)
	Coarse Silt	630 (26%)	110 (5.5%)	370 (15%)
	Fine Silt	110 (4.5%)	160 (8.1%)	100 (4.1%)
	Clay	73 (3.0%)	190 (9.6%)	58 (2.3%)
	Dissolved	18 (0.7%)	96 (4.8%)	53 (2.1%)
6-9 cm	Gravel	0.00 (0.0%)	0.36 (0.02%)	0.28 (0.01%)
	Sand	9.3 (0.4%)	21 (1.0%)	52 (2.1%)
	Coarse Silt	260 (11%)	96 (4.8%)	160 (6.5%)
	Fine Silt	100 (4.2%)	30 (1.5%)	76 (3.0%)
	Clay	84 (3.5%)	41 (2.1%)	80 (3.2%)
	Dissolved	14 (0.6%)	4.7 (0.2%)	25 (1.0%)
9-12 cm	Gravel	0.5 (0.02%)	1.3 (0.1%)	0.00 (0.0%)
	Sand	2.3 (0.1%)	7.8 (0.4%)	27 (1.1%)
	Coarse Silt	110 (4.6%)	53 (2.7%)	96 (3.8%)
	Fine Silt	65 (2.7%)	21 (1.0%)	47 (1.9%)
	Clay	77 (3.2%)	18 (0.9%)	31 (1.2%)
	Dissolved	5.6 (0.2%)	0.31 (0.02%)	5.4 (0.2%)

Table C.3. $^{239,240}Pu$ inventory distribution per microplot, Bq (and percent of total microplot inventory contained in each size fraction).

Sampling depth	Size Fraction	Microplot designation		
		CX15	CX16	CX17
0-3 cm	Sand	140 (1.5%)	200 (1.5%)	1100 (8.0%)
	Coarse Silt	2200 (22%)	3000 (23%)	3700 (26%)
	Fine Silt	61 (0.6%)	3900 (29%)	990 (6.7%)
	Clay	380 (3.8%)	350 (2.6%)	380 (2.6%)
	Dissolved	390 (3.9%)	380 (2.9%)	420 (2.9%)
3-6 cm	Sand	86 (0.9%)	70 (0.5%)	970 (6.6%)
	Coarse Silt	2600 (26%)	1500 (11%)	2600 (18%)
	Fine Silt	480 (4.8%)	690 (5.2%)	520 (3.5%)
	Clay	270 (2.7%)	980 (7.4%)	260 (1.8%)
	Dissolved	310 (3.1%)	350 (2.6%)	360 (2.4%)
6-9 cm	Sand	68 (0.7%)	87 (0.7%)	280 (1.9%)
	Coarse Silt	920 (9.2%)	780 (5.9%)	950 (6.4%)
	Fine Silt	420 (4.2%)	170 (1.3%)	420 (2.8%)
	Clay	340 (3.4%)	170 (1.3%)	240 (1.7%)
	Dissolved	230 (2.3%)	65 (0.5%)	260 (1.7%)
9-12 cm	Sand	19 (0.2%)	36 (0.3%)	170 (1.2%)
	Coarse Silt	280 (2.8%)	370 (2.8%)	460 (3.1%)
	Fine Silt	270 (2.7%)	89 (0.7%)	280 (1.9%)
	Clay	340 (3.4%)	99 (0.7%)	130 (0.9%)
	Dissolved	120 (1.2%)	22 (0.2%)	80 (0.5%)

87

Table C.4. ^{238}Pu inventory distribution per microplot, Bq (and percent of total microplot inventory contained in each size fraction).

Sampling depth	Size Fraction	Microplot designation		
		CX15	CX16	CX17
0-3 cm	Sand	2.4 (1.7%)	3.8 (8.1%)	21 (4.2%)
	Coarse Silt	34 (22%)	51 (25%)	6 (23%)
	Fine Silt	0.94 (28%)	64 (6.4%)	16 (13%)
	Clay	6.3 (2.5%)	5.6 (2.4%)	6.1 (2.8%)
	Dissolved	6.2 (2.7%)	6.2 (2.9%)	7.3 (3.1%)
3-6 cm	Sand	1.3 (0.7%)	1.6 (7.5%)	19 (3.4%)
	Coarse Silt	42 (12%)	26 (20%)	50 (18%)
	Fine Silt	7.9 (5.4%)	12 (3.5%)	8.9 (4.5%)
	Clay	4.5 (8.1%)	18 (1.8%)	4.6 (4.3%)
	Dissolved	5.6 (2.7%)	6.1 (1.0%)	2.7 (2.2%)
6-9 cm	Sand	1.2 (0.7%)	1.6 (2.3%)	5.9 (1.3%)
	Coarse Silt	15 (6.1%)	14 (6.5%)	17 (7.1%)
	Fine Silt	7.1 (1.2%)	2.7 (3.0%)	7.6 (2.7%)
	Clay	5.7 (1.3%)	2.9 (1.7%)	4.3 (2.0%)
	Dissolved	3.9 (0.6%)	1.3 (1.7%)	4.3 (1.5%)
9-12 cm	Sand	0.52 (0.2%)	0.56 (0.1%)	0.17 (0.2%)
	Coarse Silt	4.7 (2.6%)	5.8 (3.3%)	8.4 (2.9%)
	Fine Silt	3.8 (0.7%)	1.5 (1.9%)	5.0 (1.6%)
	Clay	5.6 (0.8%)	1.8 (0.8%)	2.0 (1.5%)
	Dissolved	2.2 (0.2%)	0.35 (0.6%)	1.5 (0.6%)

88

Table C. 6 Water migration experiment

Water volume, mls	Column I.D.	Slice Depth, mm	Net Mass, g	Gross cpm	Net cpm	Normalized count rate per column	Natural log of normalized count rate
0	2	3.5	25.26	5157	5033.99	0.9828	-0.02
0	2	10.5	24.56	147	26.13	0.0051	-5.28
0	2	17.5	22.97	129	13.01	0.0025	-5.98
0	2	24.5	20.54	122	13.47	0.0026	-5.94
0	2	31.5	23.76	127	8.59	0.0017	-6.39
0	2	38.5	24.69	136	14.73	0.0029	-5.85
0	2	45.5	20.57	121	12.37	0.0024	-6.03
0	7	3.5	20.04	107	0	0	-39.74
0	7	10.5	25.09	137	14.51	0.1649	-1.8
0	7	17.5	23.43	131	13.6	0.1546	-1.87
0	7	24.5	23.8	137	18.46	0.2099	-1.56
0	7	31.5	24.29	138	17.96	0.2042	-1.59
0	7	38.5	22.5	127	12.45	0.1416	-1.95
0	7	45.5	19.4	116	10.96	0.1247	-2.08
0	12	3.5	25.38	1571	1447.62	0.9422	-0.06
0	12	10.5	22.9	133	17.23	0.0112	-4.49
0	12	17.5	19.96	126	19.25	0.0125	-4.38
0	12	24.5	21.62	124	12.15	0.0079	-4.84
0	12	31.5	21.11	116	5.72	0.0037	-5.59
0	12	38.5	20.5	127	18.59	0.0121	-4.41
0	12	45.5	19.44	121	15.84	0.0103	-4.57
0	18	3.5	31.87	7629	7485.71	0.9891	-0.01
0	18	10.5	25.47	138	14.34	0.0019	-6.27
0	18	17.5	21.16	131	20.56	0.0027	-5.91
0	18	24.5	19.72	120	13.98	0.0018	-6.29

Table C. 6 Water migration experiment

Water volume, mls	Column I.D.	Slice Depth, mm	Net Mass, g	Gross cpm	Net cpm	Normalized count rate per column	Natural log of normalized count rate
0	18	31.5	23.23	125	8.21	0.0011	-6.83
0	18	38.5	23.16	135	18.43	0.0024	-6.02
0	18	45.5	16.36	103	7.29	0.001	-6.95
0	23	3.5	23.63	25154	25035.99	0.9041	-0.1
0	23	10.5	25.81	2436	2311.3	0.0835	-2.48
0	23	17.5	18.23	392	290.55	0.0105	-4.56
0	23	24.5	22.26	137	23.19	0.0008	-7.09
0	23	31.5	25.01	134	11.75	0.0004	-7.76
0	23	38.5	18.64	113	10.29	0.0004	-7.9
0	23	45.5	22.7	125	9.84	0.0004	-7.94
0	32	3.5	30.26	10125	9986.65	0.9945	-0.01
0	32	10.5	21.59	128	16.24	0.0016	-6.43
0	32	17.5	25.16	142	19.29	0.0019	-6.25
0	32	24.5	20.88	120	10.42	0.001	-6.87
0	32	31.5	23.55	132	14.23	0.0014	-6.56
0	32	38.5	19.04	121	17.07	0.0017	-6.38
0	32	45.5	19.83	116	9.64	0.001	-6.95
0	33	3.5	26.6	1393	1265.88	0.7911	-0.23
0	33	10.5	21.11	358	247.72	0.1548	-1.87
0	33	17.5	20.24	142	34.39	0.0215	-3.84
0	33	24.5	23.88	141	22.22	0.0139	-4.28
0	33	31.5	22.05	123	9.83	0.0061	-5.09
0	33	38.5	20.19	117	9.54	0.006	-5.12
0	33	45.5	20.81	120	10.64	0.0066	-5.01

Table C. 6 Water migration experiment

Water volume, mls	Column I.D.	Slice Depth, mm	Net Mass, g	Gross cpm	Net cpm	Normalized count rate per column	Natural log of normalized count rate
0	34	3.5	19.94	23188	23081.31	0.7828	-0.24
0	34	10.5	28.57	5715	5581.83	0.1893	-1.66
0	34	17.5	24.77	857	735.49	0.0249	-3.69
0	34	24.5	19.44	123	17.84	0.0006	-7.41
0	34	31.5	19.9	131	24.43	0.0008	-7.1
0	34	38.5	22.34	152	37.94	0.0013	-6.66
0	34	45.5	16.65	104	7.4	0.0003	-8.29
0	35	52.5	21.76	2072	1959.72	0.953	-0.05
0	35	3.5	24.64	152	30.89	0.015	-4.2
0	35	10.5	21.97	124	11.08	0.0054	-5.22
0	35	17.5	17.53	108	8.7	0.0042	-5.47
0	35	24.5	20.74	118	8.85	0.0043	-5.45
0	35	31.5	19.99	120	13.15	0.0064	-5.05
0	35	38.5	18.21	114	12.61	0.0061	-5.09
0	35	45.5	14.72	102	11.32	0.0055	-5.2
0	38	3.5	26.95	18152	18023.8	0.9598	-0.04
0	38	10.5	21.82	731	618.54	0.0329	-3.41
0	38	17.5	21.8	160	47.6	0.0025	-5.98
0	38	24.5	19.53	138	32.56	0.0017	-6.36
0	38	31.5	19.63	126	20.26	0.0011	-6.83
0	38	38.5	19.79	125	18.77	0.001	-6.91
0	38	45.5	18.06	118	17.07	0.0009	-7
0	41	3.5	16.92	6344	6246.57	0.9777	-0.02
0	41	10.5	22.67	181	65.93	0.0103	-4.57
0	41	17.5	23.8	132	13.46	0.0021	-6.16

Table C. 6 Water migration experiment

Water volume, mls	Column I.D.	Slice Depth, mm	Net Mass, g	Gross cpm	Net cpm	Normalized count rate per column	Natural log of normalized count rate
0	41	24.5	21.72	132	19.85	0.0031	-5.77
0	41	31.5	22.36	130	15.88	0.0025	-6
0	41	38.5	18.26	119	17.46	0.0027	-5.9
0	41	45.5	21.6	122	10.21	0.0016	-6.44
0	45	3.5	25.82	11016	10891.27	0.9916	-0.01
0	45	10.5	23.65	127	8.93	0.0008	-7.12
0	45	17.5	19.17	119	14.67	0.0013	-6.62
0	45	24.5	23.12	132	15.55	0.0014	-6.56
0	45	31.5	19.52	120	14.6	0.0013	-6.62
0	45	38.5	21.16	132	21.56	0.002	-6.23
0	45	45.5	18.93	120	16.41	0.0015	-6.51
0	49	3.5	29.96	9364	9226.57	0.985	-0.02
0	49	10.5	18.48	158	55.79	0.006	-5.12
0	49	17.5	20.22	118	10.45	0.0011	-6.8
0	49	24.5	22.45	130	15.61	0.0017	-6.4
0	49	31.5	21.12	126	15.69	0.0017	-6.39
0	49	38.5	23.88	145	26.22	0.0028	-5.88
0	49	45.5	16.88	114	16.69	0.0018	-6.33
0	64	3.5	25	10783	10660.78	0.9921	-0.01
0	64	10.5	26.96	146	17.77	0.0017	-6.4
0	64	17.5	22.62	129	14.09	0.0013	-6.64
0	64	24.5	27.19	142	13.07	0.0012	-6.71
0	64	31.5	18.38	112	10.09	0.0009	-6.97
0	64	38.5	20.43	128	19.8	0.0018	-6.3

Table C. 6 Water migration experiment

Water volume, mls	Column I.D.	Slice Depth, mm	Net Mass, g	NaI cpm	Net cpm	Normalized count rate per column	Natural log of normalized count rate
0	64	45.5	19.61	116	10.32	0.001	-6.95
0	79	3.5	16.23	10788	10692.69	0.9902	-0.01
0	79	10.5	18.86	130	26.62	0.0025	-6.01
0	79	17.5	23.33	137	19.91	0.0018	-6.3
0	79	24.5	24.12	133	13.48	0.0012	-6.69
0	79	31.5	19.55	126	20.5	0.0019	-6.27
0	79	38.5	20.24	119	11.39	0.0011	-6.85
0	79	45.5	18.15	115	13.8	0.0013	-6.66
0	81	3.5	29.1	7376	7241.21	0.9886	-0.01
0	81	10.5	24.38	138	17.69	0.0024	-6.03
0	81	17.5	20.16	116	8.63	0.0012	-6.74
0	81	24.5	22.99	130	13.95	0.0019	-6.26
0	81	31.5	22.9	128	12.23	0.0017	-6.4
0	81	38.5	23.4	139	21.69	0.003	-5.82
0	81	45.5	17.23	108	9.62	0.0013	-6.64
0	82	3.5	5.62	911	848.24	0.1454	-1.93
0	82	10.5	22.1	5012	4898.68	0.84	-0.17
0	82	17.5	25.19	143	20.2	0.0035	-5.67
0	82	24.5	21.5	131	19.52	0.0033	-5.7
0	82	31.5	21.01	127	17.02	0.0029	-5.84
0	82	38.5	25.01	137	14.75	0.0025	-5.98
0	82	45.5	16.57	110	13.65	0.0023	-6.06

Table C. 6 Water migration experiment

Water volume, mls	Column I.D.	Slice Depth, mm	Net Mass, g	NaI cpm	Net cpm	Normalized count rate per column	Natural log of normalized count rate
0	88	3.5	31.37	9010	8868.24	0.9919	-0.01
0	88	10.5	20.02	120	13.06	0.0015	-6.53
0	88	17.5	20.09	124	14.36	0.0016	-6.43
0	88	24.5	19.61	115	9.32	0.001	-6.87
0	88	31.5	20.14	127	19.69	0.0022	-6.12
0	88	38.5	16.48	112	15.92	0.0018	-6.33
2100	1	3.5	31.4	4038	3896.15	0.9725	-0.03
2100	1	10.5	12.42	116	32.38	0.0081	-4.82
2100	1	17.5	24.81	145	23.37	0.0058	-5.14
2100	1	24.5	25.08	140	17.54	0.0044	-5.43
2100	1	31.5	16.42	108	12.11	0.003	-5.8
2100	1	38.5	22.11	123	9.65	0.0024	-6.03
2100	1	45.5	20.06	122	14.94	0.0037	-5.59
2100	3	3.5	15.82	6386	6291.95	0.9354	-0.07
2100	3	10.5	29.98	471	333.51	0.0496	-3
2100	3	17.5	22.15	126	12.53	0.0019	-6.29
2100	3	24.5	22.11	128	14.65	0.0022	-6.13
2100	3	31.5	22.32	126	12.01	0.0018	-6.33
2100	3	38.5	22.33	135	20.97	0.0031	-5.77
2100	3	45.5	21.58	122	10.28	0.0015	-6.48
2100	3	52.5	21.11	128	17.72	0.0026	-5.94
2100	3	59.5	19.85	119	12.58	0.0019	-6.28
2100	15	3.5	21.56	8565	8453.34	0.9865	-0.01
2100	15	10.5	24.89	133	11.12	0.0013	-6.65
2100	15	17.5	20.31	118	10.17	0.0012	-6.74

Table C. 6 Water migration experiment

Water volume, mls	Column I.D.	Slice Depth, mm	Net Mass, g	NaI cpm	Net cpm	Normalized count rate per column	Natural log of normalized count rate
2100	15	24.5	18.87	116	12.59	0.0015	-6.52
2100	15	31.5	20.87	122	12.45	0.0015	-6.53
2100	15	38.5	20.39	119	10.93	0.0013	-6.66
2100	15	45.5	19.65	116	10.2	0.0012	-6.73
2100	15	52.5	20.29	110	2.23	0.0003	-8.25
2100	15	59.5	16.93	105	7.54	0.0009	-7.04
2100	15	66.5	20.82	122	12.61	0.0015	-6.52
2100	15	73.5	17.74	111	11.06	0.0013	-6.65
2100	15	80.5	17.27	113	14.5	0.0017	-6.38
2100	16	3.5	24.609	23711	23589.98	0.8244	-0.19
2100	16	10.5	19.18	4991	4886.64	0.1708	-1.77
2100	16	17.5	20.61	145	36.25	0.0013	-6.67
2100	16	24.5	18.24	118	16.52	0.0006	-7.46
2100	16	31.5	18.04	111	10.14	0.0004	-7.95
2100	16	38.5	19.36	119	14.09	0.0005	-7.62
2100	16	45.5	17.5	109	9.79	0.0003	-7.98
2100	16	52.5	16.43	106	10.07	0.0004	-7.95
2100	16	59.5	19.44	121	15.84	0.0006	-7.5
2100	16	66.5	17.75	114	14.03	0.0005	-7.62
2100	16	73.5	19.21	108	3.55	0.0001	-9
2100	16	80.5	18.34	109	7.22	0.0003	-8.29
2100	24	3.5	24.68	11904	11782.77	0.0428	-3.15
2100	24	10.5	16.48	263263	0.9569	-0.04	
2100	24	17.5	26.03	135	9.62	0	-10.26
2100	24	24.5	19.15	125	20.73	0.0001	-9.49
2100	24	31.5	18.81	113	9.77	0	-10.24

Table C. 6 Water migration experiment

Water volume, mls	Column I.D.	Slice Depth, mm	Net Mass, g	NaI cpm	Net cpm	Normalized count rate per column	Natural log of normalized count rate
2100	24	38.5	19.17	117	12.67	0	-9.99
2100	24	45.5	21.19	129	18.47	0.0001	-9.61
2100	29	3.5	18.3	9008	8906.34	0.7225	-0.33
2100	29	10.5	13.33	3456	3369.59	0.2733	-1.3
2100	29	17.5	22.38	134	19.82	0.0016	-6.43
2100	29	24.5	25.05	133	10.63	0.0009	-7.06
2100	29	31.5	23.25	122	5.15	0.0004	-7.78
2100	29	38.5	19.23	110	5.48	0.0004	-7.72
2100	29	45.5	22.57	125	10.24	0.0008	-7.09
2100	30	3.5	14.93	7527	7435.68	0.9401	-0.06
2100	30	10.5	19.99	488	381.15	0.0482	-3.03
2100	30	17.5	20.89	120	10.39	0.0013	-6.63
2100	30	24.5	20.94	126	16.24	0.0021	-6.19
2100	30	31.5	19.25	115	10.42	0.0013	-6.63
2100	30	38.5	19.92	118	11.37	0.0014	-6.55
2100	30	45.5	19.17	112	7.67	0.001	-6.94
2100	30	52.5	17.1	100	2.02	0.0003	-8.27
2100	30	59.5	20.55	115	6.44	0.0008	-7.11
2100	30	66.5	18.47	109	6.82	0.0009	-7.06
2100	30	73.5	18.28	112	10.4	0.0013	-6.63
2100	30	80.5	19.41	116	10.93	0.0014	-6.58
2100	31	3.5	25.41	10123	9999.53	0.9771	-0.02
2100	31	10.5	14.52	266	175.93	0.0172	-4.06
2100	31	17.5	22.17	130	16.47	0.0016	-6.43
2100	31	24.5	23.16	127	10.43	0.001	-6.89

Table C. 6 Water migration experiment

Water volume, mls	Column I.D.	Slice Depth, mm	Net Mass, g	NaI cpm	Net cpm	Normalized count rate per column	Natural log of normalized count rate
2100	31	31.5	19.83	116	9.64	0.0009	-6.97
2100	31	38.5	22.44	129	14.64	0.0014	-6.55
2100	31	45.5	18.3	109	7.34	0.0007	-7.24
2100	39	3.5	23.75	6976	6857.62	0.9287	-0.07
2100	39	10.5	20.28	547	439.26	0.0595	-2.82
2100	39	17.5	21.75	133	20.75	0.0028	-5.87
2100	39	24.5	22.48	129	14.51	0.002	-6.23
2100	39	31.5	20.19	121	13.54	0.0018	-6.3
2100	39	38.5	20.95	138	28.21	0.0038	-5.57
2100	39	45.5	20.98	120	10.12	0.0014	-6.59
2100	47	3.5	7.93	1938	1868.15	0.4886	-0.72
2100	47	10.5	26.64	1961	1833.75	0.4796	-0.73
2100	47	17.5	20.07	131	23.91	0.0063	-5.07
2100	47	24.5	22.94	136	20.1	0.0053	-5.25
2100	47	31.5	21.71	127	14.88	0.0039	-5.55
2100	47	38.5	19.97	126	19.21	0.005	-5.29
2100	47	45.5	23.64	147	28.96	0.0076	-4.88
2100	47	52.5	17.14	113	14.9	0.0039	-5.55
2100	50	3.5	3.31	3165	3109.32	0.1039	-2.26
2100	50	10.5	29.31	26226	26090.56	0.8715	-0.14
2100	50	17.5	22.27	760	646.16	0.0216	-3.84

Table C. 6 Water migration experiment

Water volume, mls	Column I.D.	Slice Depth, mm	Net Mass, g	NaI cpm	Net cpm	Normalized count rate per column	Natural log of normalized count rate
2100	50	24.5	17.68	124	24.24	0.0008	-7.12
2100	50	31.5	25.08	136	13.54	0.0005	-7.7
2100	50	38.5	18.97	113	9.28	0.0003	-8.08
2100	50	45.5	18.04	117	16.14	0.0005	-7.53
2100	50	52.5	19.62	114	8.29	0.0003	-8.19
2100	50	59.5	16.98	106	8.39	0.0003	-8.18
2100	50	66.5	22.61	125	10.12	0.0003	-7.99
2100	51	3.5	3.31	3165	3109.32	0.1039	-2.26
2100	51	10.5	29.31	26226	26090.56	0.8715	-0.14
2100	51	17.5	21.07	121	10.84	0.0013	-6.64
2100	51	24.5	20.88	122	12.42	0.0015	-6.51
2100	51	31.5	20.15	122	14.66	0.0018	-6.34
2100	51	38.5	20.12	118	10.75	0.0013	-6.65
2100	51	45.5	19.55	123	17.5	0.0021	-6.16
2100	54	3.5	9.15	5974	5900.41	0.6501	-0.43
2100	54	10.5	22	3204	3090.99	0.3405	-1.08
2100	54	17.5	21.84	123	10.48	0.0012	-6.76
2100	54	24.5	20.03	118	11.03	0.0012	-6.71
2100	54	31.5	19.78	116	9.8	0.0011	-6.83
2100	54	38.5	19.66	114	8.17	0.0009	-7.01
2100	54	45.5	22.21	131	17.34	0.0019	-6.26
2100	54	52.5	17.36	105	6.22	0.0007	-7.29

98

Table C. 6 Water migration experiment

Water volume, mls	Column I.D.	Slice Depth, mm	Net Mass, g	NaI cpm	Net cpm	Normalized count rate per column	Natural log of normalized count rate
2100	54	59.5	18.84	116	12.68	0.0014	-6.57
2100	54	66.5	18.52	112	9.66	0.0011	-6.85
2100	55	3.5	35.53	2746	2591.48	0.9794	-0.02
2100	55	10.5	26.57	147	19.97	0.0075	-4.89
2100	55	17.5	24.51	131	10.29	0.0039	-5.55
2100	55	24.5	26.11	142	16.38	0.0062	-5.08
2100	55	31.5	22.07	121	7.77	0.0029	-5.83
2100	56	3.5	18.88	1951	1847.56	0.8003	-0.22
2100	56	10.5	14.57	465	374.78	0.1623	-1.82
2100	56	17.5	21.75	125	12.75	0.0055	-5.2
2100	56	24.5	18.14	104	2.83	0.0012	-6.7
2100	56	38.5	17.44	119	19.98	0.0087	-4.75
2100	56	45.5	21.37	123	11.92	0.0052	-5.27
2100	56	52.5	19.62	117	11.29	0.0049	-5.32
2100	56	59.5	21.64	126	14.09	0.0061	-5.1
2100	56	66.5	16.61	102	5.52	0.0024	-6.04
2100	57	3.5	19.96	8049	7942.25	0.9882	-0.01
2100	57	10.5	25.64	172	47.82	0.0059	-5.12
2100	57	17.5	18.76	112	8.93	0.0011	-6.8
2100	57	24.5	23.65	123	4.93	0.0006	
2100	57	31.5	20.61	120	11.25	0.0014	-6.57
2100	57	38.5	18.06	110	9.07	0.0011	-6.79
2100	57	45.5	23.65	131	12.93	0.0016	-6.43
2100	65	3.5	17.46	2098	1998.91	0.522	-0.65

Table C. 6 Water migration experiment

Water volume, mls	Column I.D.	Slice Depth, mm	Net Mass, g	NaI cpm	Net cpm	Normalized count rate per column	Natural log of normalized count rate
2100	65	10.5	23.67	1746	1627.86	0.4251	-0.86
2100	65	17.5	19.15	179	74.73	0.0195	-3.94
2100	65	24.5	19.95	150	43.28	0.0113	-4.48
2100	65	31.5	20.31	123	15.17	0.004	-5.53
2100	65	38.5	19.83	119	12.64	0.0033	-5.71
2100	65	45.5	18	110	9.26	0.0024	-6.02
2100	65	52.5	20.49	117	8.62	0.0023	-6.1
2100	65	59.5	17.97	110	9.35	0.0024	-6.02
2100	65	66.5	18.79	111	7.83	0.002	-6.19
2100	65	73.5	17.21	108	9.68	0.0025	-5.98
2100	65	80.5	23.23	129	12.21	0.0032	-5.75
2100	66	3.5	14.79	7418	7327.11	0.8046	-0.22
2100	66	10.5	23.58	1841	1723.14	0.1892	-1.66
2100	66	17.5	23.1	125	8.61	0.0009	-6.96
2100	66	24.5	21.06	119	8.87	0.001	-6.93
2100	66	31.5	19.21	115	10.55	0.0012	-6.76
2100	66	38.5	24.11	133	13.51	0.0015	-6.51
2100	66	45.5	18.44	117	14.91	0.0016	-6.41
2100	69	3.5	11.49	9786	9705.23	0.5469	-0.6
2100	69	10.5	26.08	8093	7967.47	0.449	-0.8
2100	69	17.5	21.41	133	21.8	0.0012	-6.7
2100	69	24.5	20.57	121	12.37	0.0007	-7.27
2100	69	31.5	22.32	130	16.01	0.0009	-7.01
2100	69	38.5	21.47	126	14.61	0.0008	-7.1
2100	69	45.5	21.55	119	7.37	0.0004	-7.79

Table C. 6 Water migration experiment

Water volume, mls	Column I.D.	Slice Depth, mm	Net Mass, g	NaI cpm	Net cpm	Normalized count rate per column	Natural log of normalized count rate
2100	72	3.5	13.73	8245	8157.36	0.279	-1.28
2100	72	10.5	22.1	20951	20837.68	0.7127	-0.34
2100	72	17.5	21.76	294	181.72	0.0062	-5.08
2100	72	24.5	25.79	144	19.36	0.0007	-7.32
2100	72	31.5	19.85	122	15.58	0.0005	-7.54
2100	72	38.5	21.09	123	12.78	0.0004	-7.74
2100	72	45.5	19.53	118	12.56	0.0004	-7.75
2100	73	3.5	6.67	1134	1068.02	0.1693	-1.78
2100	73	10.5	27.3	4496	4366.73	0.6923	-0.37
2100	73	17.5	23.56	744	626.2	0.0993	-2.31
2100	73	24.5	12.54	254	170.01	0.027	-3.61
2100	73	31.5	27.23	142	12.94	0.0021	-6.19
2100	73	45.5	19.48	117	11.72	0.0019	-6.29
2100	73	52.5	18.88	123	19.56	0.0031	-5.78
2100	73	59.5	18.14	113	11.83	0.0019	-6.28
2100	73	66.5	19.02	115	11.13	0.0018	-6.34
2100	84	3.5	19.87	4472	4365.52	0.9465	-0.05
2100	84	10.5	24.41	329	208.59	0.0452	-3.1
2100	84	17.5	21.16	115	4.56	0.001	-6.92
2100	84	24.5	20.36	117	9.02	0.002	-6.24
2100	84	31.5	18.64	111	8.29	0.0018	-6.32
2100	84	38.5	20.26	113	5.33	0.0012	-6.76
2100	84	45.5	20.71	120	10.94	0.0024	-6.04
2100	87	3.5	18.39	9559	9457.06	0.921	-0.08
2100	87	10.5	13.51	767	680.03	0.0662	-2.71

(01

Table C. 6 Water migration experiment

Water. volume, mls	Column I.D.	Slice Depth, mm	Net Mass, g	NaI cpm	Net cpm	Normalized count rate per column	Natural log of normalized count rate
2100	72	3.5	13.73	8245	8157.36	0.279	-1.28
2100	72	10.5	22.1	20951	20837.68	0.7127	-0.34
2100	72	17.5	21.76	294	181.72	0.0062	-5.08
2100	72	24.5	25.79	144	19.36	0.0007	-7.32
2100	72	31.5	19.85	122	15.58	0.0005	-7.54
2100	72	38.5	21.09	123	12.78	0.0004	-7.74
2100	72	45.5	19.53	118	12.56	0.0004	-7.75
2100	73	3.5	6.67	1134	1068.02	0.1693	-1.78
2100	73	10.5	27.3	4496	4366.73	0.6923	-0.37
2100	73	17.5	23.56	744	626.2	0.0993	-2.31
2100	73	24.5	12.54	254	170.01	0.027	-3.61
2100	73	31.5	27.23	142	12.94	0.0021	-6.19
2100	73	45.5	19.48	117	11.72	0.0019	-6.29
2100	73	52.5	18.88	123	19.56	0.0031	-5.78
2100	73	59.5	18.14	113	11.83	0.0019	-6.28
2100	73	66.5	19.02	115	11.13	0.0018	-6.34
2100	84	3.5	19.87	4472	4365.52	0.9465	-0.05
2100	84	10.5	24.41	329	208.59	0.0452	-3.1
2100	84	17.5	21.16	115	4.56	0.001	-6.92
2100	84	24.5	20.36	117	9.02	0.002	-6.24
2100	84	31.5	18.64	111	8.29	0.0018	-6.32
2100	84	38.5	20.26	113	5.33	0.0012	-6.76
2100	84	45.5	20.71	120	10.94	0.0024	-6.04
2100	87	3.5	18.39	9559	9457.06	0.921	-0.08
2100	87	10.5	13.51	767	680.03	0.0662	-2.71

Table C. 6 Water migration experiment

Water volume, mls	Column I.D.	Slice Depth, mm	Net Mass, g	NaI cpm	Net cpm	Normalized count rate per column	Natural log of normalized count rate
2100	87	17.5	20.86	152	42.48	0.0041	-5.49
2100	87	24.5	24.07	156	36.64	0.0036	-5.64
2100	87	31.5	16.53	121	24.77	0.0024	-6.03
2100	87	38.5	22.32	125	11.01	0.0011	-6.84
2100	87	45.5	22.23	130	16.28	0.0016	-6.45
2100	90	3.5	11.21	6846	6766.09	0.3024	-1.2
2100	90	10.5	22.18	15504	15390.43	0.6879	-0.37
2100	90	17.5	24.58	217	96.07	0.0043	-5.45
2100	90	24.5	20.01	152	45.09	0.002	-6.21
2100	90	31.5	21.29	141	30.17	0.0013	-6.61
2100	90	38.5	21.7	129	16.91	0.0008	-7.19
2100	90	45.5	21.71	141	28.88	0.0013	-6.65
100000	13	3.5	24.19	5066	4946.27	0.9309	-0.07
100000	13	10.5	23.18	366	249.37	0.0469	-3.06
100000	13	17.5	21.61	149	37.18	0.007	-4.96
100000	13	24.5	22.15	143	29.53	0.0056	-5.19
100000	13	31.5	21.57	126	14.31	0.0027	-5.92
100000	13	38.5	21.41	130	18.8	0.0035	-5.64
100000	13	45.5	19.46	123	17.78	0.0033	-5.7
100000	14	3.5	18.35	2681	2579.18	0.7312	-0.31
100000	14	10.5	18.61	967	864.39	0.245	-1.41
100000	14	17.5	23.59	145	27.11	0.0077	-4.87
100000	14	24.5	24.28	136	15.99	0.0045	-5.4
100000	14	31.5	22.23	131	17.28	0.0049	-5.32
100000	14	38.5	21.46	126	14.64	0.0042	-5.48

Table C. 6 Water migration experiment

Water volume, mls	Column I.D.	Slice Depth, mm	Net Mass, g	NaI cpm	Net cpm	Normalized count rate per column	Natural log of normalized count rate
2100	87	17.5	20.86	152	42.48	0.0041	-5.49
2100	87	24.5	24.07	156	36.64	0.0036	-5.64
2100	87	31.5	16.53	121	24.77	0.0024	-6.03
2100	87	38.5	22.32	125	11.01	0.0011	-6.84
2100	87	45.5	22.23	130	16.28	0.0016	-6.45
2100	90	3.5	11.21	6846	6766.09	0.3024	-1.2
2100	90	10.5	22.18	15504	15390.43	0.6879	-0.37
2100	90	17.5	24.58	217	96.07	0.0043	-5.45
2100	90	24.5	20.01	152	45.09	0.002	-6.21
2100	90	31.5	21.29	141	30.17	0.0013	-6.61
2100	90	38.5	21.7	129	16.91	0.0008	-7.19
2100	90	45.5	21.71	141	28.88	0.0013	-6.65
100000	13	3.5	24.19	5066	4946.27	0.9309	-0.07
100000	13	10.5	23.18	366	249.37	0.0469	-3.06
100000	13	17.5	21.61	149	37.18	0.007	-4.96
100000	13	24.5	22.15	143	29.53	0.0056	-5.19
100000	13	31.5	21.57	126	14.31	0.0027	-5.92
100000	13	38.5	21.41	130	18.8	0.0035	-5.64
100000	13	45.5	19.46	123	17.78	0.0033	-5.7
100000	14	3.5	18.35	2681	2579.18	0.7312	-0.31
100000	14	10.5	18.61	967	864.39	0.245	-1.41
100000	14	17.5	23.59	145	27.11	0.0077	-4.87
100000	14	24.5	24.28	136	15.99	0.0045	-5.4
100000	14	31.5	22.23	131	17.28	0.0049	-5.32
100000	14	38.5	21.46	126	14.64	0.0042	-5.48

Table C. 6 Water migration experiment

Water volume, mls	Column I.D.	Slice Depth, mm	Net Mass, g	NaI cpm	Net cpm	Normalized count rate per column	Natural log of normalized count rate
100000	14	45.5	19.11	113	8.85	0.0025	-5.99
100000	20	3.5	31.37	5187	5045.24	0.9827	-0.02
100000	20	10.5	21.41	125	13.8	0.0027	-5.92
100000	20	17.5	24.8	134	12.4	0.0024	-6.03
100000	20	24.5	23.56	132	14.2	0.0028	-5.89
100000	20	31.5	22.9	128	12.23	0.0024	-6.04
100000	20	38.5	22.45	137	22.61	0.0044	-5.43
100000	20	45.5	16.28	109	13.54	0.0026	-5.94
100000	21	3.5	24.03	5392	5272.76	0.9793	-0.02
100000	21	10.5	18.04	128	27.14	0.005	-5.29
100000	21	17.5	22.3	132	18.07	0.0034	-5.7
100000	21	24.5	20.73	120	10.88	0.002	-6.2
100000	21	31.5	22.54	139	24.33	0.0045	-5.4
100000	21	38.5	20.17	123	15.6	0.0029	-5.84
100000	21	45.5	18.89	119	15.53	0.0029	-5.85
100000	26	3.5	26.32	20311	20184.73	0.9906	-0.01
100000	26	10.5	22.67	177	61.93	0.003	-5.8
100000	26	17.5	21.39	149	37.86	0.0019	-6.29
100000	26	24.5	21.74	137	24.78	0.0012	-6.71
100000	26	31.5	21.65	136	24.06	0.0012	-6.74
100000	26	38.5	19.94	129	22.31	0.0011	-6.82
100000	26	45.5	19.21	125	20.55	0.001	-6.9
100000	28	3.5	5.65	2741	2678.15	0.0881	-2.43
100000	28	10.5	34.739	27380	27227.91	0.8958	-0.11

Table C. 6 Water migration experiment

Water volume, mls	Column I.D.	Slice Depth, mm	Net Mass, g	NaI cpm	Net cpm	Normalized count rate per column	Natural log of normalized count rate
100000	28	17.5	19.099	140	35.89	0.0012	-6.74
100000	28	24.5	23.621	145	27.01	0.0009	-7.03
100000	28	31.5	22.075	135	21.76	0.0007	-7.24
100000	28	38.5	22.704	135	19.83	0.0007	-7.34
100000	28	45.5	22.78	133	17.59	0.0006	-7.45
100000	28	52.5	21.995	136	23	0.0008	-7.19
100000	28	59.5	21.09	124	13.78	0.0005	-7.7
100000	28	66.5	21.484	131	19.57	0.0006	-7.35
100000	28	73.5	21.683	135	22.96	0.0008	-7.19
100000	28	80.5	19.788	125	18.77	0.0006	-7.39
100000	28	87.5	19.151	120	15.73	0.0005	-7.57
100000	28	94.5	20.13	122	14.72	0.0005	-7.63
100000	28	101.5	29.39	159	23.32	0.0008	-7.17
100000	28	108.5	21.42	131	19.77	0.0007	-7.34
100000	28	115.5	19.24	122	17.45	0.0006	-7.46
100000	28	122.5	19.815	120	13.69	0.0005	-7.71
100000	28	129.5	19.901	115	8.43	0.0003	-8.19
100000	28	136.5	18.03	113	12.17	0.0004	-7.82
100000	28	143.5	23.743	136	17.64	0.0006	-7.45
100000	28	150.5	15.56	99	5.74	0.0002	-8.57
100000	28	157.5	19.735	119	12.94	0.0004	-7.76
100000	28	164.5	18.024	115	14.18	0.0005	-7.67
100000	28	171.5	21.287	131	20.17	0.0007	-7.32
100000	28	178.5	19.205	115	10.56	0.0003	-7.96
100000	28	185.5	18.557	117	14.55	0.0005	-7.64
100000	28	192.5	13.592	95	7.78	0.0003	-8.27
100000	28	197.5	20.053	128	20.96	0.0007	-7.28

Table C. 6 Water migration experiment

Water volume, mls	Column I.D.	Slice Depth, mm	Net Mass, g	NaI cpm	Net cpm	Normalized count rate per column	Natural log of normalized count rate
100000	37	3.5	13.52	8040	7953	0.7608	-0.27
100000	37	10.5	20.03	2352	2245.03	0.2147	-1.54
100000	37	17.5	21.91	204	91.26	0.0087	-4.74
100000	37	24.5	20.15	118	10.66	0.001	-6.89
100000	37	31.5	23.67	131	12.86	0.0012	-6.7
100000	37	38.5	19.62	116	10.29	0.001	-6.92
100000	37	45.5	24.2	146	26.24	0.0025	-5.99
100000	37	52.5	19.07	116	11.98	0.0011	-6.77
100000	37	59.5	19.45	118	12.81	0.0012	-6.7
100000	37	66.5	19.3	122	17.27	0.0017	-6.41
100000	37	73.5	21.33	135	24.04	0.0023	-6.07
100000	37	80.5	16.97	111	13.42	0.0013	-6.66
100000	37	87.5	21.9	138	25.29	0.0024	-6.02
100000	46	3.5	26.06	12403	12277.53	0.9115	-0.09
100000	46	10.5	23.51	1144	1026.35	0.0762	-2.57
100000	46	17.5	22.12	199	85.62	0.0064	-5.06
100000	46	24.5	24.33	142	21.84	0.0016	-6.42
100000	46	31.5	22.32	128	14.01	0.001	-6.87
100000	46	38.5	18.23	123	21.55	0.0016	-6.44
100000	46	45.5	24.36	143	22.75	0.0017	-6.38
100000	58	3.5	37.56	22673	22512.25	0.9865	-0,01
100000	58	10.5	21.92	192	79.23	0.0035	-5.66
100000	58	17.5	22.66	153	37.96	0.0017	-6.4
100000	58	24.5	20.12	128	20.75	0.0009	-7

Table C. 6 Water migration experiment

Water volume, mls	Column I.D.	Slice Depth, mm	Net Mass, g	NaI cpm	Net cpm	Normalized count rate per column	Natural log of normalized count rate
100000	58	31.5	20.46	124	15.71	0.0007	-7.28
100000	58	38.5	20.86	127	17.48	0.0008	-7.17
100000	58	45.5	18.45	117	14.88	0.0007	-7.34
100000	58	52.5	19.9	125	18.43	0.0008	-7.12
100000	58	59.5	21.25	135	24.29	0.0011	-6.85
100000	58	66.5	20.9	132	22.36	0.001	-6.93
100000	58	73.5	19.75	124	17.89	0.0008	-7.15
100000	58	80.5	18.91	120	16.47	0.0007	-7.23
100000	58	87.5	20.15	130	22.66	0.001	-6.91
100000	67	3.5	23.33	13631	13513.91	0.9548	-0.05
100000	67	10.5	23.8	655	536.46	0.0379	-3.27
100000	67	17.5	19.87	128	21.52	0.0015	-6.49
100000	67	24.5	21.54	143	31.4	0.0022	-6.11
100000	67	31.5	22.81	132	16.5	0.0012	-6.75
100000	67	38.5	20.14	128	20.69	0.0015	-6.53
100000	67	45.5	19.86	120	13.55	0.001	-6.95
100000	74	3.5	31.58	3047	2904.6	0.7718	-0.26
100000	74	10.5	19.92	640	533.37	0.1417	-1.95
100000	74	17.5	22.24	348	234.25	0.0622	-2.78
100000	74	24.5	20.57	147	38.37	0.0102	-4.59
100000	74	31.5	20.7	127	17.98	0.0048	-5.34
100000	74	38.5	20.24	123	15.39	0.0041	-5.5
100000	74	45.5	19.3	124	19.27	0.0051	-5.27

Table C. 6 Water migration experiment

Water volume, mls	Column I.D.	Slice Depth, mm	Net Mass, g	NaI cpm	Net cpm	Normalized count rate per column	Natural log of normalized count rate
100000	75	3.5	37.23	3944	3784.26	0.9471	-0.05
100000	75	10.5	20.96	147	37.18	0.0093	-4.68
100000	75	17.5	23.18	132	15.37	0.0038	-5.56
100000	75	24.5	23.17	137	20.4	0.0051	-5.28
100000	75	31.5	20.88	122	12.42	0.0031	-5.77
100000	75	38.5	22.04	127	13.86	0.0035	-5.66
100000	75	45.5	19.73	127	20.95	0.0052	-5.25
100000	75	52.5	22.38	130	15.82	0.004	-5.53
100000	75	59.5	20.75	126	16.82	0.0042	-5.47
100000	75	66.5	21.42	128	16.77	0.0042	-5.47
100000	75	73.5	17.43	110	11.01	0.0028	-5.89
100000	75	80.5	22.18	129	15.43	0.0039	-5.56
100000	75	87.5	16	110	15.39	0.0039	-5.56
100000	78	3.5	36.742	26682	26523.76	0.9882	-0.01
100000	78	10.5	22.93	212	96.13	0.0036	-5.63
100000	78	17.5	22.181	156	42.43	0.0016	-6.45
100000	78	24.5	21.47	143	31.61	0.0012	-6.74
100000	78	31.5	20.55	127	18.44	0.0007	-7.28
100000	78	38.5	20.522	129	20.52	0.0008	-7.18
100000	78	45.5	19.542	121	15.53	0.0006	-7.46
100000	78	52.5	20.138	127	19.7	0.0007	-7.22
100000	78	59.5	19.976	124	17.2	0.0006	-7.35
100000	78	66.5	20.28	133	25.26	0.0009	-6.97
100000	78	73.5	18.994	111	7.21	0.0003	-8.22
100000	78	80.5	19.113	117	12.84	0.0005	-7.64

Table C. 6 Water migration experiment

Water volume, mls	Column I.D.	Slice Depth, mm	Net Mass, g	NaI cpm	Net cpm	Normalized count rate per column	Natural log of normalized count rate
100000	78	87.5	20.068	118	10.91	0.0004	-7.81
100000	80	3.5	18.64	7539	7436.29	0.9713	-0.03
100000	80	10.5	21.63	254	142.12	0.0186	-3.99
100000	80	17.5	25.95	139	13.87	0.0018	-6.31
100000	80	24.5	22.33	136	21.97	0.0029	-5.85
100000	80	31.5	21.22	128	17.38	0.0023	-6.09
100000	80	38.5	22.93	130	14.13	0.0018	-6.29
100000	80	45.5	20.31	118	10.17	0.0013	-6.62
100000	86	3.5	16.81	7703	7605.91	0.6515	-0.43
100000	86	10.5	30.845	3840	3699.85	0.3169	-1.15
100000	86	17.5	22.503	142	27.44	0.0024	-6.05
100000	86	24.5	23.338	133	15.88	0.0014	-6.6
100000	86	31.5	24.826	138	16.32	0.0014	-6.57
100000	86	38.5	24.418	133	12.57	0.0011	-6.83
100000	86	45.5	21.058	124	13.88	0.0012	-6.73
100000	86	52.5	23.854	133	14.3	0.0012	-6.7
100000	86	59.5	22.721	127	11.78	0.001	-6.9
100000	86	66.5	22.517	126	11.4	0.001	-6.93
100000	86	73.5	22.574	132	17.23	0.0015	-6.52
100000	86	80.5	21.457	128	16.65	0.0014	-6.55
100000	86	87.5	21.979	129	16.05	0.0014	-6.59
100000	86	94.5	22.344	132	17.93	0.0015	-6.48
100000	86	101.5	22.798	127	11.54	0.001	-6.92
100000	86	108.5	21.62	124	12.15	0.001	-6.87

Table C. 6 Water migration experiment

Water volume, mls	Column I.D.	Slice Depth, mm	Net Mass, g	NaI cpm	Net cpm	Normalized count rate per column	Natural log of normalized count rate
100000	86	115.5	21.166	123	12.55	0.0011	-6.84
100000	86	122.5	21.009	122	12.03	0.001	-6.88
100000	86	129.5	18.642	117	14.29	0.0012	-6.71
100000	86	136.5	21.519	124	12.46	0.0011	-6.84
100000	86	143.5	19.369	116	11.06	0.0009	-6.96
100000	86	150.5	19.111	116	11.85	0.001	-6.89
100000	86	157.5	20.469	120	11.68	0.001	-6.91
100000	86	164.5	17.163	109	10.83	0.0009	-6.98
100000	86	171.5	19.472	127	21.74	0.0019	-6.29
100000	86	178.5	18.319	119	17.28	0.0015	-6.52
100000	86	185.5	14.492	100	10.02	0.0009	-7.06
100000	86	192.5	23.901	126	7.16	0.0006	-7.4
100000	89	3.5	29.24	6059	5923.78	0.9838	-0.02
100000	89	10.5	24.26	138	18.05	0.003	-5.81
100000	89	17.5	21.83	132	19.51	0.0032	-5.73
100000	89	24.5	23.73	137	18.68	0.0031	-5.78
100000	89	31.5	21.58	131	19.28	0.0032	-5.74
100000	89	38.5	22.82	125	9.47	0.0016	-6.45
100000	89	45.5	21.53	124	12.43	0.0021	-6.18

Table C.7 Column data for freeze thaw experiments

Freeze/ thaw cycle	segment position	column I.d.	slice depth, mm	net sample mass, g	sample counts per min	net sample counts per minute	net sample counts per minute per g	normalized counts per minute
0	inner	4	2.5	6.147	1816	1740.584	283.365	0.617
0	outer	4	2.5	5.396	903	830.782	154.168	0.336
0	inner	4	7.5	8.783	150	63.358	7.419	0.016
0	outer	4	7.5	8.113	129	45.212	5.778	0.013
0	inner	4	12.5	5.98	92	17.295	3.097	0.007
0	outer	4	12.5	5.73	92	18.36	3.409	0.007
0	inner	4	17.5	8.01	83	-0.35	0.161	0
0	outer	4	17.5	6.086	77	1.844	0.508	0.001
0	inner	4	22.5	7.462	80	-1.016	0.069	0
0	outer	4	22.5	5.862	73	-1.202	0	0
0	inner	4	27.5	7.244	83	2.912	0.607	0.001
0	outer	4	27.5	6.32	78	1.847	0.497	0.001
0	inner	5	2.5	2.297	5577	5517.98	2402.595	0.935
0	outer	5	2.5	3.134	172	109.415	35.252	0.014
0	inner	5	7.5	8.943	1170	1082.677	121.404	0.047
0	outer	5	7.5	6.598	126	48.663	7.715	0.003
0	inner	5	12.5	6.096	74	-1.199	0.143	0
0	outer	5	12.5	4.983	69	-1.459	0.047	0
0	inner	5	17.5	8.626	87	1.027	0.459	0
0	outer	5	17.5	6.91	77	-1.665	0.099	0
0	inner	5	22.5	5.484	73	0.408	0.414	0
0	outer	5	22.5	5.702	73	-0.521	0.248	0
0	inner	5	27.5	6.961	80	1.118	0.5	0
0	outer	5	27.5	5.603	72	-1.099	0.144	0
0	inner	5	32.5	5.553	71	-1.886	0	0
0	outer	5	32.5	4.62	71	2.087	0.791	0

Table C.7 Column data for freeze thaw experiments

Freeze/ thaw cycle	segment position	column I.d.	slice depth, mm	net sample mass, g	sample counts per min	net sample counts per minute	net sample counts per minute per g	normalized counts per minute
0	Inner	68	2.5	10.285	401	307.962	30.417	0.805
0	outer	68	2.5	7.968	104	20.829	3.088	0.082
0	Inner	68	7.5	7.733	84	1.83	0.71	0.019
0	outer	68	7.5	5.844	74	-0.126	0.452	0.012
0	Inner	68	12.5	7.892	81	-1.847	0.24	0.006
0	outer	68	12.5	6.293	75	-1.038	0.309	0.008
0	Inner	68	17.5	5.73	77	3.36	1.06	0.028
0	outer	68	17.5	5.787	73	[illegible]	[illegible]	[illegible]
0	Inner	68	[illegible]	[illegible]	78	3.133	1.008	0.011
0	Inner	83	7.5	6.018	73	-0.904	0.331	0.004
0	outer	83	7.5	5.792	76	0.754	0.611	0.007
0	Inner	83	12.5	6.107	78	0.059	0.496	0.005
0	outer	83	12.5	6.74	78	4.841	1.349	0.015
0	Inner	83	17.5	5.617	75	-2.907	0.056	0.001
0	outer	83	17.5	6.732	76	0.15	0.511	0.005
0	Inner	83	22.5	6.249	79	-3.847	0	0
0	outer	83	22.5	7.892	75	-1.936	0.19	0.002
0	Inner	83	27.5	6.504	78	2.294	0.857	0.009
0	outer	83	27.5	6.215	72	-0.018	0.484	0.005
0	Inner	83	32.5	5.349	76	1.836	0.801	0.009
0	outer	83	32.5	5.853				

Table C.7 Column data for freeze thaw experiments

Freeze/ thaw cycle	segment position	column I.d.	slice depth, mm	net sample mass, g	sample counts per min	net sample counts per minute	net sample counts per minute per g	normalized counts per minute
0	Inner	83	37.5	3.649	63	-1.778	0	0
0	outer	83	37.5	7.03	79	-0.176	0.462	0.005
0	Inner	83	42.5	5.669	75	1.62	0.773	0.008
0	outer	83	42.5	8.004	84	0.676	0.572	0.006
1	Inner	9	2.5	7.053	5822	5742.726	814.397	0.896
1	outer	9	2.5	5.068	363	292.179	57.824	0.064
1	Inner	9	7.5	6.333	135	58.792	9.456	0.01
1	outer	9	7.5	5.431	121	48.633	9.127	0.01
1	Inner	9	12.5	7.412	89	8.197	1.279	0.001
1	outer	9	12.5	6.116	98	22.716	3.887	0.004
1	Inner	9	17.5	6.125	76	0.678	0.283	0
1	outer	9	17.5	6.448	108	31.302	5.027	0.006
1	Inner	9	22.5	5.467	89	16.48	3.187	0.004
1	outer	9	22.5	7.12	85	5.44	0.937	0.001
1	Inner	9	27.5	5.525	74	1.233	0.396	0
1	outer	9	27.5	7.505	97	15.801	2.278	0.003
1	Inner	9	32.5	5.326	71	-0.92	0	0
1	outer	9	32.5	6.696	83	5.246	0.956	0.001
1	Inner	10	2.5	4.002	4678	4611.719	1152.963	0.84
1	outer	10	2.5	2.133	195	136.678	64.688	0.047
1	Inner	10	7.5	8.886	1309	1221.92	138.12	0.101
1	outer	10	7.5	7.065	126	46.675	7.216	0.005
1	Inner	10	12.5	4.731	71	1.614	0.951	0.001
1	outer	10	12.5	5.198	73	1.625	0.923	0.001
1	Inner	10	17.5	9.877	90	-1.301	0.478	0

Table C.7 Column data for freeze thaw experiments

Freeze/ thaw cycle	segment position	column I.d.	slice depth, mm	net sample mass, g	sample counts per min	net sample counts per minute	net sample counts per minute per g	normalized counts per minute
1	outer	10	17.5	9.43	87	-2.397	0.356	0
1	Inner	10	22.5	5.417	72	-0.307	0.553	0
1	outer	10	22.5	6.781	77	-1.116	0.445	0
1	Inner	10	27.5	6.497	75	-1.906	0.316	0
1	outer	10	27.5	8.585	83	-2.798	0.284	0
1	Inner	10	32.5	5.888	75	0.687	0.726	0.001
1	outer	10	32.5	6.444	77	0.319	0.659	0
1	Inner	10	37.5	4.882	72	1.971	1.014	0.001
1	outer	10	37.5	9.186	88	-0.358	0.571	0
1	Inner	10	42.5	5.171	72	0.74	0.753	0.001
1	outer	10	42.5	9.075	89	1.115	0.733	0.001
1	Inner	10	47.5	5.35	74	1.978	0.98	0.001
1	outer	10	47.5	5.69	70	-3.47	0	0
1	Inner	61	2.5	9.973	247	155.291	16.011	0.287
1	outer	61	2.5	6.201	187	111.354	18.397	0.33
1	Inner	61	7.5	6.728	86	8.11	1.645	1
1	outer	61	7.5	5.568	144	71.05	13.2	0.237
1	Inner	61	12.5	8.282	86	1.492	0.62	0.011
1	outer	61	12.5	6.429	95	18.383	3.299	0.059
1	Inner	61	17.5	7.054	79	-0.279	0.401	0.007
1	outer	61	17.5	9.388	90	0.782	0.523	0.009
1	Inner	61	22.5	10.105	95	2.728	0.71	0.013
1	outer	61	22.5	7.064	81	1.679	0.678	0.012
1	Inner	61	27.5	6.953	78	-0.848	0.318	0.006
1	outer	61	27.5	7.532	78	-3.314	0	0

Table C.7 Column data for freeze thaw experiments

Freeze/ thaw cycle	segment position	column I.d.	slice depth, mm	net sample mass, g	sample counts per min	net sample counts per minute	net sample counts per minute per g	normalized counts per minute
1	Inner	70	2.5	8.487	4057	3971.619	468.101	0.648
1	outer	70	2.5	4.271	905	837.573	196.243	0.272
1	Inner	70	7.5	5.225	92	20.511	4.062	0.006
1	outer	70	7.5	4.399	168	100.028	22.875	0.032
1	Inner	70	12.5	5.525	95	22.233	4.16	0.006
1	outer	70	12.5	3.055	121	58.752	19.367	0.027
1	Inner	70	17.5	9.681	93	2.534	0.398	0.001
1	outer	70	17.5	7.319	114	33.593	4.726	0.007
1	Inner	70	22.5	6.478	80	3.174	0.626	0.001
1	outer	70	22.5	6.707	85	7.199	1.209	0.002
1	Inner	70	27.5	6.825	81	2.697	0.531	0.001
1	outer	70	27.5	8.037	85	1.535	0.327	0
1	Inner	70	32.5	6.249	75	-0.85	0	0
1	outer	70	32.5	6.549	77	-0.128	0.117	0
4	Inner	8	2.5	9.733	1644	1553.313	159.911	0.394
4	outer	8	2.5	7.416	1550	1469.18	198.428	0.489
4	Inner	8	7.5	8.588	88	2.189	0.573	0.001
4	outer	8	7.5	7.442	222	141.069	19.274	0.047
4	Inner	8	12.5	9.584	87	-3.053	0	0
4	outer	8	12.5	8.191	138	53.879	6.896	0.017
4	Inner	8	17.5	7.447	82	1.048	0.459	0.001
4	outer	8	17.5	6.052	114	38.989	6.761	0.017
4	Inner	8	22.5	9.852	92	0.806	0.4	0.001
4	outer	8	22.5	8.407	143	57.96	7.213	0.018
4	Inner	8	27.5	6.003	73	-1.803	0.018	0
4	outer	8	27.5	7.899	107	24.123	3.372	0.008

Table C.7 Column data for freeze thaw experiments

Freeze/ thaw cycle	segment position	column I.d.	slice depth, mm	net sample mass, g	sample counts per min	net sample counts per minute	net sample counts per minute per g	normalized counts per minute
4	Inner	8	32.5	9.274	87	-1.733	0.132	0
4	outer	8	32.5	7.066	96	16.67	2.678	0.007
4	Inner	42	2.5	6.338	1884	1807.771	286.548	0.497
4	outer	42	2.5	5.645	728	654.722	117.304	0.203
4	Inner	42	7.5	8.39	592	507.032	61.754	0.107
4	outer	42	7.5	7.418	454	373.171	51.627	0.09
4	Inner	42	12.5	7.73	80	-2.157	1.042	0.002
4	outer	42	12.5	9.118	245	156.932	18.532	0.032
4	Inner	42	17.5	5.86	72	-2.194	0.947	0.002
4	outer	42	17.5	8.778	219	132.38	16.402	0.028
4	Inner	42	22.5	6.938	80	1.215	1.496	0.003
4	outer	42	22.5	7.078	148	68.619	11.016	0.019
4	Inner	42	27.5	7.306	77	-3.352	0.862	0.001
4	outer	42	27.5	8.101	114	30.263	5.057	0.009
4	Inner	42	32.5	6.192	80	4.392	2.03	0.004
4	outer	42	32.5	6.724	74	-3.873	0.745	0.001
4	Inner	42	37.5	6.387	68	-8.438	0	0
4	outer	42	37.5	6.34	76	-0.238	1.284	0.002
4	Inner	76	2.5	11.002	1213	1116.908	101.714	0.293
4	outer	76	2.5	9.58	1247	1156.964	120.964	0.348
4	Inner	76	7.5	8.928	92	4.741	0.726	0.002
4	outer	76	7.5	6.132	237	161.648	26.556	0.076
4	Inner	76	12.5	10.277	91	-2.004	0	0
4	outer	76	12.5	9.287	367	278.212	30.152	0.087
4	Inner	76	17.5	6.914	137	58.318	8.63	0.025

Table C.7 Column data for freeze thaw experiments

Freeze/ thaw cycle	segment position	column i.d.	slice depth, mm	net sample mass, g	sample counts per min	net sample counts per minute	net sample counts per minute per g	normalized counts per minute
4	outer	76	17.5	5.668	164	90.624	16.184	0.047
4	inner	76	22.5	9.06	87	-0.821	0.104	0
4	outer	76	22.5	8.619	317	231.057	27.003	0.078
4	inner	76	27.5	6.278	75	-0.974	0.04	0
4	outer	76	27.5	8.953	221	133.634	15.121	0.044
4	inner	77	2.5	6.66	2175	2097.399	315.283	0.599
4	outer	77	2.5	6.335	828	751.783	119.03	0.226
4	inner	77	7.5	10.311	159	65.851	6.745	0.013
4	outer	77	7.5	8.501	307	221.559	26.421	0.05
4	inner	77	12.5	8.144	81	-2.92	0	0
4	outer	77	12.5	6.522	163	85.987	13.543	0.026
4	inner	77	17.5	9.124	88	-0.094	0.348	0.001
4	outer	77	17.5	7.174	163	83.21	11.957	0.023
4	inner	77	22.5	7.252	88	7.878	1.445	0.003
4	outer	77	22.5	8.157	136	52.024	6.736	0.013
4	inner	77	27.5	7.26	91	10.844	1.852	0.004
4	outer	77	27.5	5.815	109	34.998	6.377	0.012
4	inner	77	32.5	11.837	102	2.353	0.557	0.001
4	outer	77	32.5	9.725	157	66.347	7.181	0.014
4	inner	77	37.5	5.391	83	10.804	2.363	0.004
4	outer	77	37.5	5.172	105	33.736	6.881	0.013
5	inner	6	2.5	5.232	827	755.481	145.045	0.427
5	outer	6	2.5	4.186	429	361.935	87.112	0.256
5	inner	6	7.5	7.088	199	119.577	17.519	0.052
5	outer	6	7.5	8.288	278	193.466	23.991	0.071

Table C.7 Column data for freeze thaw experiments

Freeze/ thaw cycle	segment position	column I.d.	slice depth, mm	net sample mass, g	sample counts per min	net sample counts per minute	net sample counts per minute per g	normalized counts per minute
5	Inner	6	12.5	8.23	86	1.713	0.857	0.003
5	outer	6	12.5	7.288	233	152.725	21.604	0.064
5	Inner	6	17.5	8.49	84	-1.394	0.484	0.001
5	outer	6	17.5	7.774	218	135.655	18.098	0.053
5	Inner	6	22.5	8.383	82	-2.938	0.298	0.001
5	outer	6	22.5	8.454	172	86.759	10.911	0.032
5	Inner	6	27.5	6.582	73	-4.268	0	0
5	outer	6	27.5	7.651	136	54.179	7.73	0.023
5	Inner	6	32.5	7.357	80	-0.569	0.571	0.002
5	outer	6	32.5	7.904	92	9.102	1.8	0.005
5	Inner	6	37.5	5.865	73	-1.215	0.441	0.001
5	outer	6	37.5	7.897	83	0.131	0.665	0.002
5	Inner	6	42.5	7.479	78	-3.088	0.236	0.001
5	outer	6	42.5	7.606	80	-1.629	0.434	0.001
5	Inner	6	47.5	6.551	84	6.864	1.696	0.005
5	outer	6	47.5	7.506	78	-3.203	0.222	0.001
5	Inner	27	2.5	8.297	1067	982.428	119.362	0.46
5	outer	27	2.5	8.102	720	636.258	79.485	0.306
5	Inner	27	7.5	6.907	100	21.348	4.045	0.016
5	outer	27	7.5	7.018	237	157.875	23.45	0.09
5	Inner	27	12.5	6.695	80	2.25	1.29	0.005
5	outer	27	12.5	6.488	110	33.132	6.061	0.023
5	Inner	27	17.5	8.674	83	-3.177	0.588	0.002
5	outer	27	17.5	6.89	134	55.42	8.998	0.035
5	Inner	27	22.5	8.477	86	0.661	1.032	0.004
5	outer	27	22.5	7.16	122	42.27	6.858	0.026

Table C.7 Column data for freeze thaw experiments

Freeze/ thaw cycle	segment position	column I.d.	slice depth, mm	net sample mass, g	sample counts per min	net sample counts per minute	net sample counts per minute per g	normalized counts per minute
5	Inner	27	27.5	6.961	80	1.118	1.115	0.004
5	outer	27	27.5	7.688	86	4.022	1.477	0.006
5	Inner	27	32.5	10.167	91	-1.536	0.803	0.003
5	outer	27	32.5	8.602	90	4.129	1.434	0.006
5	Inner	27	37.5	6.888	72	-6.572	0	0
5	outer	27	37.5	7.918	79	-3.958	0.454	0.002
5	Inner	27	42.5	8.281	88	3.496	1.376	0.005
5	outer	27	42.5	8.815	83	-3.778	0.525	0.002
5	Inner	27	47.5	5.079	68	-2.868	0.389	0.002
5	outer	27	47.5	8.749	85	-1.497	0.783	0.003
5	Inner	40	2.5	7.324	1861	1780.572	243.794	0.635
5	outer	40	2.5	6.221	360	284.269	46.375	0.121
5	Inner	40	7.5	7.229	239	158.976	22.671	0.059
5	outer	40	7.5	6.492	206	129.115	20.568	0.054
5	Inner	40	12.5	6.71	85	7.186	1.751	0.005
5	outer	40	12.5	6.76	169	90.974	14.137	0.037
5	Inner	40	17.5	12.215	96	-5.257	0.249	0.001
5	outer	40	17.5	9.154	166	77.778	9.176	0.024
5	Inner	40	22.5	5.893	71	-3.334	0.114	0
5	outer	40	22.5	6.566	140	62.8	10.244	0.027
5	Inner	40	27.5	7.067	79	-0.334	0.632	0.002
5	outer	40	27.5	7.07	114	34.653	5.581	0.015
5	Inner	40	32.5	8.036	78	-5.46	0	0
5	outer	40	32.5	9.094	106	18.034	2.663	0.007
5	Inner	40	37.5	5.632	71	-2.223	0.285	0.001
5	outer	40	37.5	7.043	85	5.768	1.499	0.004

Table C.7 Column data for freeze thaw experiments

Freeze/ thaw cycle	segment position	column I.d.	slice depth, mm	net sample mass, g	sample counts per min	net sample counts per minute	net sample counts per minute per g	normalized counts per minute
5	Inner	40	42.5	7.439	81	0.082	0.691	0.002
5	outer	40	42.5	9.463	96	6.462	1.362	0.004
5	Inner	40	47.5	5.834	78	3.917	1.351	0.004
5	outer	40	47.5	5.636	73	-0.24	0.637	0.002
5	Inner	92	2.5	5.197	309	237.63	46.287	0.125
5	outer	92	2.5	4.757	513	443.504	93.794	0.254
5	Inner	92	7.5	5.033	79	8.328	2.217	0.006
5	outer	92	7.5	9.389	670	580.778	62.42	0.169
5	Inner	92	12.5	11.751	101	1.719	0.709	0.002
5	outer	92	12.5	7.622	562	480.303	63.578	0.172
5	Inner	92	17.5	8.07	87	3.395	0.983	0.003
5	outer	92	17.5	7.695	388	305.992	40.328	0.109
5	Inner	92	22.5	8.906	89	1.835	0.769	0.002
5	outer	92	22.5	6.863	282	203.535	30.22	0.082
5	Inner	92	27.5	6.205	77	1.337	0.778	0.002
5	outer	92	27.5	9.543	158	68.122	7.701	0.021
5	Inner	92	32.5	9.482	95	5.382	1.13	0.003
5	outer	92	32.5	10.979	119	23.006	2.658	0.007
5	Inner	92	37.5	6.976	85	6.054	1.43	0.004
5	outer	92	37.5	8.497	112	26.576	3.69	0.01
5	Inner	92	42.5	7.887	81	-1.826	0.331	0.001
5	outer	92	42.5	8.691	120	33.75	4.446	0.012
5	Inner	92	47.5	5.888	71	-3.313	0	0
5	outer	92	47.5	8.549	132	46.355	5.985	0.016
6	Inner	22	2.5	7.954	1234	1150.889	145.207	0.731

Table C.7 Column data for freeze thaw experiments

Freeze/ thaw cycle	segment position	column I.d.	slice depth, mm	net sample mass, g	sample counts per min	net sample counts per minute	net sample counts per minute per g	normalized counts per minute
6	outer	22	2.5	5.905	212	137.615	23.818	0.12
6	Inner	22	7.5	7.895	132	49.14	6.738	0.034
6	outer	22	7.5	6.393	115	38.536	6.542	0.033
6	Inner	22	12.5	5.903	72	-2.377	0.111	0.001
6	outer	22	12.5	4.877	101	30.993	6.869	0.035
6	Inner	22	17.5	11.304	97	-0.378	0.48	0.002
6	outer	22	17.5	8.294	102	17.441	2.617	0.013
6	Inner	22	22.5	7.091	81	1.564	0.734	0.004
6	outer	22	22.5	9.506	93	3.279	0.859	0.004
6	Inner	22	27.5	8.984	91	3.502	0.904	0.005
6	outer	22	27.5	9.51	90	0.262	0.541	0.003
6	Inner	22	32.5	7.1	78	-1.474	0.306	0.002
6	outer	22	32.5	9.071	84	-3.868	0.087	0
6	Inner	22	37.5	7.655	83	1.162	0.666	0.003
6	outer	22	37.5	5.277	69	-2.711	0	0
6	Inner	22	42.5	7.513	86	4.767	1.148	0.006
6	outer	22	42.5	10.686	91	-3.746	0.163	0.001
6	Inner	22	47.5	6.197	73	-2.629	0.09	0
6	outer	22	47.5	9.086	89	1.068	0.631	0.003
6	Inner	25	2.5	9.549	136	46.096	5.056	0.056
6	outer	25	2.5	9.562	348	258.041	27.214	0.303
6	Inner	25	7.5	9.653	104	13.653	1.643	0.018
6	outer	25	7.5	6.429	203	126.383	19.887	0.222
6	Inner	25	12.5	7.486	103	21.882	3.151	0.035
6	outer	25	12.5	6.184	159	83.426	13.719	0.153
6	Inner	25	17.5	8.018	90	6.616	1.054	0.012

Table C.7 Column data for freeze thaw experiments

Freeze/ thaw cycle	segment position	column I.d.	slice depth, mm	net sample mass, g	sample counts per min	net sample counts per minute	net sample counts per minute per g	normalized counts per minute
6	outer	25	17.5	7.5	130	48.822	6.738	0.075
6	inner	25	22.5	7.836	91	8.391	1.299	0.014
6	outer	25	22.5	5.292	90	18.225	3.672	0.041
6	inner	25	27.5	9.222	95	6.489	0.932	0.01
6	outer	25	27.5	7.972	95	11.812	1.71	0.019
6	inner	25	32.5	8.129	82	-1.857	0	0
6	outer	25	32.5	6.737	82	4.071	0.833	0.009
6	inner	25	37.5	8.244	84	-0.346	0.186	0.002
6	outer	25	37.5	6.946	82	3.181	0.686	0.008
6	inner	25	42.5	8.114	85	1.207	0.377	0.004
6	outer	25	42.5	6.831	79	0.671	0.327	0.004
6	inner	25	47.5	5.711	76	2.441	0.656	0.007
6	outer	25	47.5	9.41	93	3.688	0.62	0.007
6	inner	36	2.5	5.218	658	586.54	113.2	0.485
6	outer	36	2.5	4.163	193	126.033	31.067	0.133
6	inner	36	7.5	8.329	259	174.292	21.718	0.093
6	outer	36	7.5	7.788	232	149.596	20.001	0.086
6	inner	36	12.5	7.77	92	9.672	2.037	0.009
6	outer	36	12.5	6.212	166	90.307	15.33	0.066
6	inner	36	17.5	9.268	90	1.293	0.932	0.004
6	outer	36	17.5	9.633	155	64.739	7.513	0.032
6	inner	36	22.5	6.567	72	-5.205	0	0
6	outer	36	22.5	7.938	130	46.957	6.708	0.029
6	inner	36	27.5	7.536	84	2.669	1.147	0.005
6	outer	36	27.5	9.122	123	34.915	4.62	0.02
6	inner	36	32.5	8.455	95	9.755	1.946	0.008
6	outer	36	32.5	10.175	98	5.43	1.326	0.006

Table C.7 Column data for freeze thaw experiments

Freeze/ thaw cycle	segment position	column I.d.	slice depth, mm	net sample mass, g	sample counts per min	net sample counts per minute	net sample counts per minute per g	normalized counts per minute
6	inner	36	37.5	6.787	79	0.859	0.919	0.004
6	outer	36	37.5	5.593	81	7.943	2.213	0.009
6	inner	36	42.5	7.908	79	-3.915	0.297	0.001
6	outer	36	42.5	9.533	93	3.164	1.124	0.005
6	inner	36	47.5	6.86	77	-1.452	0.581	0.002
6	outer	36	47.5	7.549	80	-1.387	0.609	0.003
6	inner	63	2.5	8.075	750	666.373	83.056	0.464
6	outer	63	2.5	7.435	279	198.099	27.177	0.152
6	inner	63	7.5	8.639	93	6.972	1.34	0.007
6	outer	63	7.5	6.437	195	118.349	18.919	0.106
6	inner	63	12.5	7.93	86	2.991	0.91	0.005
6	outer	63	12.5	7.943	168	84.936	11.226	0.063
6	inner	63	17.5	5.651	82	8.696	2.072	0.012
6	outer	63	17.5	7.041	142	62.777	9.449	0.053
6	inner	63	22.5	8.617	89	3.065	0.889	0.005
6	outer	63	22.5	7.145	152	72.334	10.657	0.06
6	inner	63	27.5	8.639	92	5.972	1.224	0.007
6	outer	63	27.5	11	131	34.917	3.707	0.021
6	inner	63	32.5	7.294	87	6.699	1.451	0.008
6	outer	63	32.5	8.4	101	15.989	2.436	0.014
6	inner	63	37.5	6.646	74	-3.541	0	0
6	outer	63	37.5	11.718	102	2.859	0.777	0.004
6	inner	63	42.5	5.191	71	-0.345	0.466	0.003
6	outer	63	42.5	9.079	97	9.098	1.535	0.009

Table C.7 Column data for freeze thaw experiments

Freeze/ thaw cycle	segment position	column I.d.	slice depth, mm	net sample mass, g	sample counts per min	net sample counts per minute	net sample counts per minute per g	normalized counts per minute
6	inner	63	47.5	9.017	88	0.362	0.573	0.003
6	outer	63	47.5	9.689	96	5.5	1.1	0.006

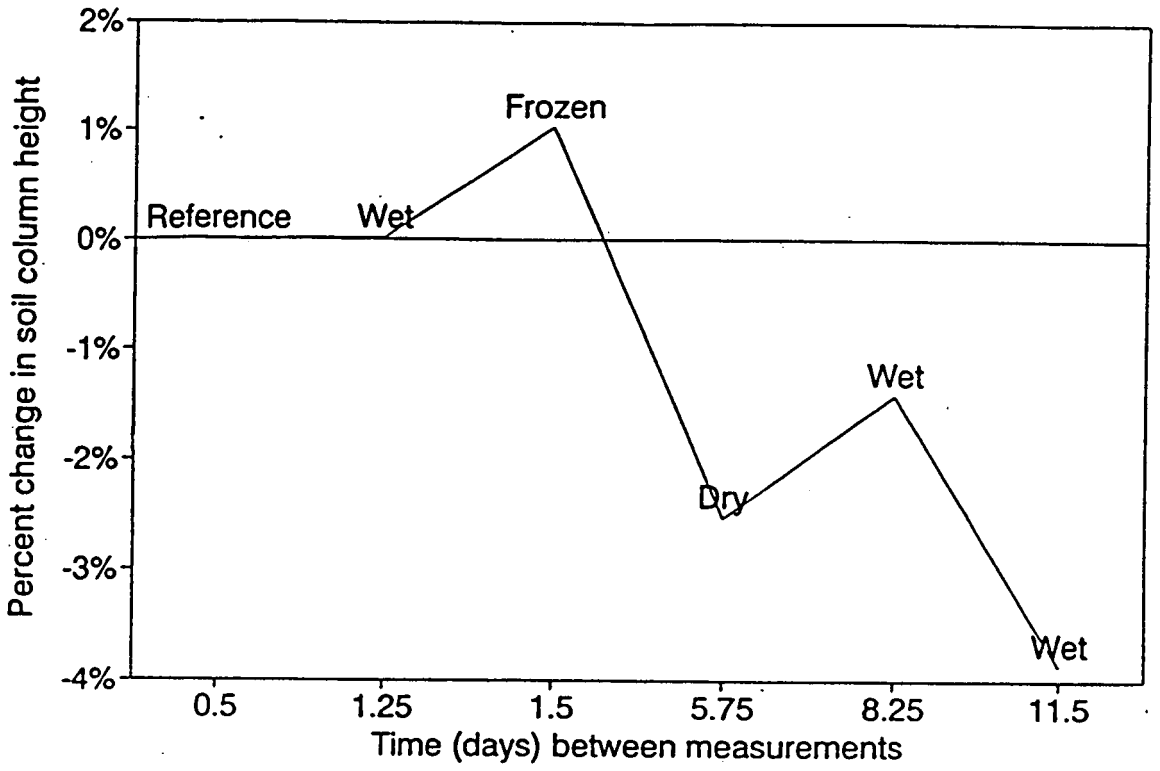

Figure C.1 Core height measurements taking during freeze/thaw experiment (prior to application of radiotracer).

126

COLORADO STATE UNIVERSITY

August 26, 1994

WE HEREBY RECOMMEND THAT THE DISSERTATION PREPARED UNDER OUR SUPERVISION BY KATHRYN A. HIGLEY ENTITLED VERTICAL MOVEMENT OF ACTINIDE-CONTAMINATED SOIL PARTICLES BE ACCEPTED AS FULFILLING IN PART REQUIREMENTS FOR THE DEGREE OF DOCTOR OF PHILOSOPHY.

Committee on Graduate Work

L. Dean Schweickhise

Thomas B. Kinchner

Leslie Trumbo

Janet L. Johnson

H. Ward Whicker

Adviser

J S Bedford

Department Head (acting)

127/127